Characterisation of solid dosing and dissolution in work ups

Arabella Marie McLaughlin

Thesis submitted for the degree of Doctor of Philosophy

Heriot-Watt University

School of Engineering and Physical Sciences

May 2019

Abstract

Continuous manufacturing (CM) in pharmaceutical industry involves work up, reaction, crystallisation, filtration and further downstream processes. This PhD work is focused on work up processes, in particular how to feed solids directly into a liquid stream. This requires the understanding of dissolution kinetics as well as parameters affecting kinetics. A Twin Screw Extruder (TSE) is used in this PhD project as a tool for continuous dissolution; acetylsalicylic acid, benzoic acid, nicotinic acid and paracetamol of different sizes are the test candidates.

It was found that faster dissolution rates were achieved within the TSE in comparison to a stirred tank vessel as a result of shorter mass transfer times and more aggressive mixing. Solubility was identified as the major parameter affecting dissolution rates, temperature is the second contributing factor, while mixing has less effect. Material with the smallest particle size has the fastest dissolution rate, however is difficult to dispense in bulk due to poor flow properties. The TSE enables the decoupling of liquid from the solid feed, thus eliminating any potential fouled solid feeding; allows solution consistency at the exit of the TSE even feeding at low solid feed rates, e.g. 2 g min^{-1}.

Variable solid and liquid flow rates in the TSE are tested, full dissolution of powder paracetamol is attained within the residence time of the TSE, while full dissolution of benzoic acid and acetylsalicylic acid is achievable by having higher barrel temperature. nicotinic acid exits the TSE as a consistent slurry. Dissolution kinetics for the four APIs (Active Pharmaceutical Ingredients) are established. This work also demonstrates that the TSE is a novel and valid tool for work up, allowing the controlled and synchronised input flows, together with intense mixing, to deliver a dissolved solution within the residence time of the barrel.

Acknowledgements

I would firstly like to thank EPSRC, the Doctoral Training Centre in Continuous Manufacturing and Crystallisation, and GSK for funding this work.

I give special thanks to my supervisor, Professor Xiong-Wei Ni, for his help and support, and I am grateful to have been given the opportunity to receive an insight into his extensive knowledge and expertise throughout my PhD, and to work amongst a group of talented researchers.

I would also like to acknowledge the help and support from Dr John Robertson for his guidance and backing, sharing his vast knowledge of Secondary Pharmaceutical Manufacturing Processes and my colleagues within CMAC at the University of Strathclyde who have provided training and assistance during my time spent at the Technology and Innovation Centre.

My appreciation goes to the other members of the COBRA team – Juliet, Guillermo, Meifen, Ross and Francisca- for their assistance in the progress of this research work. I also really appreciate the invaluable help of the technicians, Mr Richard Kinsella, Mr Cameron Smith, Mr Douglas Wagener and Mr Craig Bell, I am grateful for their continued support.

I would like to thank Dr Andrew Rutter and Dr Gareth Alford from GSK, for being my industrial mentors and providing guidance, support and an insight into the current industrial processes.

Finally, and most importantly, I would like to thank my sons, Riagan and Byron, my parents, and my family and friends for their continued love and support.

ACADEMIC REGISTRY

Research Thesis Submission - Declaration Statement

Name*:*	Arabella Marie McLaughlin		
School:	Engineering and Physical Sciences		
Version: *(i.e. First, Resubmission, Final)*	Final	Degree Sought:	Doctor of Philosophy

Declaration

In accordance with the appropriate regulations I hereby submit my thesis and I declare that:

1. The thesis embodies the results of my own work and has been composed by myself
2. Where appropriate, I have made acknowledgement of the work of others
3. Where the thesis contains published outputs under Regulation 6 (9.1.2) these are accompanied by a critical review which accurately describes my contribution to the research and, for multi-author outputs, a signed declaration indicating the contribution of each author (complete Inclusion of Published Works Form – see below)
4. The thesis is the correct version for submission and is the same version as any electronic versions submitted*.
5. My thesis for the award referred to, deposited in the Heriot-Watt University Library, should be made available for loan or photocopying and be available via the Institutional Repository, subject to such conditions as the Librarian may require
6. I understand that as a student of the University I am required to abide by the Regulations of the University and to conform to its discipline.
7. Inclusion of published outputs under Regulation 6 (9.1.2) shall not constitute plagiarism.
8. I confirm that the thesis has been verified against plagiarism via an approved plagiarism detection application e.g. Turnitin.

* *Please note that it is the responsibility of the candidate to ensure that the correct version of the thesis is submitted.*

Signature of Candidate*:*		Date:	

Submission

Submitted By *(name in capitals):*	Arabella McLaughlin
Signature of Individual Submitting:	
Date Submitted:	

For Completion in the Student Service Centre (SSC)

Received in the SSC by *(name in capitals):*			
Method of Submission *(Handed in to SSC; posted through internal/external mail):*			
E-thesis Submitted **(mandatory for final theses)**			
Signature:		Date:	

Table of Contents

List of Tables

List of Figures

Glossary

ΔG	=	Change in Gibbs free energy (J)
ΔH	=	Change in enthalpy (J)
T	=	Temperature (K)
ΔS	=	Change in entropy (J K^{-1})
pH	=	Concentration of hydrogen ions in an aqueous solution (no units)
pKa	=	Log acid dissociation constant (no units)
$[A-]$	=	Concentration of a conjugate base (M)
$[HA]$	=	Concentration of an undissociated weak acid (M)
S	=	Solubility of the ionised drug (g L^{-1})
S_0	=	Solubility of the un-ionised drug (g L^{-1})
$\gamma\left(\frac{s}{a}\right)$	=	Surface tension of the solid at the solid-air boundary (N m^{-1})
$\gamma\left(\frac{s}{l}\right)$	=	Solid-liquid interfacial tension (N m^{-1})
$\gamma\left(\frac{l}{a}\right)$	=	Surface tension of the liquid-air boundary (N m^{-1})

θ	=	Contact angle between solid and liquid (º)
dc/dt	=	Rate of dissolution (kg s^{-1})
k	=	Dissolution rate constant
Cs	=	Concentration in the diffusion layer (saturated) (kg L^{-1})
Cb	=	Concentration of the solid in the bulk dissolution medium (kg L^{-1})
t	=	Time (s)
A	=	Surface area of the solute particle (m^2)
D	=	Diffusion coefficient (m s^{-1})
d	=	Thickness of the concentration gradient (m)
κ	=	Boltzmann constant ($1.38064852 \times 10^{-23}$ m^2 kg s^{-2} K^{-1})
η	=	Viscosity of solvent (kg m^{-1} s^{-1})
r	=	Radius of the solute molecule (m)
A	=	Absorbance (no units),
ε	=	molar extinction coefficient ($Lmol^{-1}cm^{-1}$)
C	=	concentration ($molL^{-1}$)

l	=	path length (cm)
k	=	rate constant (s^{-1})
Ea	=	Activation energy (J mol^{-1})
R	=	gas constant (8.314 J mol^{-1} K)
T	=	Absolute temperature (K)
A	=	Arrhenius factor (s^{-1})
P/V	=	Power density (W m^{-3})
ρ	=	fluid density (kg m^{-3})
N_s	=	Speed of the stirrer (rps)
D_S	=	Diameter of the stirrer (m)
V_L	=	Volume of liquid in the STV (m^3)
P_O	=	Dimensionless power number of the agitator

List of Publications

McLaughlin, A. M.; Robertson, J.; Ni, X., Material characterisation and parameter effects on bulk solid dissolution rate of paracetamol in a stirred tank vessel using an in situ UV-ATR probe. *International Journal of Engineering Research & Science* **2018,** *4*, 10-20.

McLaughlin, A. M.; Robertson, J.; Ni, X., On the use of a twin screw extruder for continuous solid feeding and dissolution for continuous flow processes. *Organic Process Research & Development* **2018***,* 22**,** 1373-1382.

McLaughlin, A. M.; Robertson, J.; Ni, X., Investigation of dissolution rates of acetylsalicylic acid, benzoic acid, nicotinic acid and paracetamol in a stirred tank vessel and a twin screw extruder. *Submitted to Pharmaceutical Development and Technology* **2019**.

List of Conference Presentations

Oral presentation

McLaughlin, A.; Ni, X. Characterisation of Solid Dosing in work ups: 10th World Congress of Chemical Engineering, Barcelona, Spain, 2017.

Poster presentation

McLaughlin, A.; Robertson J.; Ni, X. An investigation of a twin screw mixer as a continuous solid dosing feed system: JPAG Symposium Continuous Manufacturing, Royal Society of Chemistry, London, 2018.

Poster presentation

McLaughlin, A.; Robertson J.; Ni, X. Characterisation of solid dissolution in work up: 4th Winter Process Chemistry Conference 2016, TIC Building, University of Strathclyde, Glasgow, UK, 2016.

Chapter 1 **Introduction**

Traditionally batch manufacture has been used throughout the production of pharmaceutical materials, from work up to reaction and from isolation to tableting. Although the use of continuous manufacture and crystallisation has been gaining momentum in the pharmaceutical industry (Lee et al., 2015, Plumb, 2005), work up technology and inventory in pharmaceutical manufacture remain batch operations (Dimian et al., 2014). "Charging solids into a tank of solvent and leaving it stirred for hours" is the current method used in industrial work up operations (Towler and Sinnott, 2013, Koganti et al., 2010, Pangarkar et al., 2002) which are too large or inflexible to modify for continuous processing (Baxendale et al., 2015, Page et al., 2015). The majority of work up operations fit into this category, and hence little effort has been devoted to development in this area.

This is reflected in the limited number of academic publications available in this area, with academic researchers largely regarding work up as being a technical problem. As a result, there has generally been a lack of scientific understanding in terms of work up operations (Wood, 2009, Hörmann et al., 2011).

Current methods in continuous crystallisation permit access to crystals with consistent properties. This consistency is necessary to obtain the reliable properties desirable in the pharmaceutical industry. Hence, with increasing interest in the application of continuous crystallisation (Kaialy et al., 2014, Kwon et al., 2014, Ferguson et al., 2012), investigation into continuous work up procedures have been identified as a crucial, unmet need (McWilliams et al., 2018). The development of continuous work up is required to feed solute solid particles and the selected solvent concurrently, accurately and continuously into a plug flow system for unit operations. This requires an understanding of dissolution

kinetics of solids under continuous feed conditions, the dissolution mechanisms and the parameters that affect them.

Dissolution kinetics have been discussed in the literature for many decades although it tends to be fundamental rather than with particular application in mind. Effectively the fundamental of dissolution is known and literature for chemical engineering processes is phenomenological. But there is no bridge between the two which means rationale design of processes is next to impossible. This thesis addresses this very subject.

1.1 Objectives and scope of project

The primary objectives of this PhD project were:

i. to gain scientific understanding of solid dissolution rates in a stationary system of various solvent compositions;
ii. to apply the science learnt in order to establish an efficient and accurate dosing device for continuous flow systems;
iii. to evaluate the flexibility and reliability of the continuous flow system using a range of solid materials.

The scope of this project is to determine the major parameter effects on dissolution rates using paracetamol as the model compound. To set up and test a continuous solid dosing and dissolution system using different grades of paracetamol as the solute. The dissolution rates obtained in the batch system are compared with the continuous system. Further compounds are then studied in both batch and continuous systems to broaden the range of solids dosed.

1.2 Structure of thesis

Following this introduction, the thesis commences in Chapter 2 with a survey of background literature relevant to this work. Beginning with the dissolution kinetics of paracetamol in a batch system in Chapter 3, the effects of temperature, solvent composition, mixing intensity and particle size on dissolution rates in a stirred tank vessel were studied. Following this, Chapter 4 describes the dissolution rates of paracetamol in a continuous system and reports the effect of operational parameters on the rate, including feed rates, barrel temperature, screw speed, and screw configuration. Continuation from this, Chapter 5 deals with the dissolution kinetics of benzoic acid, acetylsalicylic acid and nicotinic acid in both a batch and continuous system. Finally, the overall conclusions from the project are given in Chapter 6 with recommendations for future work.

Chapter 2 **Literature Review**

As stated previously, the overall aims of this project were to develop a continuous solid dosing platform and to evaluate dissolution kinetics in batch and continuous processes. The three key areas of interest in this PhD work are: (i) current batch systems, (ii) solubility, dissolution and dissolution kinetics (iii) continuous processing techniques. The relevant literature relating to each of these topics is reviewed in turn in this chapter.

2.1 Current Batch Systems

2.1.1 Pharmaceutical Manufacture

A pharmaceutical product contains two groups of materials, active ingredients and excipients. The active ingredients are those materials that have a therapeutic effect, whilst the excipients have no therapeutic effect but are necessary to ensure that the final dosage form acts as intended. Typical excipients include lubricants, lactose, starch, sugar and colouring although in practice there are a very large number of excipients in common usage.

Pharmaceutical manufacturing can be broken down into several stages, frequently simplified into two major stages known as primary and secondary. These stages are commonly concludedat different sites and often involve a number of manufacturers. The Primary stage incorporates manufacture of the active pharmaceutical ingredients (APIs), which can be made by either chemical synthesis or biological processing followed by physical manipulation processes such as purification, drying and size reduction. In most cases the API in bulk is then shipped to a Secondary manufacturing site where the formulation of the final product in a bulk form is performedand involves one or more APIs mixed with excipients. These may undergo further physical manipulations such as

drying, size reduction, size enlargement, filtration and sterilisation. The bulk material is then convertedinto the final dosage form. In most cases the final form is a tablet, but may be capsules, a liquid in ampoules, vials, or bottles, creams in tubes or jars, aerosols in canisters or suppositories. Finally, the product undergoes packaging, such as bottles, blister packs or foil wraps.

The research focus of this thesis falls within the remit of Primary manufacture, and in particular, work up. Work up can be defined as the processing steps prior to and intermediately preceeding the main unit operations, specifically reaction synthesis and crystallisation. Generally, there are several work up operations required during the manufacturing stages. The steps involved in work up include any unit operation required to purify the API by means of concentration, extraction and separation, including:

- Solid dosing and dissolution
- Distillation
- Degassing
- Solvent Exchange
- Liquid-Liquid Extraction
- Various separations

As solid dosing and dissolution are the key focus areas of this thesis, the main features of those unit operations are summarised here. To establish a work up system for continuous solid dosing and dissolution, it is essential to understand the principles of batch work ups that are currently used in the pharmaceutical industry.

The introduction of raw materials and intermediates for continuous pharmaceutical manufacturing processes are currently based on batch feed systems, e.g. using stirred tank vessels for dissolution of solid particles (Wood, 2009, Hörmann et al., 2011). It is clear

that a large number of vessels are required in work ups in batch productions, although some of the vessels are flexible and can be used for more than one product and more than one unit operation.

Solids are usually added to a liquid in a stirred tank at atmospheric pressure. In order to allow more accurate control of dissolved solid concentration, mixing of solids and liquids is often carried out as a batch operation (Towler and Sinnott, 2013). Previous work on batch dissolution of scale-up (Koganti et al., 2010), used UV Spectroscopy and HPLC to determine the dissolution concentration; mass transfer coefficients were also employed as the indicator for dissolution in stirred tank reactors (Pangarkar et al., 2002).

Depending on the physical properties of the solids, such as non-wetting (hydrophobic), cohesive or adhesive, dissolution of solids in batch vessels is often a labour intensive and time-consuming operation. Moreover, it is accompanied by common problems involving mass transfer limitation for solids dissolution, non-uniformity of slurry composition on discharge, and nozzles plugged by solids. If solids are cohesive there is potential for agglomeration. For adhesive solids accumulation on the impellers, baffles and supports occur readily. This leads to batch to batch variations on product quality.

For suspension of high bulk density solids, adequate mixing of particles is essential to maintain suspension and prevent particle from resting on the bottom of the vessel. This however leads to overmixing overall, potentially causing foaming in solid-liquid suspensions, reducing dissolution characteristics (Paul et al., 2004). For suspension of low bulk density solids, entrainment is often achieved using a mixer designed to provide downward pulling drag force to offset the upward buoyancy force, leading to incomplete solids wetting, shearing and breaking up of agglomerates (Atiemo-Obeng et al., 2004, Hemrajani and Tatterson, 2004).

The use of static mixers has addressed various mixing issues (Thakur et al., 2003, Ghanem et al., 2014), including solids blending in a fluid phase, the dispersion of additives in a suspension, and solid dispersion by breaking agglomerates in a fluid phase and in pulp and paper processes (Baker, 1991). Adhesive solids in these dispersions can accumulate on the walls and blades inside these mixers. The motivation for the use of these mixers is to achieve a dispersion as the output. There are however still problems in maintaining slurry homogeneity in flow, resulting blockages in valves and nozzles during downstream processing when solids are present. A continuous solid dosing system incorporating complete dissolution would overcome the above issues; this is the focus of this work where a twin screw extruder is investigated as a novel solid dosing and dissolution system.

2.1.2 Solid Dosing

The methods used for solid dosing and liquid delivery of raw materials and intermediates vary greatly between manufacturing processes depending on the quantities used and the hazards associated with the material. Typical solid dosing techniques include drumming booth, glovebox, mass flow meter and manual loading *via* the manway. Accurate dispensing of solid forms can however be problematic depending on the physical properties of the material, e.g. bulk density, particle size, particle shape, adhesion and cohesion of the particles. Agglomeration and compressability can impact the flow of material.

Solids can generally be added manually through the manway of a reactor vessel; drum lifters and other manual handling aids are available to assist during loading operations. Split butterfly valves are used for dosing small volumes of solids directly into the reactor. Such an operation introduces the possibility of contamination of the batch from the environment, while loading activities are taking place in an non-contained area.

Contained areas can address this issue such as discharging solids *via* a loading booth and followed by a chute wash, both to clean the booth and to ensure that the correct quantity of solids has been charged, thereby maintaining reaction stoichiometry. Laminar flow booths for solids loading of low density materials, which have a tendency to back-flow out the hopper, have a reverse jet filter attached to the hopper, which collects particulate material leaving the holding hopper and returns the material back to the hopper.

Hazardous products are dispensed from a contained area with sufficient extraction, e.g. a glove box. Access is restrictive for the operator and blockages can occur if the solid is not free flowing. Vibration is often required to assist flow of solids from hoppers, or alternatively the solids are added in small aliquots to prevent blockages in the chute between the glove box and the reaction vessel. When there are sixteen 25 kg bags of raw material to be loaded into the glove box this is a time consuming and physically demanding task. In addition, solids discharge dust extract filters are required in the solids loading area to prevent the release of solid particulates during charging operations.

The time taken for addition of raw materials and the temperature control during these additions is critical. The addition of raw materials for reaction often involves an exotherm. Slow addition rates are often required to control the temperature, as high temperature may lead to elevated impurity levels. However lower temperatures will slow the reaction, leading to formation of impurities *via* side reactions. This is accompanied by lower reaction yields. Up to ten solid raw materials can be required for each pharmaceutical process. These can be prepared before the start of batch production and can then be dispensed gravimetrically in a designated dispensing area. Well-ventilated dispensing areas are required for preparing solid batching materials using a gravimetric (weighing) component.

Continuous and consistent feeds of solid materials are challenging and require an accurate account of both solid and liquid ratios at any given time. The properties of particulate solids in bulk include their shapes, sizes and size distribution. Each individual batch of solid material will contain a varying degree of non-uniform particle shapes and sizes which are often altered due to aggregation and attrition during packaging, handling and distribution from the supplier. This batch to batch variation results in the dispensing and metering of dry powders being much more complex than those of liquids, as such general theories of flow cannot be applied to diverse powders (Alsenz, 2011).

Currently there are several methods for dispensing solids in batch manufacturing which have a gravimetric component, while solid is transported by different mechanisms e.g. volumetric, Archimedes screw, tapping, shaking (Yang and Evans, 2007). These feeders dose bulk material or sequentially feed multiple ingredients into a weigh hopper mounted on load cells (load cell is a device that converts a force (mass multiplied by gravity) to an electrical signal). This allows the increase in the weight of the collection hopper to be measured with high accuracy. Once all ingredients have been delivered, the batch is complete, and the mixture is delivered to the process thereafter.

For current batch solid dosing systems, it is often enough to totalise material throughput without the requirement to control flow rate. To this end a weigh meter can be used. A weigh meter merely totalises material throughput whereas a weigh feeder controls flow rate. A feeder can perform all the functions of a meter, but a meter can't do what a feeder does. For a continuous solid dosing system, the flow rate must be controlled therefore a weigh feeder is required.

Solid dosing weigh feeders are commonly used in the food industry for a range of free-flowing or sluggish bulk solids, granules and powders. Customised programmable controls provide doses or continuous delivery by volumetric or gravimetric feeders (Ricciardi and Laidlaw, 1995). Metered or controlled flow of solid from a storage

container to a destination vessel gives real time feedback on the amount of material that is transferred. This is done by monitoring the increase in weight in the destination vessel or weight-loss in the storage container as a function of time (Thiry et al., 2015). However periodic refill of hopper feeders can lead to inconsistent and poor feeding performance (Engisch and Muzzio, 2015).

There are many types of feeders available for feeding powder (Todd M. Francis, 2006, Amit Suri, 2009, Briens et al., 2008, Jamaleddine et al., 2015, Woodruff et al., 2012), all of which have advantages and limitations depending on the bulk properties of the material being dispensed. For example, vibratory feeders (see Figure 2.1) are well suited for better dosing of a variety of powders provided that material is allowed to flow freely out from the conical hopper (Chen et al., 2012, Gabriel I. Tardos, 1996). An electromagnetic drive creates high frequency, low amplitude vibration. The tray is suspended above the base using leaf springs, a magnet is attached to the tray and an electromagnetic coil attached to the base. The magnet is attracted to the coil when activated and released when the coil is deactivated causing spring forward motion using tension in the leaf springs. This vibration results in the material hopping forward along the tray. The addition of a spinning wheel to a vibratory feeder can break apart loose particle aggregates of powder as the powder is sheared by the wheel. Spinning wheel feeders (see Figure 2.2) also reduce the particle size distribution after de-aggregation. Entrainment feeders (see Figure 2.3) use a rotating plunger to transfer material but they have the same difficulties as fluidisation feeders since they do not provide a means of breaking down loosely formed particle aggregates, hence do not provide a steady feed of powder. Spinning wheel and entrainment feeders both require a carrier gas flow and it is the flow rate of this gas that limits residence time in the reactor. The gas flow is generally higher for the entrainment feeder than for a fluidisation feeder.

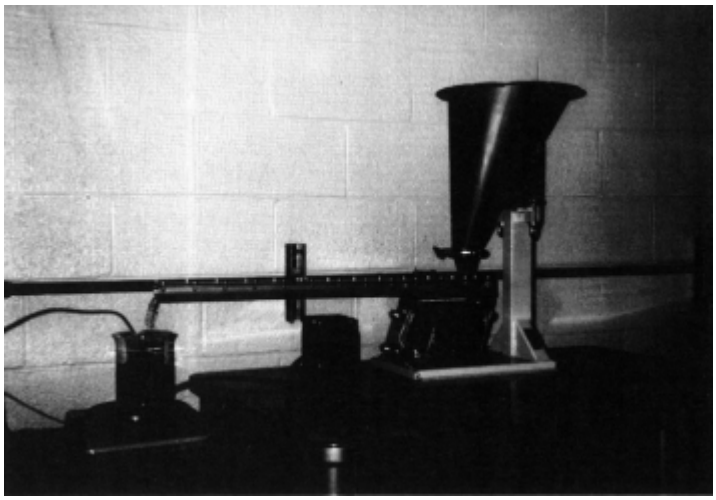

Figure 2.1 Experimental set up of vibratory feeder (Tardos and Lu, 1996)

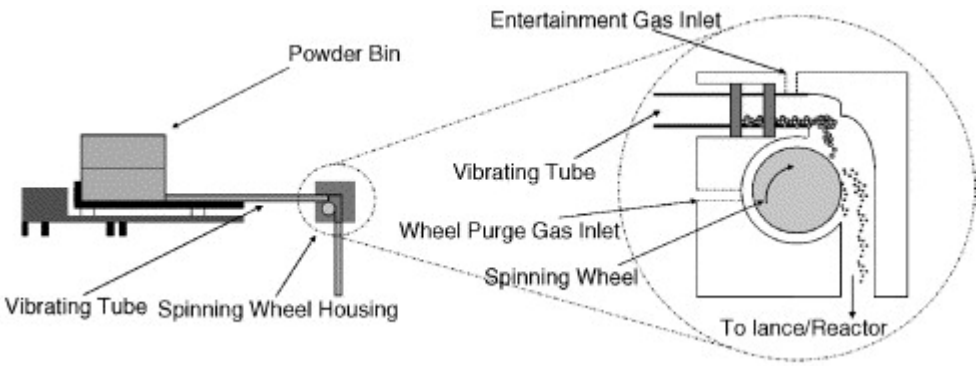

Figure 2.2 Spinning wheel feeder design and spinning wheel feeder housing (Todd M. Francis, 2006)

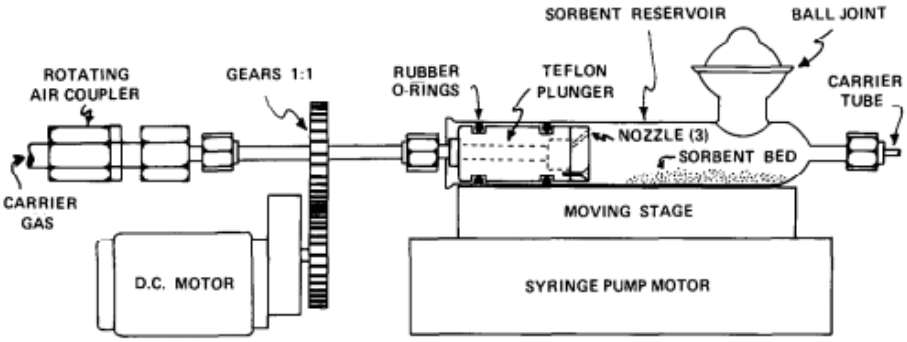

Figure 2.3 The entrainment feeder uses a rotating plunger that travels the length of the sorbent bed, blowing particles into the carrier tube (Gullett and Gillis, 1987)

Piston feeders (see Figure 2.4) use a piston to maintain the powder bed at a constant level relative to the exit tube such that the feed rate becomes equal to the characteristics of the powder bed and the carrier gas flow. However, piston feeders also cannot break apart loose particle aggregates. Some advantages of using a rotary valve feeder (see Figure 2.5) would be the low cost and the ability to feed at high and low flow rates (Gundogdu, 2004). Rotary valves are gravity fed and can be connected to a flow meter. The combined output from the load cells in the flow meter determine the mass flow rate which is then used for corrective adjustments to the rotary valve speed. Difficulties however, include no reliable means to disperse loose particle aggregates which creates inconsistencies in fill volumes in the rotary valve. Screw feeders (see Figure 2.6) using a selection of available screw designs, are commonly used to dispense solids and can easily be modified to fit the type of powder and process involved (Jia et al., 2009).

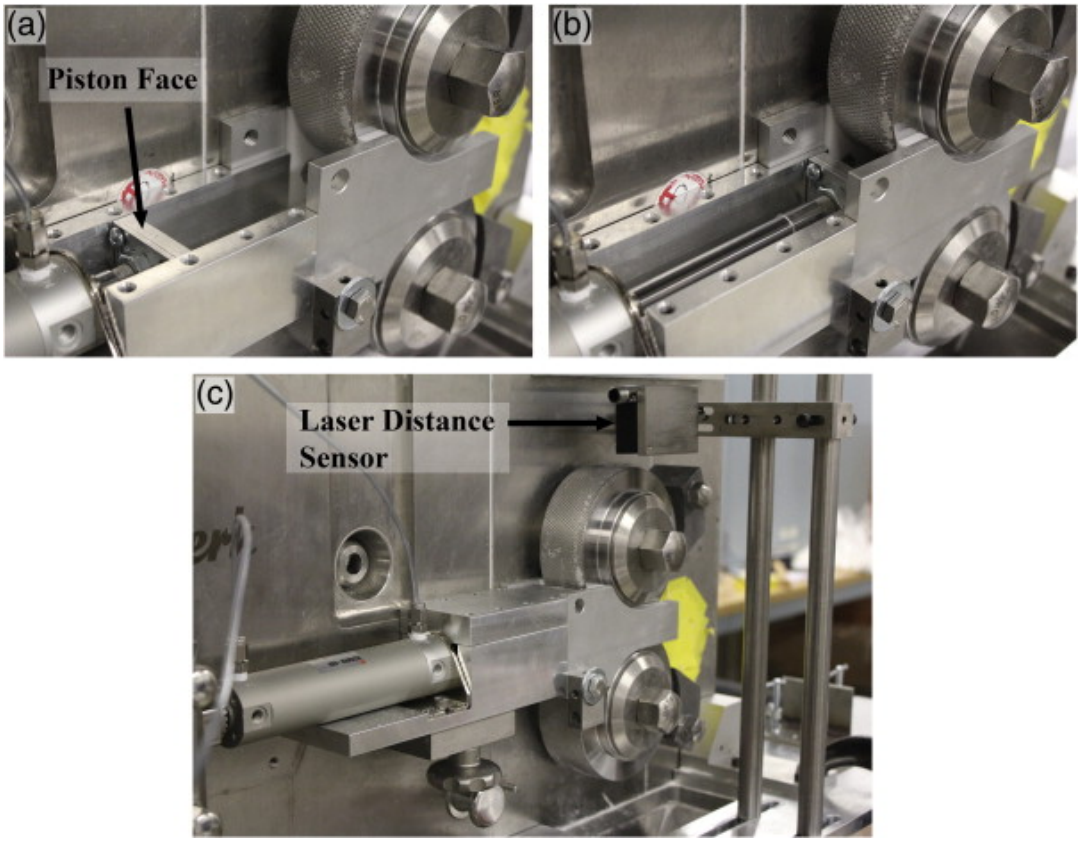

Figure 2.4 Photographs of the WP120-40V, showing (a) the (empty) piston feeder with the piston face at its initial position, (b) the piston feeder with the piston face at its full stroke, and (c) the fully assembled piston feeder (Muliadi et al., 2013)

Figure 2.5 Rotary valve utilised in feeding solid materials

Figure 2.6 . K-Tron KT35 feeder with Schenck Accurate AccPro II catch scale (William E. Engisch, 2012)

Continuous solids feeders fall into two broad categories: gravimetric feeders, which measure and control feed rate by weighing the material; and volumetric feeders which control the volume of material fed per unit time. Gravimetric (measurement by weight) solids feeders have been around for a long time and volumetric feeders for even longer, but only in the last 30 years could most feeders be called truly reliable. The early mechanical, pneumatic and analogue – electrical feeders were temperamental and required close attention to maintain even crude control. Today, more is known about solids flow, and advanced mechanical and electrical components have made feeders highly accurate and reliable (Thiry et al., 2015). Within each category the chief aim is to deliver a certain weight of solid material continuously per unit time. Thus, measuring

accuracy on a weight basis is the same for gravimetric and volumetric feeders. What is different for volumetric feeders is that the overall accuracy depends not only on feeder performance but also on variations in the density of the solid material.

Thus, volumetric feeders can achieve their maximum accuracy only when bulk density is very nearly constant. This is a rare condition, because a material's density is affected by load, moisture content, particle size and other factors. Accuracy in volumetric feeders is also affected by material build-up and flowability, so even when bulk density does not vary, a volumetric feeder is likely to be less accurate than a gravimetric feeder. In loss in weight, the entire feeder, hopper and material are weighed. Loss in weight depends on a reliable weight signal to control material flow. Loss in weight in unit time dw/dt gives the real feeding amount. The difference between the default set feeding amount and the real feeding amount is controlled by a microprocessor. Required adjustments are made and the feeding reaches the set value (see Figure 2.7). Loss in weight feeders provide high accuracy for batch or continuous processes, when dosing pharmaceutical bulk solids (Nowak, 2013, William E. Engisch, 2012). Loss in weight feeders operating in continuous mode have a load cell with feedback control. This allows monitoring and control of the feed rate, and minimises flow variability caused by bulk density changes associated with the emptying of the feeding hopper (Engisch and Muzzio, 2015). The loss in weight gravimetric feeders can be used to continuously dose solids into flow processes, as these are accurate even at micro scale volumes. Each raw material could be dosed separately from its own feeders without the requirement for changeover or cleaning between dosing.

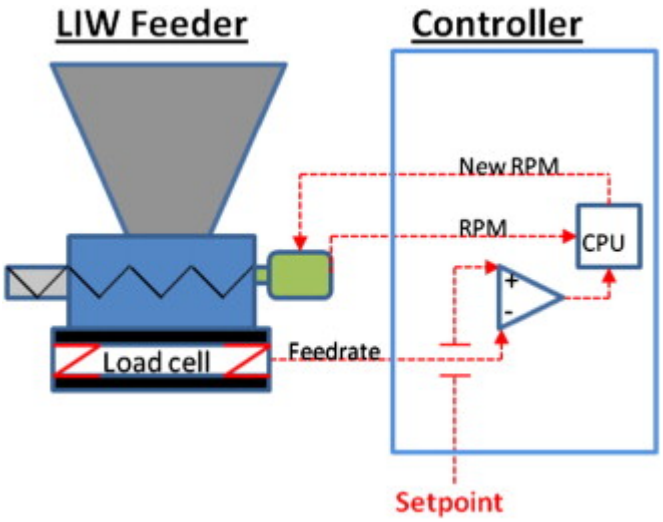

Figure 2.7 Loss-in-weight feeder characterisation setup for monitoring feedrate and determining steady state performance. The catch scale is used to collect gain-in-weight data from the outlet of the feeder (Engisch and Muzzio, 2012).

Micro feeding (see Figure 2.8) is defined as the ability to feed powders consistently and in a dynamic method to a process, at rates as low as 20 g hr^{-1} (5.56 x 10^{-6} kg s^{-1} feed rate). It is well known that pharmaceutical processes seek a more precise dispensing due to the strict regulatory requirements on dose uniformity. With this regard, a micro dosing system for fine powder in the milligram range using a vibrating capillary was developed (Chen et al., 2012). The piezo actuator provides short strokes of motion and force with high frequency and fast response time. Setting the frequency and amplitude of the vibration controls the flow rate.

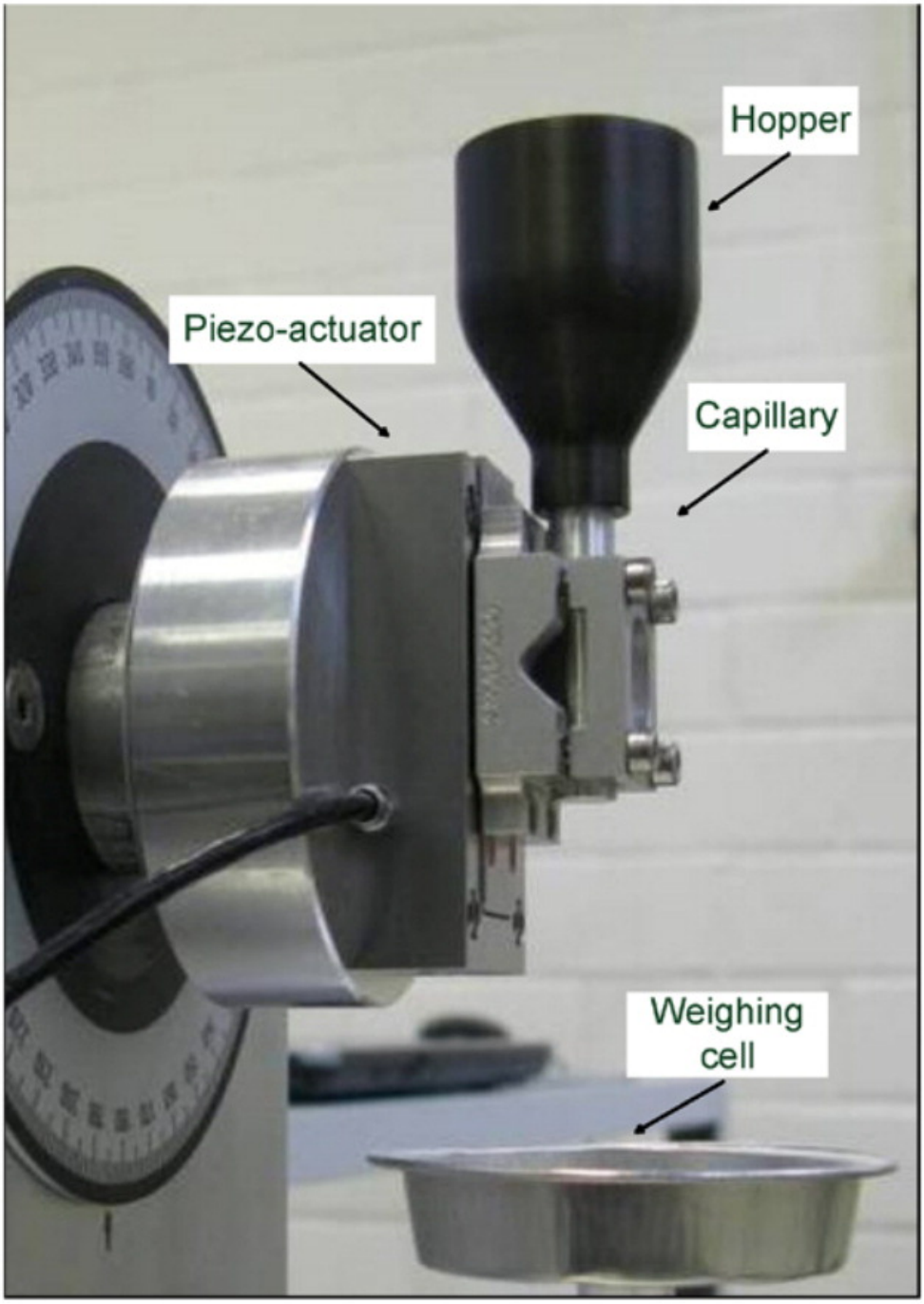

Figure 2.8 Micro feeding system based on a vibrating capillary (Chen et al., 2012)

Improvements on a particle feeder for experiments requiring low feed rates have been achieved by modifying the centre piece by sweeping the particles upward into a concentric tube which also serves as the piston support (Tang and Chen, 1999). The use of ultrasonic micro feeding (see Figure 2.9) highlighted the inaccuracies obtained in feed rates when operations were frequently stopped and restarted (Lu et al., 2007). Micro feeding with different ultrasonic nozzle designs (Lu et al., 2009) concluded that plugs and bubbles often appeared alternately at low voltages; this behaviour prevents quantitative dosing.

In continuous manufacturing, it is the absolute requirement to feed powders consistently and accurately into subsequent unit operations. At typical small flowrates of pharmaceutical processes (10–100 kg hr^{-1}), inaccuracies in dispensed ingredient flowrates, driven typically by powder cohesion or by electrostatics, can cause large variability in the composition of flowing powder blends. Laboratory development trials either require even smaller machines than those currently available or alternatively use can be made of current equipment if operated intermittently rather than continuously. However, the associated start up and shut down problems become more pertinent. This scale down issue needs to be addressed if progress is to be made in this area.

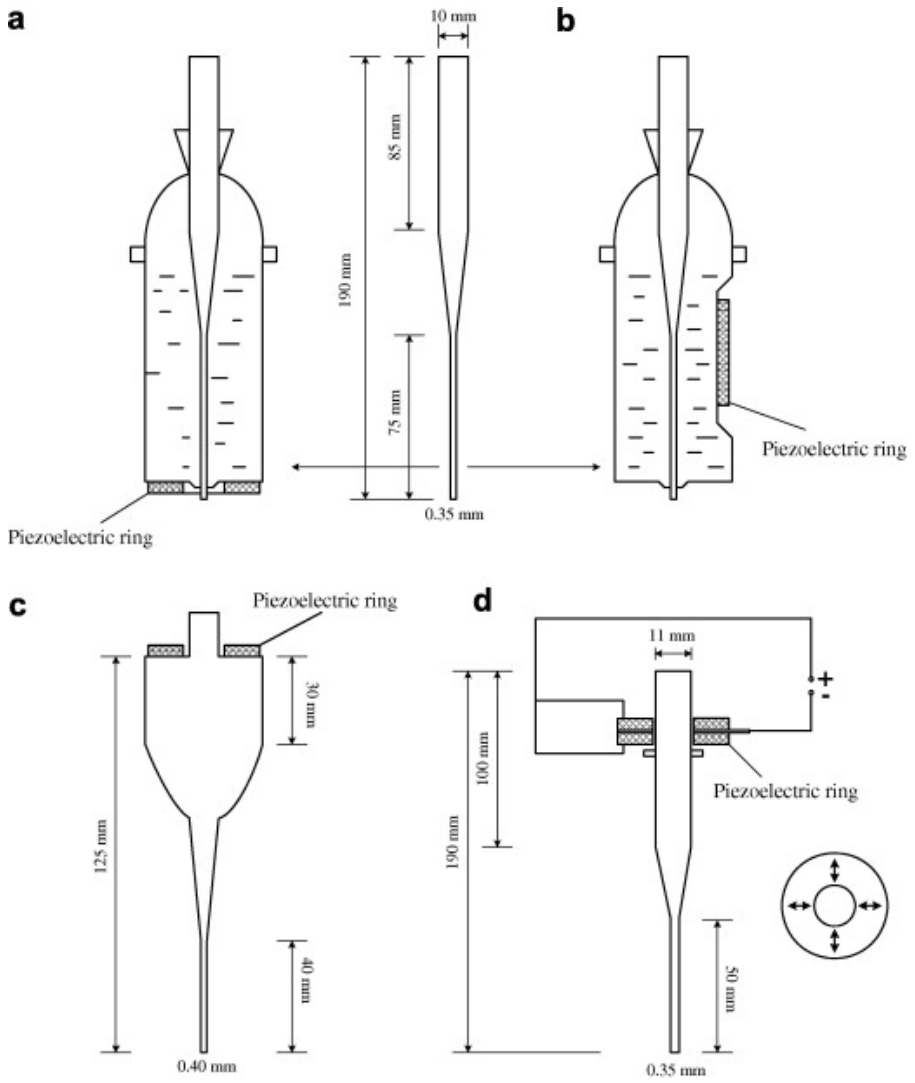

Figure 2.9 The four nozzle designs used in ultrasonic micro feeding systems (a Type I; b Type II; c, Type III; d, Type IV) (Lu et al., 2009)

There has been a continued focus towards developing an understanding of the influence of materials and processes on product performance within pharmaceutical research (Davé et al., 2013, Juha A. Kurkela, 2008). A system for solid materials to be continuously transported into vessels under high pressure (Nuennerich et al., 2008) has been integrated in a pilot plant for industrial dyeing of polyester fibres (Eggers, 2002). Powder material, which is stored in a small container, can quasi-continuously be

transported from ambient pressure (storage container) into a supercritical fluid (inside the high pressure vessel). This is done by small transport-holes in a shaft, which is horizontally moved through a vertically mounted pressure vessel. The main advantages of this process are a homogeneous loading of the super critical carbon dioxide, a better control of the dyeing process, reduced inventory of raw materials due to a better utilisation of the solid material, and, as a result of these effects, shorter process times.

In summary, critical components in any system handling bulk solids are the feeders. Numerous designs are available to accommodate the diverse properties of materials handled in the pharmaceutical industry. The general practice is to use a screw, vibration or belt feeder combined with a loss by weight device and an appropriate controller (Gabriel I. Tardos, 1996). However, it would be challenging to select a type and capacity without first thoroughly defining the flow characteristics of the material. The behaviour of the solid must be determined as it passes into a hopper, rests under a weight of overlying material, flows under varying pressures through the hopper, and expands into the feeding device. Quantitative methods for predicting flow behaviour focus on material properties that affect flow and can determine flowability, cohesiveness, bulk density, compressibility, deaeration time and permeability of solids using a shear tester (Feeley et al., 1998).

Variations in particle size and shape give rise to a range of flow behaviours which can impact solid dosing. These include granular materials and pellet-shaped plastics which are generally free-flowing materials. They feed under gravity without the need for special design considerations or flow enhancements. Plastic pellets are currently used in the processing of polymer materials in a twin screw extruder.

Poor flowability materials include powders with a smaller particle size than granules. Adhesive powders have a tendency to to bond and adhere to contact surfaces, creating a resistance to flow. While cohesive powders can agglomerate resulting in variations in

output flow from the feeder. These powders are typically associated with a high angle of repose which can impact the fill volume in the hopper during hopper refills. They require flow aids such as internal agitation, air sweeps, or air pads to create movement or external vibration to break up the aggregates formed. Powders with small spherical shaped particles i.e. micronised powders, can easily compact in the feeder and around the screw. These materials are typically associated with a low angle of repose and oftenbehave like a fluid when aerated. Aeration can occur during the loading and feeder filling processes which can often lead to the aerated material in the feeder flooding out. This increases variability in the feeder output. Some powders that are very cohesive may present hindered filling of the screw flights at higher feed rates due to bridging over the screws. This can cause phenomena such as hopper "rat holes" as shown in Figure 2.10, whereby the powder flows only from one side of the hopper, or in extreme cases complete bridging above the screws. Under such conditions no material would enter the screw, thereby stopping the flow. Powder adhering and coating the screws can also change the effective flight volume and lead to inconsistent flight filling and varying output concentration. Gravimetric feeder performance is mostly affected by how well the material feeds volumetrically. The closer one can fill the flights of the feed screw volumetrically to 100%, the better the feeder (Messmer, 2013).

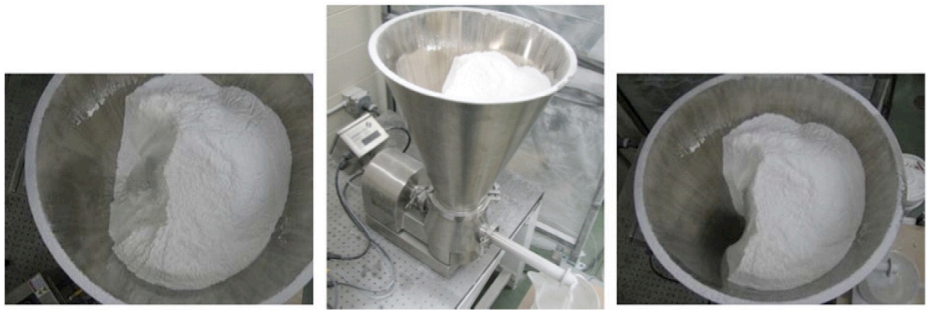

Figure 2.10 "Rat holing" and bridging shown in the hopper of a Schenck Accurate Purefeed feeder feeding a very cohesive powder (William E. Engisch, 2012)

Hygroscopic materials are difficult to dispense as they retain moisture very easily therefore, the material can quickly solidify if exposed to the environment or left in the feeder hopper overnight. These materials have been identified as potential materials to investigate in future work.

Three grades of paracetamol were chosen to determine the flow characteristics of free-flowing, cohesive and aeratable powders. These characteristics were measured using a FT4 Rheometer and are discussed in Chapter 4. A gravimetric loss in weight feeder can assure the accuracy required for continuous feeding, however investigation of the screw type (single spiral or twin concave) and any feeding aids, to agitate the powder and reduce compaction, is necessary in the design of a continuous system. Both a twin screw loss in weight feeder and a single screw loss in weight feeder with flexible wall, were chosen for investigation of continuous solid dosing in this project. These feeder types meet the requirements of accurate continuous feeding for a range of materials (granular, powder and micronised powder) and are capable of operating at small feed rates. Connecting these feeders to a twin screw extruder creates a potential device for continuous solid feeding to downstream pharmaceutical processes, further descriptions are given later.

2.1.3 Liquid Delivery

Solid dissolution requires a liquid phase or a liquid mixture. In current batch processing liquid material can be charged manually into a head flask, using a drum wand, to a visual level indicator marked on the head flask. This manual control can often lead to errors, e.g. an overcharge of material leads to lower quality product as the level of impurities is increased, while an undercharge of material results in lower yields. The drum wand requires regular maintenance and cleaning to prevent blockages. Flow rate and temperature are critical parameters during the addition of material from the head flask. Blocked vent pipe work to a head flask will result in a negative pressure to the head flask and therefore restrict flow to the reactor vessel. Any deviations during this step will lead

to increased impurities which will remain in the final product and can result in batch failures.

Liquids are often added to the reactor vessel via a mass flow meter. These additions can be automated, and the valves set to close after a pre-set volume has been dispensed. Viscoelastic liquids can adhere to the surfaces causing these valves to fail or only partially close, leading to an undercharge or overcharge of material. Liquids are also dispensed from a drumming booth using weigh scales. These scales require regular calibration to ensure that the correct weight is being dispensed.

During solids loading into a dissolution vessel, adequate mixing is required to avoid the 'flour on water effect' where the low bulk density solids float on the surface and do not go into solution. The solids remain on the vessel walls after the solution is transferred into the next vessel. The solids are usually dissolved in a solvent by agitation and heating to reflux. This can take several hours for materials with low solubility in the dissolving solvent. Separate dissolution vessels are often used to prepare the solution several hours before they are required to prevent holding up the process. The material can be added as either a solution or slurry (in portions at low temperature over several hours) to the reaction vessel. This increases the number of vessels required for manufacture. Problems during the dissolution of the starting material include the formation of a paste around the agitator causing it to trip or overheating the batch temperature due to poor control of feed addition rate. An orifice plate, with a small diameter to restrict the flow, can be inserted into the line to help to control the feed rate.

The choice of solvent used for dissolution is dependent upon wettability and solubility. The ability of a solvent to wet a solute is dependent on surface tension. Young's equation (Lee, 2014) (Equation (2.1)) is a method of accounting for and using surface tension values to predict how easily a solute will be wetted and ultimately dissolved.

$$\gamma\left(\frac{s}{a}\right) = \gamma\left(\frac{s}{l}\right) + \gamma\left(\frac{l}{a}\right) cos\theta \qquad (2.1)$$

where $\gamma\left(\frac{s}{a}\right)$ = surface tension of the solid at the solid-air boundary (N m^{-1}), $\gamma\left(\frac{s}{l}\right)$ = solid-liquid interfacial tension (N m^{-1}), $\gamma\left(\frac{l}{a}\right)$ = surface tension of the liquid-air boundary (N m^{-1}), θ = contact angle between solid and liquid (º).

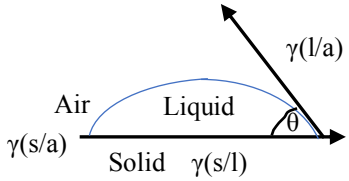

Spontaneous wetting occurs if the contact angle θ is 0º. When the liquid is water, if θ is less than 90º, the substance is considered hydrophilic and ifθ is greater than 90º, the substance is considered hydrophobic. When water is the solvent, a hydrophilic solute is desirable. Aqueous systems were chosen in this study.

The addition of a co-solvent can reduce the surface tension of the solvent. IPA has lower polarity and lower surface tension than water and has been chosen as the solvent mixture, in various water/IPA ratios, for the dissolution studies in this work.

2.2 Solubility, Dissolution, and Dissolution Kinetics

Solubility and dissolution are related, albeit unique, concepts. Solubility is a thermodynamic process which determines the maximum concentration of solute which can dissolve at a given temperature. Whereas dissolution is governed by the rate at which the solute dissolves i.e. the dissolution kinetics.A solute may have poor solubility in a solvent, yet its dissolution rate may be rapid.

2.2.1 Solubility

Solubility of pharmaceuticals is an important parameter during drug development and manufacturing processes. It is often enhanced by increasing the temperature to create a supersaturated solution or by the use of a cosolvent. Measurements of the solubility of a solid in a liquid have been documented in the literature for many decades (Zimmerman, 1952, Baka et al., 2008, Breon and Paruta, 1970). More recent publications have focused on solubility predictions using mathematical modelling developed from experimental data, classical molecular mechanics and quantum mechanical techniques (Abolghasem Jouyban, 2008, Matsuda et al., 2015, Paus and Ji, 2016, Rohani, 2006a, William L. Jorgensen, 2002, Xu et al., 2016). Solubilities of pharmaceutical products are often measured over a temperature span and plotted as van't Hoff Solubility Curves (D.J.W. Grant, 1984). Crystal engineering has been used to improve solubility and dissolution rates of active pharmaceutical ingredients (Blagden, 2007, Ebrahimi et al., 2016, Huang et al., 2013). For example, the solubility of paracetamol in various solvent systems is well documented in the literature (Rohani, 2006a, Rasmuson, 1999, Janicki et al., 2001, Ribeiro et al., 2012, Rohani, 2006b).

There are several methods of determining solubility measurements experimentally, by heating a suspension of solid and solvent until dissolution has completed (clear point). A solubility curve can be plotted using the temperature and concentration data. The most common method is to sample a saturated solution at a known temperature, and then analyse for the solute either gravimetrically or using spectroscopy (Horst, 2016). The isothermal solubility measurement method (Myerson, 2002) allows for an extended time for the solution to reach equilibrium, then to sample and weigh the residue and to determine the concentration of a dissolved compound. This is an accurate but time consuming method and requires a lot of material.

The supersolubility can be determined by cooling a solution and detecting the first appearance of solid (cloud point). This can be done visually or using optical instruments to detect turbidity (Barrett and Glennon, 2002). The temperature difference between the clear point and the cloud point is known as the Meta Stable Zone Width (MSZW). Turbidity measurements are often used to determine the MSZW of pharmaceutical compounds (Parsons et al., 2003), which provides useful information to aid the development of the crystallisation process for that compound. A semi-automated device for solubility measurements in solution volumes as low as 1ml has been developed for pharmaceutical applications (Yongjin Yi, 2005).

The solubility of paracetamol in water- propan-2-ol mixtures was evaluated by Hojjati and Rohani (Rohani, 2006) using an ATR-FTIR method, in comparison with measurements taken gravimetrically. The results were in good agreement with each other, and comparable to the results obtained by (Fujiwara et al., 2002). Granberg and Rasmuson used a gravimetric technique to determine the solubilities of paracetamol in 26 different pure solvents including propan-2-ol and water over the temperature range from -5 to +30°C (Granberg and Rasmuson, 1999). Fujiwara et al. measured the solubility of paracetamol in water from 20 to 50°C using in situ ATR-FTIR probe and chemometric techniques (Fujiwara et al., 2002). The agreement among the aforementioned solubilities was good. The solubility data for paracetamol in water- propan-2-ol mixtures (Rohani, 2006) is used in this thesis and verified using a gravimetric technique.

The thermodynamics of solubility

Solubility thermodynamics are considered from the equilibrium of chemical potentials. To be thermodynamically favourable, the change in Gibbs free energy, G (energy to do work) must be negative, i.e. large values for entropy (S) means large -ve G. It is desirable to have both -ve enthalpy (H) and big +ve S values, but both must be large, as shown in Equation (2.2) (Wang et al., 2011). This equation can be used to determine the

spontaneity of the process. Processes with ΔG values < 0 are spontanaeous, whereas ΔG values = 0 indicate this system is in equilibrium and ΔG > 0 show that the process is not spontaneous. Even though a thermodynamically favourable change can occur, there is no indication of how long it will take to occur.

$$\Delta G = \Delta H - T\Delta S \qquad (2.2)$$

where ΔG = change in Gibbs free energy (J), ΔH = change in enthalpy (J), T = temperature (K), ΔS = change in entropy (J K^{-1}).

ΔG depends only on the conditions describing the system and not how the changes occur. Entropy is a measure of the degree of disorder i.e. the number of states that the system can take on and the increasing number of positions available to the molecules when the dissolution process progresses from one state to another. The effect of temperature on solubility impacts the entropy of the system and is dependent upon whether the dissolution process is endothermic or exothermic in nature, as well as on the ambient environmental conditions. If the ambient temperature is relatively high, exothermic dissolution processes will be inhibited, while endothermic dissolution processes will be improved. As a result, high ambient temperatures will increase the solubility of solutes with endothermic dissolution processes but decrease the solubility of those with exothermic processes.

The pH of the solvent can greatly impact the solubility of ionisable solutes according to the Henderson-Hasselbalch equation (Sinclair et al., 1968) (see Equation (2.3)). The lower the pH, the higher the concentration of hydrogen ions, [H+]. The lower the pKa, the stronger the acid and the greater its ability to donate protons.

$$pH = pKa + log\ (\frac{[A-]}{[HA]}) \qquad (2.3)$$

where pH = Concentration of hydrogen ions in an aqueous solution (no units), pKa =Acid dissociation constant, $[A-]$ = Concentration of a conjugate base (M), $[HA]$= Concentration of an undissociated weak acid (M)(Po and Senozan, 2001).

Acidic drugs are less soluble in acidic solutions due to more of the drug in the un-ionised form, which is less able to interact with the solvent than the ionised form. The dependence of the solubility of an acidic drug on ionisation of the drug, in acidic conditions, is represented by Equation (2.4). The solubility of basic drugs in relation to pH is represented by Equation (2.5).

$$pH - pKa = log\left(\frac{S-S0}{S0}\right) \quad (2.4)$$

where S= solubility of the ionised drug (g L^{-1}), $S0$= solubility of the un-ionised drug (g L^{-1})

$$pH - pKa = log\left(\frac{S}{S0-S}\right) \quad (2.5)$$

For pH values above the isoelectric point (pI), i.e. the pH at which a molecule carries no net electrical charge, the acidic Equation (2.4) is used, and at pH values below the pI, the basic Equation (2.5) is used. The pI value can affect the solubility of a molecule at a given pH in that molecules have minimum solubility in water or salt solutions at the pH that corresponds to their pI and often precipitate out of solution.

2.2.2 Dissolution and Dissolution Kinetics

Dissolution is the process of a solute dispersing in a solvent, forming a chemically and physically homogeneous dispersion called a solution. There are two types of dissolution

within the solid-in-liquid solutions. In the first type of dissolution, the solution's phase contains the same solute chemical entity as is found in the original solid phase. Upon removal of the solvent, the solute can be recovered unaltered by the dissolution process, e.g. dissolution of sucrose in water (Figure 2.11) (www.pharmpress.com).

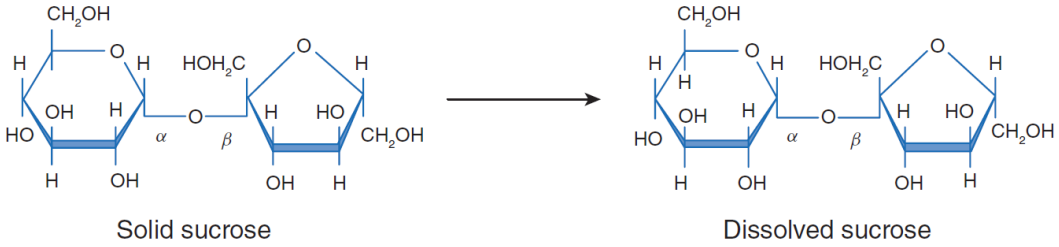

Figure 2.11 Dissolution where the solute remains the same chemical entity (www.pharmpress.com)

For the second type of dissolution, the original solute is neither recoverable nor completely recoverable. The resulting solution contains a compound that is different from that of the original solid phase. This change is generally due to some chemical reaction between the solute and solvent, e.g. dissolution of acetylsalicylic acid (aspirin) in water (Figure 2.12). While in solution, some of the acetylsalicylic acid hydrolyses: forming salicylic acid and acetic acid. When water is removed, some of the original acetylsalicylic acid may be recovered, so are salicylic acid and acetic acid. Here, in order for dissolution to occur, the solute was required to ionise, and the solvent was then required to exert enough influence on the ions to overcome their cohesive forces (www.pharmpress.com).

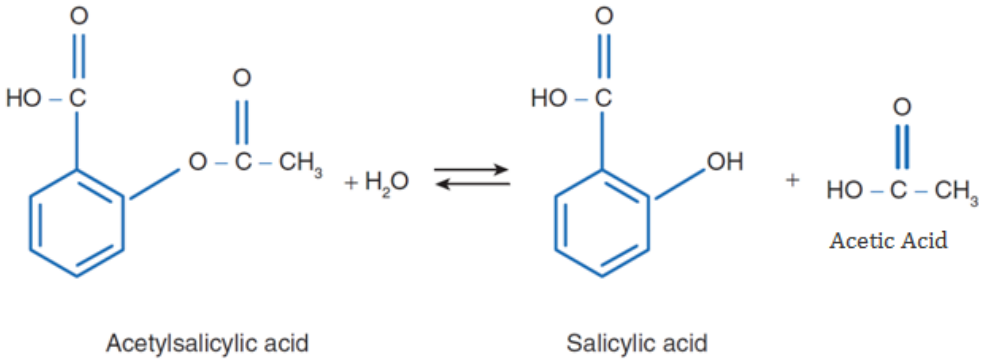

Figure 2.12 Dissolution where the solute chemical entity changes upon dissolution (www.pharmpress.com)

Dissolution of a solid in a liquid, e.g. tablet or capsule dissolution (Figure 2.13) (www.pharmpress.com), often involves three steps (Mangin et al., 2006): disintegration, de-aggregation and dissolution. The most important step of dissolution is the movement of fine particles into solution. The process of fine particle dissolution follows three steps: wetting, immersion and diffusion. The initial step of wetting is the spreading of the solvent over the solute. Wetting of the solute by the solvent can be hindered by air pockets that are trapped in the powder, which slows the initial ability of the powder to contact the solvent. Spreading of a liquid on a solid is favoured when forces between different molecules exceed those between similar molecules. The ability of a solvent to wet a solute is dependent on surface tension (see Equation (2.1)).

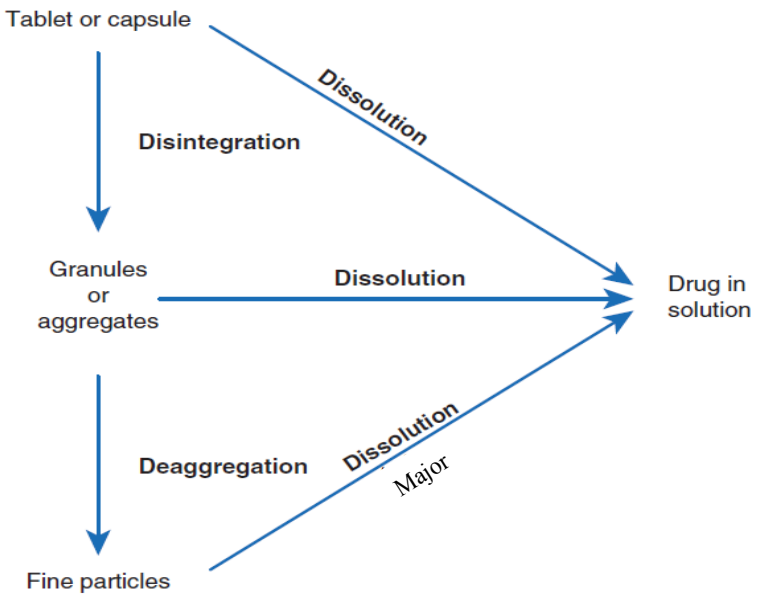

Figure 2.13 The dissolution process (www.pharmpress.com)

Immersional wetting, which is the immersion of the solute in the solvent, is the subsequent step for spreading and is also dictated by the angle the solute surface makes with the air-liquid interface. If the work of adhesion exceeds the work of cohesion, wetting will tend to occur. In order to improve wetting, the surface tension must be reduced. When a solid dissolves, the components pass down a diffusion gradient until the particle completely dissolves and enters the bulk solution. The diffusion gradient is thought of as a 'film' very near the solid surface around the particle. At the particle surface the solution is saturated. Molecules first traverse through the diffusion gradient almost instantaneously, then diffuse into the bulk solution. This diffusion step is slower and often rate limiting. The bulk solution has a concentration that varies with time until the dissolution process has been completed.

Dissolution research began in 1897 when Noyes and Whitney (Whitney, 1897) conducted the first dissolution experiments of two sparingly soluble compounds, benzoic

acid and lead chloride; noticed that the rate of dissolution was proportional to the difference between the instantaneous concentration, C at time t, and the saturation solubility Cs. The authors attributed the mechanism of dissolution to a thin diffusion layer which was formed around the solid surface and through which the molecules diffused to the bulk aqueous phase. Further work on the diffusion layer model was investigated by Higuchi (Higuchi, 1961).

The dissolution rate is a measure of the actual release rate of the compound under the given experimental conditions, and depends on many physical properties, including particle size and shape, crystallinity, and solution composition. It often varies considerably with solid form, the dissociation barrier from solute particle, mixing and diffusion coefficients. Dissolution rate can be expressed using the Noyes-Whitney equation (Whitney, 1897) (see Equation (2.6)).

$$\frac{dc}{dt} = k(Cs - Cb) \tag{2.6}$$

where dc/dt = rate of dissolution (kg s^{-1}), k = rate constant, Cs = concentration in the diffusion layer (saturated) (kg L^{-1}), Cb = concentration of the solid in the bulk dissolution medium (kg L^{-1}).

Integrating Equation (2.6) gives Equation (2.7).

$$\int_{C_1}^{C_2} \frac{dC}{C} = \int_{t_1}^{t_2} k\, dt \tag{2.7}$$

First order kinetics are confirmed using Equation (2.8).

$$\ln\left(\frac{C2}{C1}\right) = kt \tag{2.8}$$

The rate constant of Equation (2.6) can be further expanded leading to:

$$k = A(\frac{D}{d}) \tag{2.9}$$

where A= surface area of the solute particle (m^2), D= diffusion coefficient (m s^{-1}), d = thickness of the concentration gradient (m).

The concentration of the solution is greatest at the particle surface, as the solvent will be saturated with the solute molecules. The time taken for the particle surface to reach saturation is the initial dissolution rate. As the concentration of the bulk solution increases with time, the saturation concentration decreases as does the dissolution rate. This implies that the dissolution rate is directly proportional to the saturated concentration, i.e. the dissolution rate will be given by the solubility of the compound. It has been shown that the relationship between the initial dissolution rate and solubility values support the dissolution rate theory which states that the initial rate of dissolution of a compound is directly proportional to its solubility (Hamlin et al., 1965). Therefore, it is possible to predict the initial rates of dissolution of a broad range of compounds when their solubility values are known.

The total surface area of the solute is also directly proportional to the dissolution rate hence smaller particles with larger total surface area (micronised particles) will dissolve faster than granule. If the solute is ionisable and/or a weak electrolyte, altering the solvent pH can affect the surface/saturation concentration, Cs. Depending on the characteristics of the solute and solvent, this change could either increase or decrease Cs and the concentration gradient, and increase or decrease dissolution rate, respectively. Stirring or agitation during dissolution will decrease the diffusion gradient, d, by removing solute molecules more quickly from the particle surface, increasing the dissolution rate.

The diffusion coefficient, D (m s^{-1}), which is in part related to the solvent viscosity, will decrease with increasing solvent viscosity and with decreasing dissolution rate, dc/dt. D is inversely proportional to viscosity. D is dependent on several parameters and is described by the Stokes-Einstein equation (Mauro and Ellison, 2011) (see Equation (2.10)).

$$D = \left(\frac{\kappa T}{6\pi\eta r}\right) \tag{2.10}$$

where D = diffusion coefficient of the solute in solution (m s^{-1}), κ = Boltzmann constant (1.38064852 × 10^{-23} m^2 kg s^{-2} K^{-1}), T = absolute temperature (K), η = viscosity of solvent (kg m^{-1} s^{-1}), r = radius of the solute molecule (m).

According to Fick's second law (see Equation (2.11)) (Fick, 1855), the diffusion occurring in a unit of time, through the diffusion layer, is directly proportional to the concentration difference and inversely proportional to the distance between the between the concentrations, i.e. the thickness of the concentration layer.

$$\frac{dC}{dt} = D\ \frac{d^2C}{dx^2} \tag{2.11}$$

where dC/dt = the dissolution rate (cm^{-3} s^{-1}), D = diffusion coefficient (cm^2 s^{-1}), $\frac{d^2C}{dx^2}$ = the 2nd derivative of the concentration (cm^{-3} cm^{-2}) or (cm^{-5}).

As temperature is directly proportional to the diffusion coefficient, increasing the temperature of the solution will increase the dissolution rate.

Inspection of the Noyes –Whitney and the Stokes-Einstein equations reveals the parameters affecting dissolution rates of solutes in solvents. However, the major

parameters influencing the dissolution rate, in bulk solid dissolution, remain to be determined in order to optimise the design of a continuous dissolution process.

In the 1950s the pharmaceutical sciences used the concept of in vitro dissolution when it became clear that the dissolution rate was the limiting step. This led to the development of the basket-stirred-flask United States Pharmacopeia (USP) Apparatus 1, as an official dissolution test kit for aqueous systems. However, in some cases the liberation of molecules from the surface into water is not ideal, and the dissolution rate will be lower or higher than theoretically calculated. Thus, in order to determine whether a compound behaves as "ideal", a measurement of the intrinsic dissolution rate (IDR) is necessary. The IDR is the dissolution rate when extrinsic factors are held constant for a pure substance. Dissolution is dependent on many factors, both intrinsic and extrinsic. Extrinsic factors include surface area, stirring speed, pH and ionic-strength of the dissolution medium being kept constant, i.e. the surface area of the compound is well defined. Thus, dissolution rate is measured as the release of API from a tablet with a flat and well-defined surface area into an aqueous solution at a given pH value (Shekunov and Montgomery, 2015).

Over the past few decades, the factors affecting the dissolution rates in USP apparatus were studied extensively and the degree of agitation, solubility and the surfaces exposed in the solvent were identified as the important factors in determining dissolution (Eric Garcia, 2002, Eric Garcia, 1999, Hanson, 1991). Solubility and dissolution measurements are necessary requirements to estimate the drugs bioavailability (Korlakunte V.R. Prasad, 2002, Prasad et al., 2002). These dissolution measurements are used in product control to secure the same particle behaviour for different batches (Parojčić et al., 2008).

More recently the focus has been on quantitative solubility history obtained from IDR and dissolution rate measurements, especially as a function of pH, to determine the extent

of regulatory concern about the different solid forms (polymorphs) (Kuminek et al., 2013, Parojčić et al., 2008, Tran et al., 2012, Smirnov and Badelin, 2014, Javadzadeh et al., 2015, Escribà-Gelonch et al., 2017, Hanson, 1991). Studies have also investigated formulations in tablet or capsule form which contain excipients to control the release rate of the API (Shah and Londhe, 2016, Leblond et al., 2016, Berthelsen et al., 2016); for single crystal dissolution (Østergaardjesper et al., 2014), for monitoring the effect of pH on dissolution rate of controlled release tablets (Khan et al., 2016, Ozturk et al., 2015) and for the dissolution rate of pure paracetamol (Lee et al., 2013).

It is clear from Equations (2.6) – (2.11) that many factors affect the dissolution kinetics of a system although temperature was not investigated further for pharmaceutical dissolution as in vitro studies are carried out isothermally at 37 ˚C. The motivation for dissolution studies using pharmaceuticals has been focused on drug release rates to determine the time for the drug to take effect after the patient has taken the dose. There has been, as yet, no motivation to study bulk solid dissolution rates of pharmaceuticals for the purposes of process design.

2.3 Continuous Processing Techniques

Continuous processing and flow chemistry have been commonplace for decades in the petrochemical and bulk chemical industry, as well as for many unit operations in drug formulation. Only recently however has continuous processing technology become a major focus of chemical process development in the pharmaceutical industry (McMullen et al., 2018).

Continuous manufacturing in the pharmaceutical industry has gained significant attractions as it offers potential flexibility, quality and economic advantages over batch operation (Ni, 2006, McGlone et al., 2015, O'Connor and Lee, 2017). The introduction

of flow chemistry enables chemistry that is difficult to scale in batch mode such as electrochemistry and photochemistry (Politano and Oksdath-Mansilla, 2018). Controlled production of polymorphic forms (Agnew et al., 2016, Agnew et al., 2017) and extreme conditions, such as high and low temperatures and pressures, are becoming more accessible. Hazardous chemistry can safely be executed due to the small amount of unstable intermediate generated and the high ratio of surface area to volume allows excellent control of exothermic chemistry (Bernhard et al., 2015). Operational advantages include process intensification, smaller equipment footprint, amenable to automated operation and process analytical technology (PAT), which can lower operating costs and improve reproducibility (Cole and Johnson, 2018). However, the handling of slurries and heterogeneous reactions remain a challenging area for flow chemistry (Hughes, 2018).

Interest towards the development of continuous manufacturing platforms has increased since 2004, when the regulatory authorities (e.g. the US Food and Drug Administration (FDA)) launched a two-year initiative to modernise and enhance regulation of pharmaceutical manufacturing and quality. New guidelines were set out in their resulting publication "Pharmaceutical cGMPs for the. 21st Century -- A Risk Based Approach". In this document, the concept of Quality by Design (QbD) was detailed, which emphasises that the quality of a product should be built with an understanding of the product and process.

Substantial research in continuous reaction, crystallisation and filtration have been reported in the past decade (Simon Lawton, 2009,, Ferguson et al., 2013, Salvatore et al., 2013, Bernhard et al., 2015, Besenhard et al., 2017). In contrast, continuous work up, e.g. solid dosing and dissolution, remains a challenging area that has yet to be addressed (McWilliams et al., 2018). End-to-end continuous manufacturing is a desirable outcome (O'Connor and Lee, 2017).

The development of an efficient flow process is often the result of designing and implementing a new concept or piece of equipment that is better suited to performing an otherwise challenging task (Baumann and Baxendale, 2015). Continuous processing can generally be conceptualised by several reactions and separation unit operations running simultaneously, with constant flow of materials in and out of each reactor or separator.

Continuous processing can be thought of as the constant pumping of one or more reagent solutions into and out of a reactor. One aspect of continuous processing for which little progress has been made concerns the way in which reagents streams are delivered into the reactors. Early investigations into flow chemistry focused on the delivery of liquid streams. This was achieved using syringe pumps, piston pumps or rotary pumps. Unfortunately syringe pump applications are significantly limited by relatively low working pressures and often needed manual intervention when recharging the syringe. Both piston and rotary pumps suffer from inaccurate flow rates and fouling due to their direct interactions with the chemicals being pumped. In addition, both pumping solutions must be homogeneous. Slurries can cause immense complications. Hence, these technologies cannot provide consistent and accurate control of reagent to flow reactors.

In order to address these issues, flow equipment has instead been based on peristaltic pumps. An early application of such a system for commercial use was reported in 2013 by the Ley group with their continuous synthesis of an important anticancer agent tamoxifen (Murray et al., 2013). The pump design allowed a smooth and consistent delivery of a solution drawn directly out of the supplier's reagent bottle.

In 2014 researchers from Eli Lilly (US) evaluated flow techniques in which peristaltic pumps were used to direct solutions via a static mixer into a plug flow reactor (Polster et al., 2014). However, the reagent solutions were prepared in situ in a batch vessel prior to delivery to the continuous flow reactor.

A continuous solid dosing system incorporating complete dissolution would overcome the above issues. Twin screw extruders have been studied extensively for hot melt extrusion (Crowley et al., 2007, Repka et al., 2007, Patil et al., 2015, Martinez-Marcos et al., 2016) and wet granulation (Vercruysse et al., 2012, Mendez Torrecillas et al., 2017, Dhenge et al., 2011, Dhenge et al., 2012, Saleh et al., 2015, Cartwright et al., 2013). The twin screw extruder has been identified as a potential platform for continuous delivery of solids to a flow process.

2.3.1 Twin screw extruders

Developed in *ca* 1897, single screw extruders are the most widely used extruders, owing largely to their mechanical simplicity (H.A.Cushman, 1897). The single screw extruder consists of one continuously rotating screw in a barrel (see Figure 2.14). It is known to result in good quality molten material (melt) and generates a stable high pressure across the screw ensuring consistent output. Different operations can be performed in single screw extruders such as feeding of raw materials, conveying, melting, devolatilising, pumping and shaping. Mixing can also be accomplished for less demanding applications.

The twin screw extruder (see Figure 2.15) has two agitator assemblies mounted on parallel shafts (see Figure 2.16). The use of two screws permits different types of configurations and can thus vary conditions across the zones of the extruder. The screws can either be co-rotating (same direction) or counter-rotating (opposite direction) and can further be classified as fully intermeshing or non-intermeshing. The former is the most popular because the design incorporates a self-cleaning feature thereby, not only reducing the non-motion but also prevents the localised overheating of the raw materials with the extruder. Therefore, the raw material does not rotate along the screw or adhere to the "first in/first out" principle of the extruder. In comparison to the fully intermeshing, the non-intermeshing is less popular in the mixing application due to its weaker screw interactions and lower self-cleaning capability. These types of screws are often used to

process highly viscous materials and for the removal of large amounts of volatile substances.

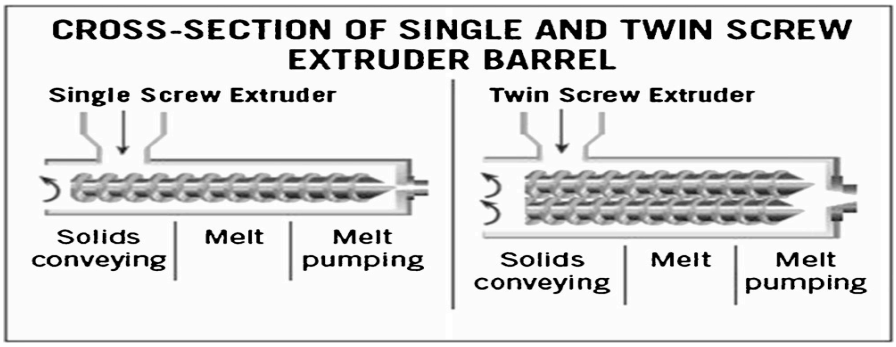

Figure 2.14 Cross-section of single- and twin-screw extruders (Patil et al., 2015)

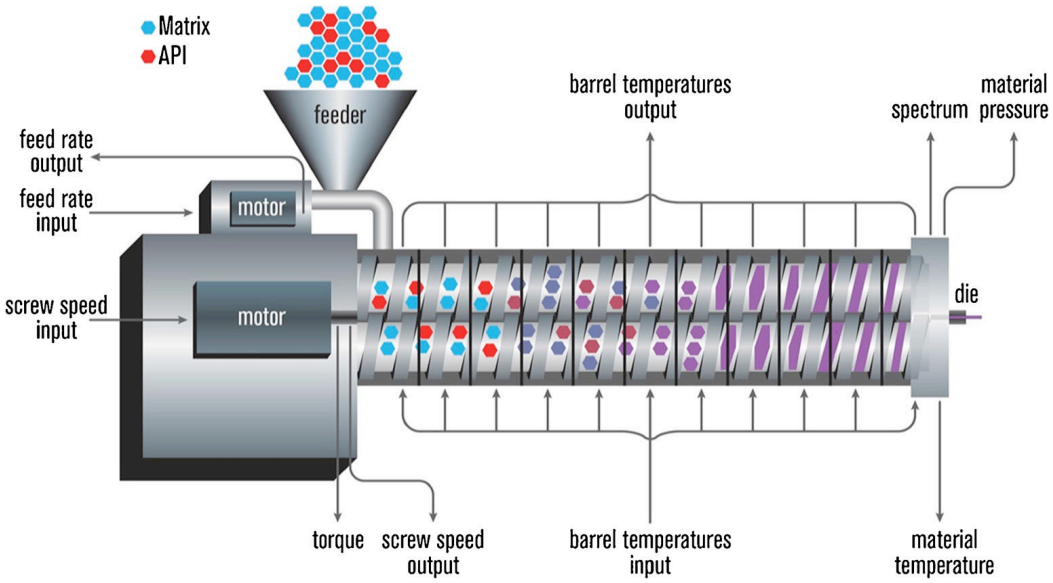

Figure 2.15 Schematic of a typical extruder system for API manufacture (Patil et al., 2015)

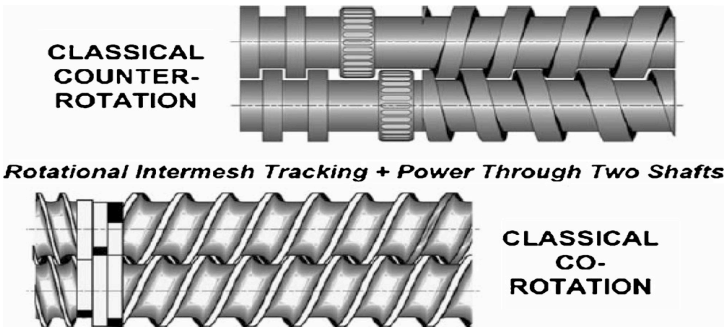

Figure 2.16 Classical intermeshing co-rotating and counter-rotating screws (Patil et al., 2015)

The twin screw extruder can be operated in two modes: as a hot melt extruder at high temperatures, and as a twin screw granulator with both solid and liquid inputs. Hot melt extrusion (HME) is the process of applying heat and pressure to melt a polymer, pumping it along a rotating screw and forcing it though an orifice in a continuous process (Crowley et al., 2007). HME is a well-known and developed process used to produce polymer products of uniform shape and density. Despite its widespread use in both the food and plastic industries (Harold F. Giles Jr, 2004), monitoring of the process and product quality requires adaptation to the specific requirements of the pharmaceutical industry (Maniruzzaman et al., 2012). For example, the materials used in the production of plastic or food products are usually less valuable and/or sensitive than pharmaceutical products. In addition, the physicochemical properties of pharmaceutical constituents may not require the same considerations as those processed in other industries (i.e., water solubility, molecular weight, polar surface area, and partition coefficient). As a continuous process, the starting materials and processing parameters have important roles in controlling the quality of the hot-melt extrudates (Pudlas et al., 2015, Aho et al., 2015).

Over the last thirty years, HME has emerged as a promising cost-effective technology for the pharmaceutical industry (Goertz et al., 1992, A. Forster, 2001) and has been used to manufacture medical devices, orally administered tablets/capsules, transdermal patches, for the production of extrudates with sustained-release properties (Islam et al.,

2014, Maniruzzaman et al., 2016) and more recently to enhance the solubility of poorly soluble drugs (Andrews and Jones, 2014, Moradiya et al., 2014a, Moradiya et al., 2014b). The advantages of this process are that it has high throughput and relatively few processing steps compared with more conventional pharmaceutical processing technologies, and are both solvent free and potentially continuous (Repka et al., 2007). Currently, HME is widely used in the production of solid dispersions and controlled release formulations (Shibata et al., 2009, Kouichi Nakamichi, 2002, Stankovic et al., 2015).

The twin screw extruder has been used to dispense solids during secondary processing of APIs (Patil et al., 2015), because they continuously convert feed material to the finished form. Various dosage forms, such as pellets, tablets and mucoadhesive films for transmucosal products, can be easily prepared from hot-melt extrudates (Patil et al., 2015). However, the potential for HME applications in pharmaceutical research and development has not yet been fully realised, mainly owing to the complexity of HME design and the non-Newtonian behaviour of the extruded materials (J.A. Covas, 2008). This makes it somewhat difficult to predict the behaviour of materials processed by HME using mathematical modelling (Ponomarev et al., 2012).

The twin screw granulator (TSG) has recently become an equipment of choice for the continuous wet granulation in the pharmaceutical industry (Saleh et al., 2015, Cartwright et al., 2013). Although this process utilises both solid and liquid dosing it does not meet the desired outcome of this work to achieve full dissolution into a solution.

Suitable equipment in Secondary Manufacturing is too large to be used for Primary Manufacturing. The scale of operation for this project is 1-10 kg per day, and thus modification to an existing twin screw extruder is required. The twin screw extruder operating at lower temperatures than currently used in HME or TSG mode facilitates the use of volatile solvents for dissolution. This system has been designed for use as a

continuous feed system as it incorporates variable solid and liquid feed rates for a range of output flows, variable temperature zones and configurable mixing zones to enhance dissolution. The current syringe pump used for TSG was replaced with a peristaltic pump (Watson Marlow, Falmouth UK) to enable higher liquid flow rates without the necessity to refill the syringe. This allowed a liquid volume of two litres (in a glass duran bottle) to be dispensed continuously. The duran bottle was immersed in a water bath and the liquid heated to temperature. Two loss-in-weight feeders were connected to the system, a labscale feeder with concave twin screws for low feed rates and a universal flexwall higher throughput feeder with a single spiral screw attachment suitable for low bulk density powders. This enables a broad range of raw materials to be dosed. A bespoke end piece was 3D printed and connected to the output end of the barrel. Tubing was connected to this end piece to direct the output flow into a collection vessel. Further design considerations included enabling the measurement of dissolution rate kinetics. This requires the implementation of in-line probes in the exit flow tubing, to monitor the concentration and temperature of the output solution and a measurement of the time taken to dissolution.

2.3.2 Process Analytical Technology (PAT)

PAT probes can be used to give real time feedback during manufacturing. PAT tools such as in-line near infrared red (NIR) probes have been implemented during extrusion processing, in line with quality by design (QbD) guidelines, in order to obtain a better understanding of the relationship between processing parameters and the extruded formulations (Islam et al., 2015, Wahl et al., 2013). Various types of PAT probes have been documented in the literature for use during real time analysis including Near Infra-Red Spectroscopy (Hattori and Otsuka, 2012, Hernandez et al., 2016, Cabassi et al., 2015, Fan et al., 2016), Focused Beam Reflectance Measurement (Mitchell et al., 2011, Mitsuko Fujiwara, 2002, Laitinen et al., 2010, Nagy et al., 2008), Fourier Transform Infra-Red Spectroscopy (Timokleia Togkalidou, 2001, Pudlas et al., 2015, Warren et al., 2016,

Calvo et al., 2015, Girard et al., 2013, Filgueiras et al., 2014) and Ultra-Violet Spectroscopy (Thompson et al., 2005), Particle Vision Measurement (Barrett and Glennon, 2002, Kim et al., 2012, Liu and Rasmuson, 2013, Brown and Ni, 2011) and UV Imaging and Raman Spectroscopy (Østergaard et al., 2014, Bumbrah and Sharma, 2015, Simonetti et al., 2016).

The probes chosen for this work were temperature, turbidity and ultraviolet- attenuated total reflectance spectroscopy (UV-ATR). Turbidity is a method of measuring the cloudiness of a solution and is based on the principle of measuring the transmittance of light passing through a solution using a fibre optic signal. The light transmittance reduces as the solution becomes cloudy due to the presence of solids when nucleation commences, for instance. Likewise the light transmittance increases as the solution becomes clear and is free of solids, e.g. during dissolution (Cheng et al., 2010a, Cheng et al., 2010b). Turbidity can effectively be used to interpret the amount of solids suspended in solution and can detect events including dissolution and nucleation (clear point and cloud point), as well as the metastable zone width (MSZW).

UV refers to absorption spectroscopy in the ultraviolet spectral region. In this region of the electromagnetic spectrum, molecules undergo electronic transitions. This technique measures transitions from the ground state to the excited state. Molecules containing π-electrons or non-bonding electrons can absorb the energy in the form of ultraviolet light to excite these electrons to higher anti-bonding molecular orbitals. The more easily excited the electrons, the longer the wavelength of light it can absorb. This type of probe can be used to determine the concentration of the solution (Zhang et al., 2011), and is useful for compounds with chromophores and conjugation. Wavelength range is from 190 nm to 400 nm. Attenuated total reflectance (ATR) is based on the attenuation effect of light when it is internally reflected at an interface between a high refractive index material (an internal reflection element) and an ultraviolet absorbing low refractive index material (the sample). The light penetrates the sample as an evanescent

wave. A beam of ultraviolet light is passed through the ATR crystal in such a way that it reflects at least once off the internal surface in contact with the sample. This reflection forms the evanescent wave which extends into the sample. The penetration depth into the sample is typically between 0.5 and 2 μm, with the exact value being determined by the wavelength of light, the angle of incidence and the indices of refraction for the ATR crystal and the medium being probed. The number of reflections may be varied by varying the angle of incidence. The beam is then collected by a detector as it exits the crystal. ATR probe with sapphire crystal is good for strongly absorbing solutions while a transflectance probe is for weakly absorbing solutions. It is very sensitive and has short measurement times but gives rise to broad spectral bands. Data analysis requires univariate or multivariate calibration. A multivariate model enables estimation of the proportion of each individual component (Hu et al., 2016). A univariate model allows quick and easy estimation of the concentration. ATR-UV/vis spectroscopy was used together with focused beam reflectance measurement (FBRM) to monitor the liquid and solid phases, respectively, during the crystallisation of a mixture of ortho- and para-aminobenzoic acid (Saleemi et al., 2012).

In summary, the probes best suited to this research project are UV-ATR and turbidity probes for solid dissolution investigations. The turbidity probe can detect the clear point at the end of the dissolution process while the UV-ATR probe can provide both qualitative and quantitative analysis of the concentration of conjugated polar solute in an aqueous solution. Univariate calibration using known amounts of solute in solution enable the concentration of the solution to be extracted from absorbance measurements.

2.4 Applications

Work up to Continuous Crystallisation

In batch solution crystallisation, pharmaceutical ingredients and intermediates are initially re-dissolved in solvents according to their solubilities, typically in 5 to 20 volumes of solvent. The dissolution takes place in a train of several batch vessels from 200L to 4000L in volume, holding typically from 8 hours to 3 days of materials. Cooling is then applied to achieve the supersaturation required for nucleation in each vessel. In continuous crystallisation, there are two likely scenarios, firstly the same dissolution process in batch vessels can be used and the dissolved solutions can then be fed into a continuous crystalliser. The advantage of this is that the existing batch vessels are utilised. Unfortunately, the long storage times of these solutions can lead to formation of by-products, and hence reduce product quality. The second methodology is to feed solids directly into a continuous plug flow crystalliser. The definition and the scientific understanding of the dissolution rates of the fed materials in question will impact on supersaturation, nucleation and crystal properties. While the question remains of how to accurately dose solids into a flow stream is a technical challenge to this course. Both of these methodologies will be the focus of this project. Since all work up in pharmaceutical industry are operated in batch and involve relatively large volume, consequently these aspects are new, and the challenges are real.

2.5 Project Aims

Limited literature on work up demonstrate the lack of research in this field and also reinforce the urgent need to address this issue. This project is a first in this area. The aims of this project are to determine the feasibility of continuous dissolution within a twin screw extruder and identify the benefits and limitations of the system.

Following on from the literature review, the dissolution process was investigated initially in a batch system using paracetamol as the model compound, followed by dissolution in a continuous system. Further classes of materials were then tested and

compared in both the batch and the continuous system. Each of which is presented in a separate chapter, beginning with the batch system in chapter 3.

Chapter 3 **Material Characterisation and Parameter Effects on Bulk Solid Dissolution Rate of Paracetamol in a Stirred Tank Vessel using an in situ UV-ATR Probe**

This chapter describes the experimental apparatus chosen for the purpose of solid dissolution, outlines the selection of model compound, and presents the experimental outcomes. This chapter was also published in the International Journal of Engineering Research & Science **2018,** 4, 10-20.

3.1 Introduction

Solubility is a commonly quoted value in literature and has been widely reported for paracetamol. Much less commonly explored, however, are the dissolution kinetics. It is the kinetics that governs the dissolution process. Knowledge of dissolution kinetics is particularly crucial for continuous processing, where the major parameter effects should be optimised in order to ensure full dissolution is obtained within the short residence time. What do we know about paracetamol, and how can it be used to rationalise its behaviour in engineering systems?

Paracetamol (p-hydroxyacetanilide) also known as Acetaminophen, is a medication used to treat pain and fever, and is classed as a mild analgesic. Chemical formula is $C_8H_9NO_2$, as indicated in Figure 3.1, Molar Mass - 151.163 g mol^{-1}. The molecular structure of paracetamol comprises two main active groups, hydroxide (OH) and amide (N-C=O), attached to an aromatic ring. The paracetamol molecules possess several potential centres at which the reaction can be initiated. Four places in the structure have been identified: the benzene ring, OH, NH and CO (C=O). These are the basic fragments for the formation of hydrogen bonds, providing the structure of the paracetamol lattice (Vasil'chenko et al., 1996). The surface structure of paracetamol carries high negative

charges which remain undetermined and unexplained. The lone pair electrons of nitrogen and oxygen atoms are good electron donors, giving paracetamol useful chemical and electrical properties. Paracetamol is available in a broad particle size distribution range and can be purchased in a variety of particle sizes. Three grades of paracetamol which were used in this project are micronised, powder and granular.

Paracetamol was selected for dissolution studies because it is soluble in water and is also soluble in a variety of solvent systems (Rohani, 2006a). The solubility has been well documented in the literature and was used for both comparison purposes with data obtained experimentally and to determine the solids loading in each solvent system during the dissolution experiments (see Appendix A 7.1.1).

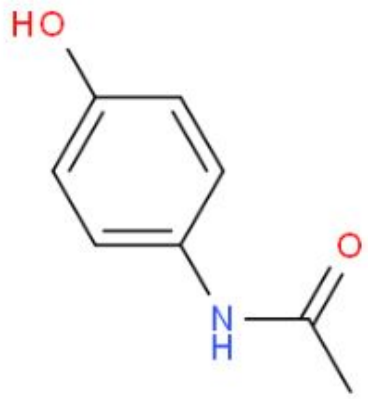

Figure 3.1 Chemical Structure of Paracetamol

3.2 Experimental Preparation and Procedures

3.2.1 Materials

Propan-2-ol (IPA) (>99.5% purity) was supplied by Sigma-Aldrich (Gillingham, UK). Deionised water was produced using the in-house Millipore Milli-Q system. Three

grades (micronised, powder and granular) of paracetamol (99% purity) were supplied by Mallinckrodt Chemical Limited (UK).

3.2.2 Methods

3.2.2.1 Solubility Measurement

Three different solvent systems were used in this study: 100% deionised water, 80% deionised water: 20% IPA, and 20% deionised water: 80% IPA. Solubility of paracetamol has been determined by a gravimetric method and compared to previously published work (Rohani, 2006a). In the gravimetric technique, a known weight of paracetamol was added to a conical flask containing 100g of solvent mixture. The flask was placed in a water bath to maintain the temperature and stirred until all solids had dissolved and solution remained clear. Further known weights of paracetamol were added until no further dissolution had occurred. The excess solid was filtered off, dried and weighed to determine the saturation concentration. Each measurement was repeated three times.

3.2.2.2 Particle Size Analysis

The mean particle size and particle size distributions (see Figure 3.2) were analysed by laser diffraction using a Mastersizer (HYDRO, Malvern 3000) and given in Table 3.1. Raw materials, directly purchased from the manufacturer, were powders rather than agglomerates. The samples were dispersed in hexane and added directly to the Mastersizer. This measurement assumes the particles are spherical and is less accurate for needle shaped particles however it is a widely accepted measurement system which give an indication of the particle size distribution of the material. The D50, the median, has been defined as the diameter where half of the population lies below this value. Similarly, 90 percent of the distribution lies below the D90, and 10 percent of the

population lies below the D10. The rate of dissolution is dependant on the particle size (see Equation 2.9).

Table 3.1 Particle sizes of three grades of paracetamol (granular, powder, micronised) measured using laser diffraction

	Dx (10) (µm)	Dx (50) (µm)	Dx (90) (µm)
Micronised	11	26.1	51.4
Powder	12.6	44.9	124
Granular	263	374	516

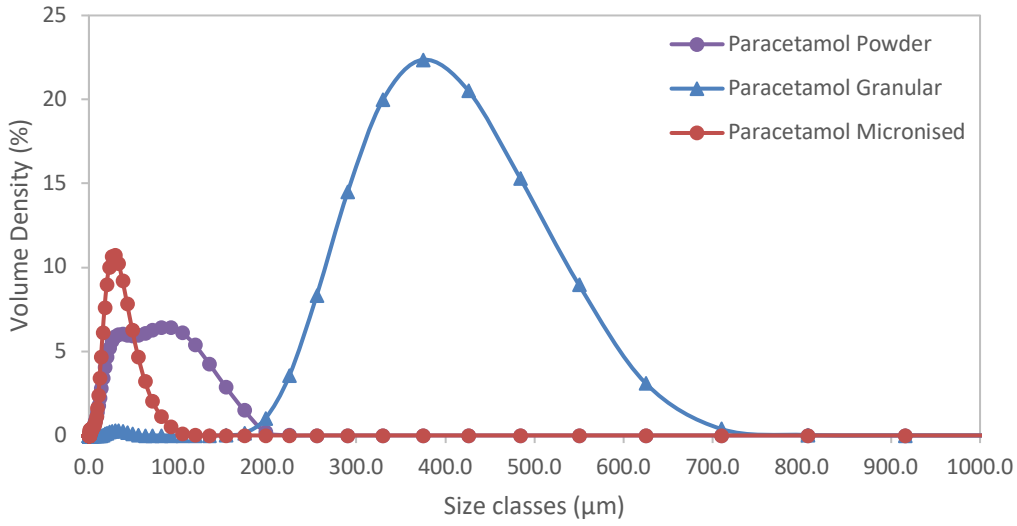

Figure 3.2 Particle size distribution of paracetamol - micronised, powder, granular obtained using laser diffraction

Scanning Electron Microscopy (SEM) is a surface analysis method for visualising particle size and shape from detailed three-dimensional (3D) topographical imaging. A

field emission gun produces a high energy narrow electron beam which is focused to a fine point on the sample surface of a sample under vacuum. Backscattered low energy secondary electrons emitted from sample surfaces are collected by the photon detector. The intensity of the electrons is a function of atomic composition of the sample and the sample geometry. The beam is scanned over the sample surface to create a high resolution, high magnification image spatially reconstructed from the intensity of the secondary electron emission at each point. SEM images (provided by Remedies Project) for each grade of paracetamol are given in Figure 3.3.

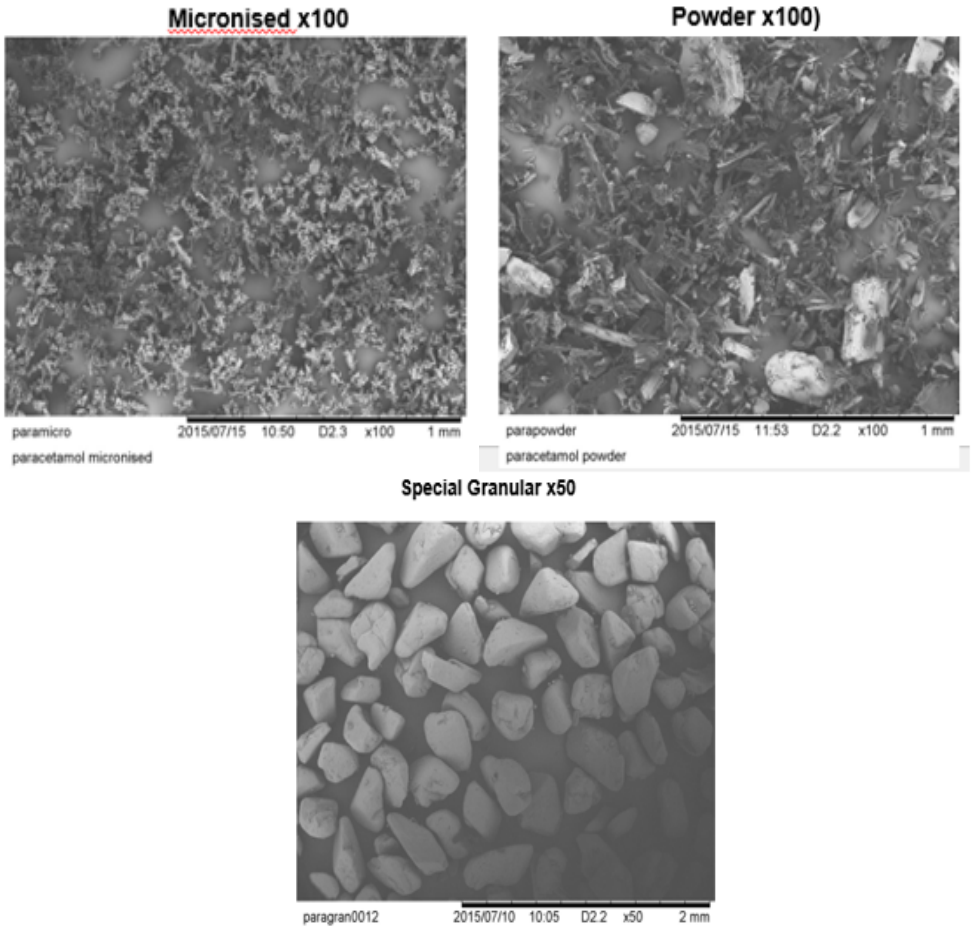

Figure 3.3 SEM images of paracetamol micronised particles, powder, and granular

The shape of the particles also impacts the dissolution rate. The dissolution rate decreases with increasing degree of particle shape irregularity (Mosharraf and Nyström, 1995). Figure 3.3 illustrates the powder and micronised particles consist of fused aggregates of irregular non spherical particulates whilst the granules are more sphere-like in shape.

3.2.2.3 BET Specific Surface area

Surface characterisation techniques are used to explore the surface area and surface energies of solid particles, identifying differences in grades of material such as wettability, and hydrophilicity. These are important parameters for understanding the mechanism of diffusion of the solute through the diffusion layer during bulk solid dissolution.

Autosorb iQ (Quantachrome Instruments) automated gas sorption analyser has been employed for the measurement of the specific surface area, an important index for dissolution as it can influence the dissolution rates of a material. This is a nitrogen gas physisorption technique for determining the Brunauer–Emmett–Teller (BET) surface area using an 11 point N_2 adsorption isotherm at 77K. Approximately 1 g of material was accurately weighed into a 9 mm diameter glass cell and degassed under vacuum for 5 h at 50°C, prior to the sorption isotherm being conducted. BET surface area was calculated within the Quantachrome® ASiQwin™ software version 3.01, using 11 points within the P/Po range 0.05 to 0.35.

3.2.2.4 Inverse Gas Chromatography Surface Energy Analyser (iGC- SEA)

SMS-iGC 2000 from Surface Measurement Systems Ltd was used to measure the surface area and surface energy of each of the paracetamol grades. Approximately 1 g of each

sample was packed by gentle tapping into a 4 mm ID silanised glass column capped with glass wool in each end. Samples were pre-conditioned at 25°C and 0% RH for 1 hour under flowing helium prior to measurements. BET surface area was determined using octane as the vapour probe. Dispersive and specific surface energies were determined from non-polar solvent probes octane, nonane, decane, and polar solvent probes ethyl acetate and dichloromethane using the Dorris-Gray calculation method (Dorris and Gray, 1980) and the peak centre of mass for surface coverages from 0.005 to 0.2 n/nm. Analysis was carried out using Analysis Software Advanced Version 1.4.1.0 (Surface Measurement Systems) to identify the wettability, hydrophilicity and surface energy. Inverse gas chromatography has been shown to be a versatile technique for surface characterisation of solid materials (Rückriem et al., 2015) and its accuracy has been verified in work by Mohammad (Mohammad, 2015).

3.2.2.5 Dissolution Studies in Stirred Tank Vessel

The STV was a jacketed glass vessel of 1 L in volume, with a PTFE four-blade pitched impeller to generate mixing. The impeller was attached to an overhead motor to control the rotation speeds. The vessel was fitted with a 5 port PTFE lid which enables the insertion of PAT probes and the dosing funnels. Different temperatures within the vessel were achieved by controlling the jacket temperature using a water bath (Grant Instruments GP 200/R2). UV-ATR, turbidity and temperature (PT100) probes (CrystalEyes system from HEL, UK) were inserted into the vessel to monitor and record the solute concentration, the cloudiness and temperatures of the solution during dissolution. The system was interfaced with a Carl Zeiss MC600 Spectrometer and PC for real-time display, logging and data analysis. The UV spectra were collected continuously over the spectral range of 220 – 280nm, using Aspect Plus software from Carl Zeiss. The schematic illustration of the STV is given in Figure 3.4. All the PAT probes also act as the baffles in the STV.

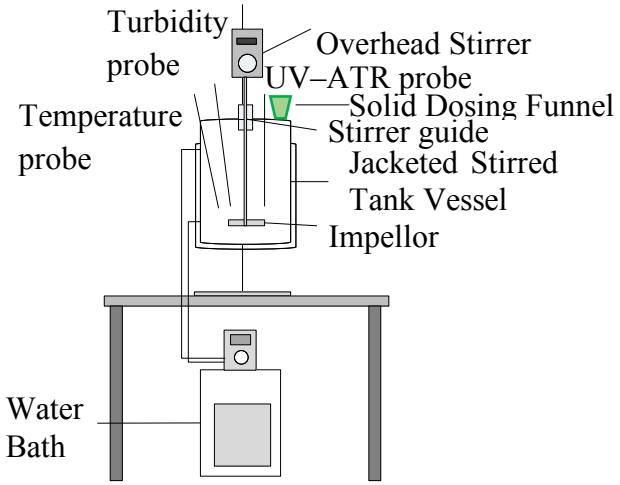

Figure 3.4 Schematic illustration of STV set-up used for dissolution experiments

For each experimental run, the volume of one litre of solvent was added to the STV and heated/cooled to the desired temperature (20°C, 30°C, or 40°C). The dissolution was carried out isothermally. A specified amount (see Appendix A 7.1.1) of technical grade paracetamol was accurately weighed (to four decimal places) using an electronic balance and was poured into the vessel using a funnel, to minimise loss. It was decided to use a solid loading of 95% of the solubility, in order to obtain an undersaturated solution. The solution was held at temperature and stirred under a fixed rotational speed until dissolution was complete. Dissolution experiments were carried out to determine the parameter effects of temperature (20 ˚C, 30 ˚C, 40 ˚C), mixing intensity (250rpm, 500rpm, 750rpm), solvent composition (water/ IPA mixtures), and particle size (micronised, powder, granular) on the dissolution rate.

3.3 Results and Discussion

3.3.1 Solubility of paracetamol in water/IPA mixtures

The solubility data (Rohani, 2006a) for paracetamol in water/IPA mixtures was verified using a gravimetric technique and used in this study. The solubility measurements are shown in Table 3.2, the corresponding values measured by Hojjati et. al. (Rohani, 2006a), along with the percentage error are also presented. Good agreement was obtained with the solubility reported in literature.

Table 3.2 Comparison of measured solubility using gravimetric technique and reported solubility using ATR-FTIR technique for paracetamol in water/IPA mixtures

IPA Mass (%)	Temperature (°C)	Solubility (g/1000 g solvent) Gravimetric measurement	% Error from Gravimetric measurement	Solubility (g/1000 g solvent) ATR-FTIR measurement	% Error between Gravimetric and ATR-FTIR
80	20	218.60	1.3	224.95	2.8
80	30	264.34	1.1	274.01	3.5
80	40	321.83	0.9	331.72	3.0
20	20	43.96	2.1	45.69	3.8
20	30	68.64	1.7	70.45	2.6
20	40	103.90	1.3	107.67	3.5
0	20	11.91	1.9	12.22	2.5
0	30	17.21	1.6	17.36	0.9
0	40	24.21	1.4	24.75	2.2

3.3.2 Dissolution Tests in STV

3.3.2.1 Calibration for concentration measurement

To quantify the solute concentration in the solution, calibration graphs were generated from known quantities of paracetamol in solvents based on the Beer-Lambert Law (see equation (3.1)) where a linear relationship is obeyed between the absorbance and the concentration of an absorbing species.

$$A = \varepsilon C l \qquad (3.1)$$

where A = Absorbance (no units), ε = molar extinction coefficient ($Lmol^{-1}cm^{-1}$), C = concentration ($molL^{-1}$), l = path length (cm).

Molar extinction coefficient is a measure of the probability of the electronic transition. The larger the molar absorptivity, the more probable the electronic transition. An unknown concentration of an analyte can be determined by measuring the amount of light that a sample absorbs. If the molar extinction coefficient is not known, the unknown concentration can be determined using a working curve of absorbance versus concentration derived from standards.

A maximum absorbance peak can be seen at 247nm (for paracetamol in deionised water) indicating that the paracetamol has dissolved (see Figure 3.5). Once the calibration curve has been established (see Figures 3.6, 3.7, and 3.8), each individual sample can be analysed. Calibration curves were generated for each solvent system at each temperature in this parametric study. Absorbance measurements at different solution temperatures can potentially lead to a wavelength shift of UV maximum absorbance and therefore absorbance measurements taken at a single wavelength may not be at the absorbance

maximum. These variations would therefore result in a deviation from the Beer-Lambert Law where the absorbance is directly proportional to concentration at the absorbance maxima. The data show that the temperature dependence of UV spectra is weak in the range of experimental temperatures (see Appendix A 7.1.2, Figures 7.1, 7.2, and 7.3). This indicates that temperature should not significantly influence solution concentration measurement which supports previously published work by Zhang et.al. (Zhang et al., 2011). Calibration curves at 40 ˚C (Figures 3.6, 3.7, and 3.8) were used to quantify the concentration measurements during the dissolution experiments. The dissolution experiments were repeated 3 times to confirm precision of the results. The error bars have not been added the graphs as they are too small to been seen (see Appendix A 7.1.2 Figure 7.4).

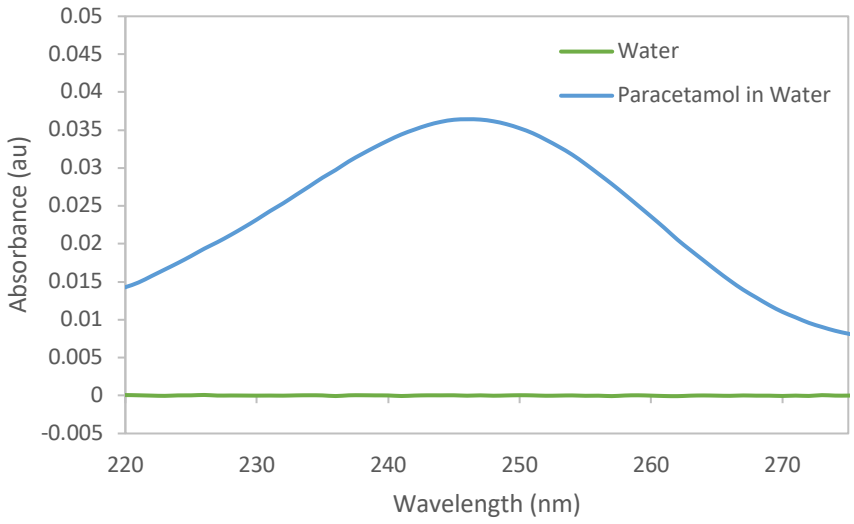

Figure 3.5 UV Spectroscopy of paracetamol dissolution in water at 220 -280 nm (Temperature = 40 ˚C)

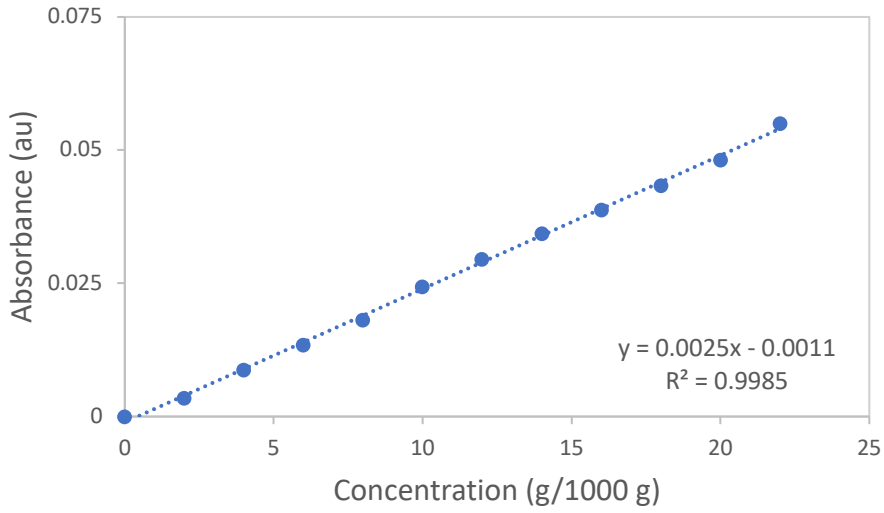

Figure 3.6 Calibration curve of paracetamol in water (Temperature = 40˚C)

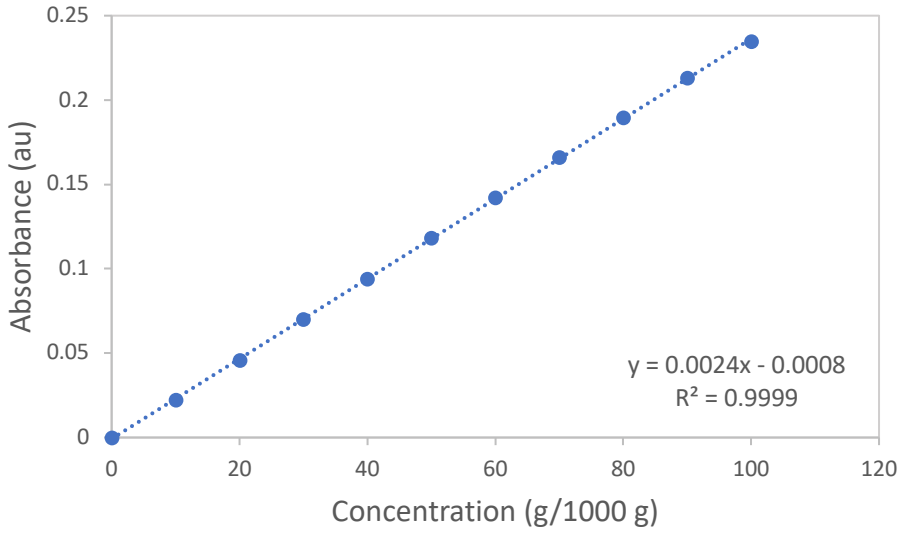

Figure 3.7 Calibration curve of paracetamol in water/IPA (80:20) (Temperature = 40˚C)

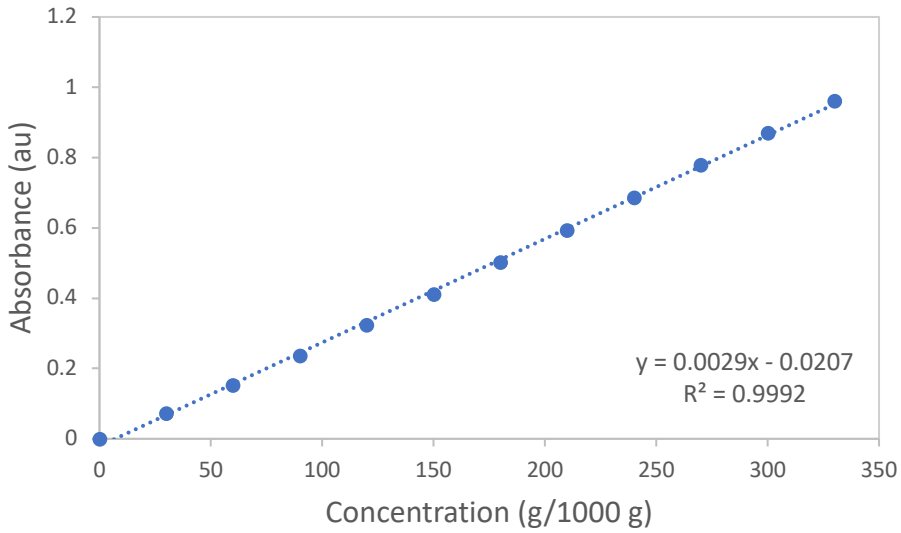

Figure 3.8 Calibration curve of paracetamol in water/IPA (20:80) (Temperature = 40˚C)

3.3.2.2 Dissolution Kinetics

The dissolution rate kinetics were evaluated by the slopes of the plot of concentration of dissolved paracetamol as a function of time as shown in Figure 3.9. We see that the slope (i.e. the rate) is relatively steep initially and then levels off monotonously as time, t increases. This is typical behaviour of solid particles whose size and total surface area gradually decrease as dissolution proceeds which is called the attrition mechanism (Hocsman et al., 2006). The curve flattens off as complete dissolution is approached. Under highly undersaturated conditions, all dissolution surface sites actively participate in the dissolution reaction, while it is only certain faces of the materials with lower activation energies of dissolution that contribute to the dissolution process as the solution becomes more saturated, as demonstrated by Guidry and Mackenzie (Guidry and Mackenzie, 2003) for alkali feldspars.

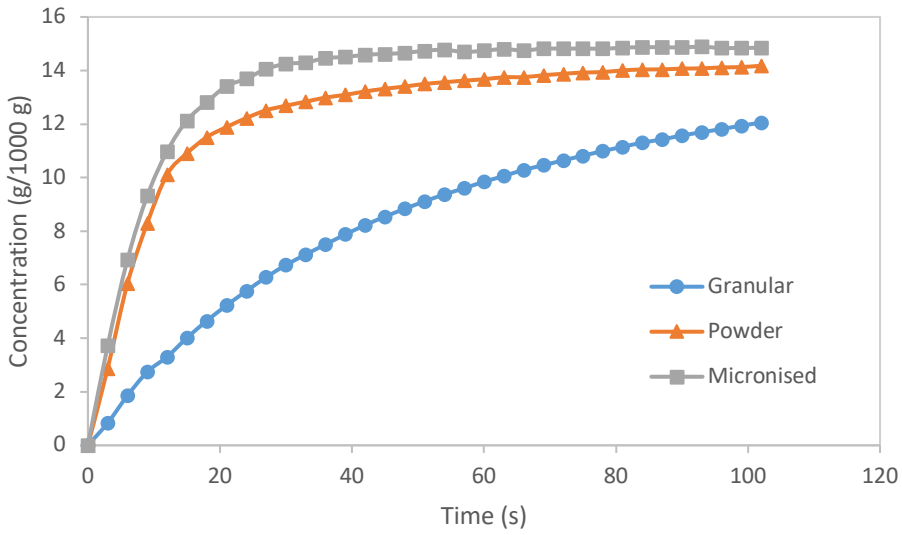

Figure 3.9 Dissolution history of paracetamol in water in a stirred tank vessel (Temperature = 30°C, Mixing Speed = 750 rpm)

For comparative purposes, the maximum dissolutions observed at the initial dissolution times, i.e. only the rising parts of the dissolution history, were used to extract dissolution kinetics, as Equation (2.6). These are the intrinsic dissolution kinetics and relate directly to the capacity of the material to dissolve, without diffusion limitation.

The effect of particle size, solvent composition, temperature and mixing intensity on the dissolution rate kinetics is presented in turn.

3.3.3 Effect of Particle Size

Specific surface area available for dissolution increases as the particle size is reduced. Each grade of paracetamol was measured using nitrogen physisorption and inverse gas chromatography techniques. Although both methods gave high correlating results (see Table 3.3) the comparison of the surface area using these two techniques as illustrated in

Figure 3.10 highlights the differences in sample preparation which has given rise to different values.

Table 3.3 Comparison of correlation coefficients for two surface area methods

Nitrogen Physisorption R^2 **value**	**iGC-SEA** R^2 **value**
0.9973	0.9975
0.9996	0.9990
1.0000	0.9990

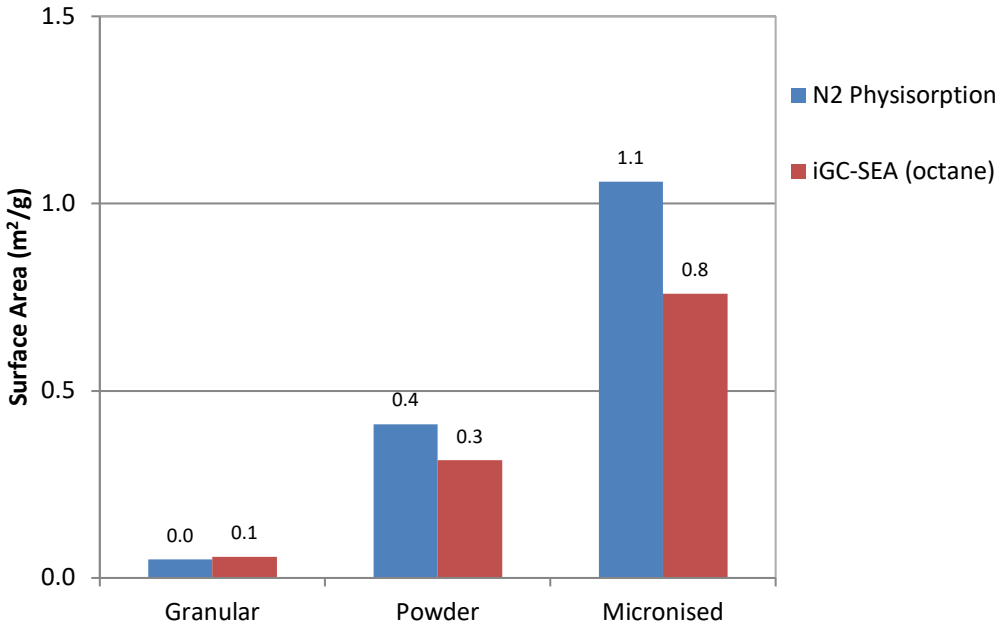

Figure 3.10 BET Surface area comparison of paracetamol using nitrogen physisorption and iGC - SEA

Sample preparation can be quite severe using the nitrogen physisorption technique as the sample is initially degassed with nitrogen under vacuum. The temperature is then reduced to liquid nitrogen temperature (77K), changing the sample and resulting this technique being less accurate at surface areas below $1 m^2 g^{-1}$. Samples exposed to very low pressures (i.e. vacuum drying) will completely dry most pharmaceutical hydrates and some fragile crystals might collapse under these conditions. BET surface area can be dependent on hydrated state. The iGC-SEA technique uses octane and is run at room temperature and this is more representative of the available surface at ambient conditions (Legras et al., 2015). Therefore, the results from the inverse gas chromatography were used to determine the specific surface areas.

As can be seen from Figure 3.10 the micronised paracetamol has the greatest surface area available for dissolution and as such should have the fastest dissolution rate, as shown in Equation (2.9). The iGC- SEA results (see Table 3.4) identified the granular material to have the highest affinity to the water molecules (hydrophilicity), the highest specific surface energy and the highest wettability (See Appendix A 7.1.3). The granular particles will therefore initially diffuse through the solvent quicker. Whereas the initial wetting step of dissolution is hindered by air pockets that are trapped in the powder and micronised material, which slows the initial ability of the particles to contact the solvent. However, these characteristics have less impact on the dissolution rate than the specific surface area which is driven by the greater number of particles diffusing through the concentration gradient. Powder and micronised material are more uniform and have less energy sites with a broader distribution of energy sites than granular material which shows that powder and micronised materials preferentially interact with each other than interact with liquid system. This tendency to agglomerate indicates these materials will be more problematic than granular to flow in a continuous system. The effect of increased specific surface area on the dissolution rate is clearly shown in Figure 3.11.

Table 3.4 iGC- SEA results for granular, powder and micronised paracetamol

	Hydrophilicity (Polarity Value)	**Wettability (mJ m^{-2})**	**Specific Surface Energy (mJ m^{-2})**	**Surface Area (m^2/g)**
Granular	0.217	132.0	14.3	0.1
Powder	0.081	110.9	4.5	0.3
Micronised	0.087	114.0	4.9	0.8

Figure 3.11 shows the dissolution history for the three materials in water at a fixed temperature; for comparative purposes, the time taken to dissolve 90% of the paracetamol concentration was used for each experiment. The granular material took 201 s to dissolve and was the slowest; the powder dissolved faster than the granular particles, taking 45 s, although the dissolution slowed considerably near equilibrium concentrations. The micronised material dissolved very quickly and complete dissolution was obtained within 21 seconds.

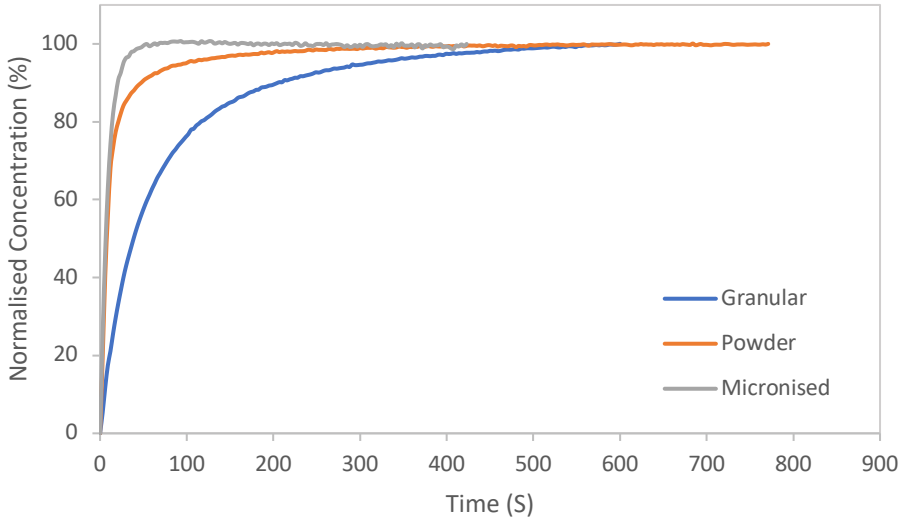

Figure 3.11 Normalised data for dissolution history of paracetamol in water in a stirred tank vessel (Temperature = 30°C, Mixing Speed = 750 rpm)

Note that both the micronised and powder particles were difficult to dose due to static force and prone to stick to the walls of the dispensing funnel and sides of the vessel when dispensing in one shot (see Figure 3.12). While dosing granular material was trouble free without loss of material. As such the total concentration of paracetamol dissolved was slightly less for micronised and powder than for granular particles, e.g. granular 15.6 g 1000 g^{-1} (solvent), powder 14.8 g 1000 g^{-1} (solvent) and micronised 14.8 g 1000 g^{-1} (solvent). The data has therefore been normalised (see Figure 3.11) to the granular concentration prior to analysis of the dissolution kinetics (see Appendix B 7.2.1).

The dissolution kinetics were determined using Equation (2.6). First order kinetics can be seen in Figure 3.13, showing that the rate of dissolution is directly proportional to the concentration. The dissolution rate constants for each grade of material are summarised in Table 3.5, which agrees with previously published work by Lee T. et.al (Lee et al., 2013).

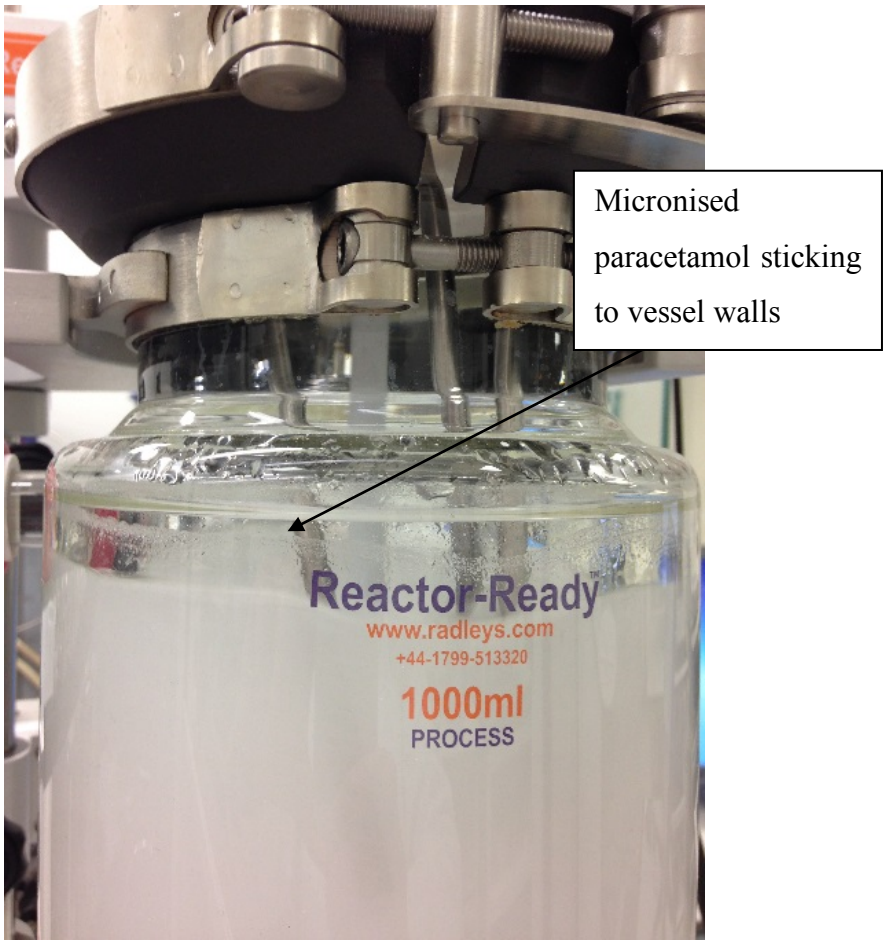

Figure 3.12 Dissolution of micronised paracetamol in a stirred tank vessel

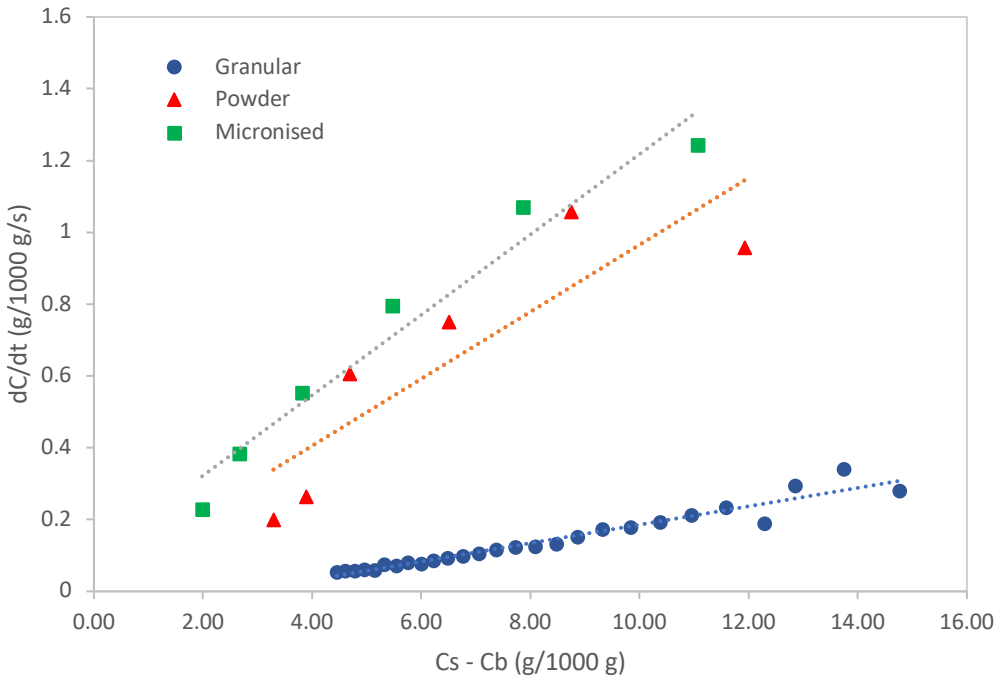

Figure 3.13 Dissolution kinetic plots of dC/dt vs Cs-Cb for micronised, granular, and powder paracetamol in a stirred tank vessel

Table 3.5 Dissolution rate constants of paracetamol dissolution in a stirred tank vessel

Particle Size	k (s^{-1})
Granular	0.026
Powder	0.093
Micronised	0.112

The results from this system are similar to that of literature (Lee et al., 2013), with the steepest slope for the smallest particles. Previous studies of paracetamol dissolution have evaluated dissolution rates in a dissolution test station (paddle method for in vitro testing

of paracetamol dissolution). Using 500mg of paracetamol and 900ml Ultrapure water of pH 1.4 with HCl as the dissolution medium, at a temperature of 37°C (Lee et al., 2013). Samples were then analysed off line, after filtration, for concentration using a UV/Vis spectrometer. Similar particle sizes and particle size distributions of paracetamol crystals were used for the dissolution study by Lee, et al.

Micronised material has fastest dissolution rates but has drawbacks such as lower wettability which often causes the material to have a tendency to float on the liquid surface during dissolution. These are cohesive powders which can agglomerate and cause problems with flow in and out of the storage hopper while processing. Granular material has good flow properties, wettability, and is easiest to dose, but has the slowest dissolution rates. Higher mixing is required to prevent sedimentation of granular material during dissolution.

The increase in dissolution rate from granular to micronised material is driven by the significant increase in specific surface area (granular 0.057, powder 0.314, micronised 0.759 m^2g^{-1}). The surface energy reduction from granular to micronised material (granular 131.9, micronised 99.9 mJm^{-2}) shows that although the granular particles have better wettability and can therefore diffuse through the solvent into solution faster than micronised particles. This effect is very small in comparison to the available surface area of the micronised particles which has the greatest impact on the dissolution rate. These values suggest that the mechanism for dissolution is surface-controlled. However, when the surface area is small as for granular particles, dissolution is not purely controlled by surface processes in water. A mixed control mechanism involving surface and transport processes is present when dissolving large particles. A transport controlled mechanism is a contributory factor for dissolution of granules and as such is playing an important role in the dissolution kinetics and hence may be the rate controlling step. However, at significantly large surface areas the dissolution is very fast, and the mechanism has not

been attributed to mixed-control, although some participation of transport in the kinetic control cannot be ruled out.

3.3.4 Effect of Solvent Composition

Solvent composition experiments comprise of varying the solubility of the system by altering the amount of IPA used in the water-IPA mixture. The magnitude of the solubility gives some clues about the mode (transport or surface reaction) that controls the dissolution rate of the solid. Lasaga (Lasaga, 1997) states that for aqueous solutions, solids with low solubility dissolve by surface control, whereas highly soluble solutes dissolve by transport control. The dissolution historyfor the three solvent systems as a function of time are illustrated in Figure 3.14 for granular paracetamol. The quantities of paracetamol added for 0 % IPA, 20 % IPA and 80 % IPA experiments were 11.56 g, 35.56 g, and 61.18 g respectively. The higher the IPA (and thus paracetamol solubility), the faster the dissolution rate, as highlighted in Table 3.6. This can be rationalised by considering the chemical structure of paracetamol, Figure 3.1. Barra and et al. studied the hydrogen bonding ability of paracetamol as a donor and an acceptor (Barra et al., 1997), focusing on H-bonding as the majority of molecule is hydrophobic. Water is very polar, while IPA is less polar; lower polarity of IPA reduces the interfacial tensions and surface tension between the solute and solvent; the solute moves faster through the diffusion gradient of the solvent, hence increasing the dissolution rate (see Table 3.6).

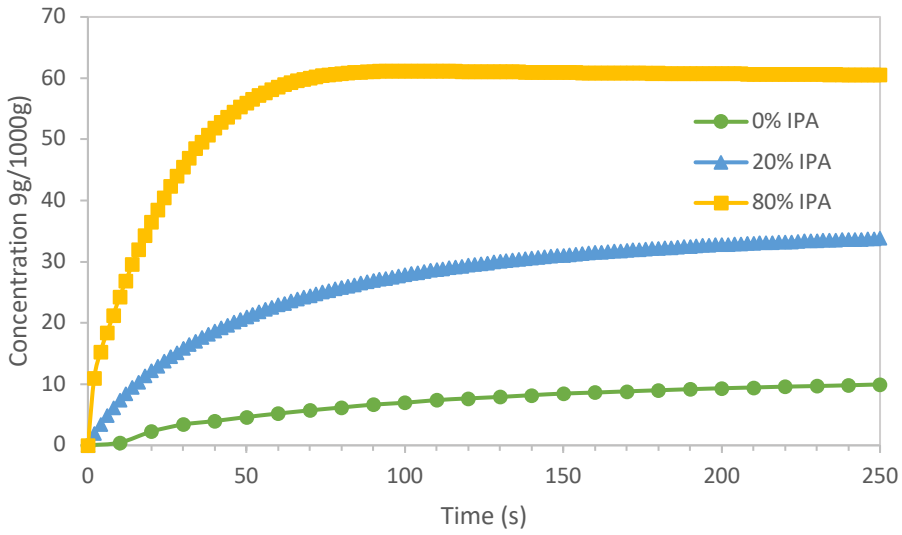

Figure 3.14 Dissolution history of granular paracetamol in water/IPA mixtures in a stirred tank vessel (Temp=20°C, Mixing Speed = 750 rpm)

Table 3.6 Time to dissolution of granular paracetamol and dissolution rate in varying solvent compositions in a stirred tank vessel

Solvent Composition	Dissolution Time (s)	k (s^{-1})
0 % IPA	440	0.01
20 % IPA	18	0.06
80 %IPA	2	0.79

Increasing the solubility of the solvent system has increased the dissolution rate. The dissolution mechanism for paracetamol is transport controlled due to its high solubility, however the solubility of paracetamol is decreased in aqueous systems suggesting there is also surface processes involved in the dissolution mechanism. The grade of paracetamol used in these experiments was granular, the solubility of which has

previously been attributed to a mixed-controlled mechanism. These results confirm both surface and transport processes are involved in the dissolution mechanism, and as the solubility increases, transport controlled mechanism become the major contributory processes. In short, solvent composition is a major factor affecting dissolution rate of solute molecules for a given particle type.

3.3.5 Effect of Temperature

The temperature effects were studied at three different temperatures (20°C, 30°C, and 40°C) for granular paracetamol particles in water. Increasing the temperature of the solvent increases the solubility of the drug and hence increases the dissolution rate as shown in Figure 3.15.

The dissolution rate constant obeys the Arrhenius equation (see Equation 3.2), higher temperatures results in an increase in the rate constant (see Table 3.7).

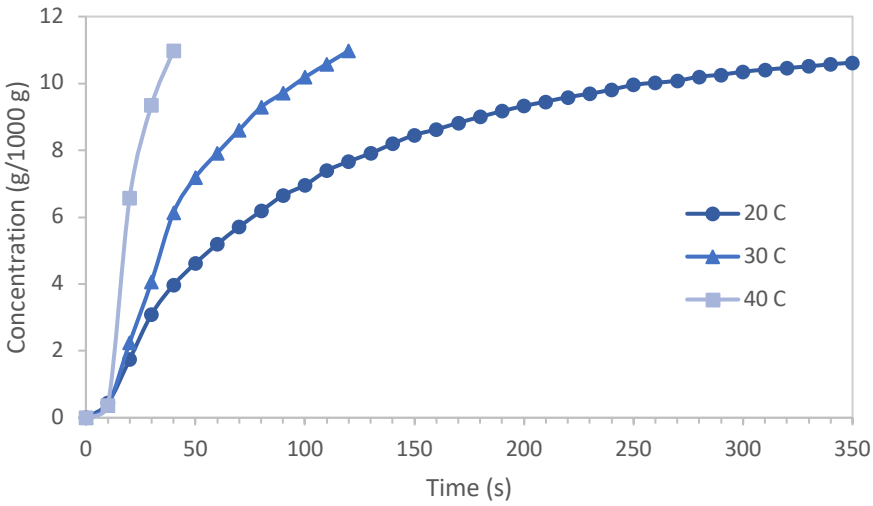

Figure 3.15 Dissolution history of granular paracetamol in water in a stirred tank vessel (Mixing Speed = 500 rpm)

Table 3.7 Dissolution rate constants at varying temperatures in a stirred tank vessel

Temperature	k (s^{-1})
20°C	0.01
30°C	0.03
40°C	0.09

The activation energy can be found algebraically by substituting two rate constants (k_1, k_2) and the two corresponding dissolution temperatures (T_1, T_2) into the Equation (3.2). Graphing ln k vs 1/T yields a straight line with a slope of $-E_a/R$ and a y-intercept of ln A.

$$ln\, k = -\frac{Ea}{R\,T} + ln\, A \qquad (3.2)$$

where, k = rate constant (s^{-1}), Ea = Activation energy (J mol^{-1}), R = gas constant (8.314 J mol^{-1} K), T = Absolute temperature (K), A = Arrhenius factor (s^{-1}), (It indicates the rate of collision and the fraction of collisions with the proper orientation for the reaction to occur).

As temperature increases, molecule velocity also increases. The kinetic energy of a molecule is proportional to the velocity of the molecules. Therefore, when temperature increases, kinetic energy also increases; as temperature increases, more molecules have higher kinetic energy, and thus the fraction of molecules that have high enough kinetic energy to overcome the energy barrier also increases.

The dissolution rate is approximately 3 times faster for every 10 degrees rise in temperature which is consistent with the reduction in dissolution time by approximately 1/3 for each 10 degrees increase as shown in Table 3.8.

Table 3.8 Time to dissolution of granular paracetamol in varying solvent compositions in a stirred tank vessel

Temperature	Dissolution Time (s)
20°C	350
30°C	100
40°C	30

Using a pair of temperatures and rate constants from Table 3.8, the activation energy (and the frequency factor) can be calculated for this dissolution as 19.45 kJ mol^{-1}. Sparks (Sparks et al., 1996) indicated that values of activation energies <21 kJ mol^{-1} were typical of transport-controlled processes in water and 42–84 kJ mol^{-1} for surface reaction controlled at solid surfaces. Intermediate values may be found for mixed-control (transport and surface) of the dissolution reaction. It must be noted that these values were established for dissolution of minerals and may not apply strictly to the dissolution of paracetamol particles. Nevertheless, the low value of activation energy (19.45 kJ mol-1) deduced from Figure 3.15 suggests that paracetamol dissolution is controlled by transport processes in water.

Strong temperature effects normally indicate surface-controlled dissolution because these effects are relatively weak for diffusion in aqueous media. The temperature effects on dissolution rate increased linearly, as the diffusion coefficient is highly temperature dependent (see Equation (2.10)). Therefore, the indication is that surface-controlled

processes are the dominant processes. This suggests a mixed control mechanism with transport control being the rate-limiting steps.

3.3.6 Effect of Mixing Intensity

The intensity of the mixing was varied by increasing the agitator speed (250 rpm, 500 rpm, and 750 rpm) for dissolution of powder paracetamol particles in water at 20°C. The impact of increasing the mixing within the STV resulted in increased dissolution rate as shown in Figure 3.16. At increased mixing intensity the solvent/solute boundary layer is replenished faster with fresh solvent increasing diffusion of solute into the solvent and therefore increases the dissolution rate (see Table 3.9).

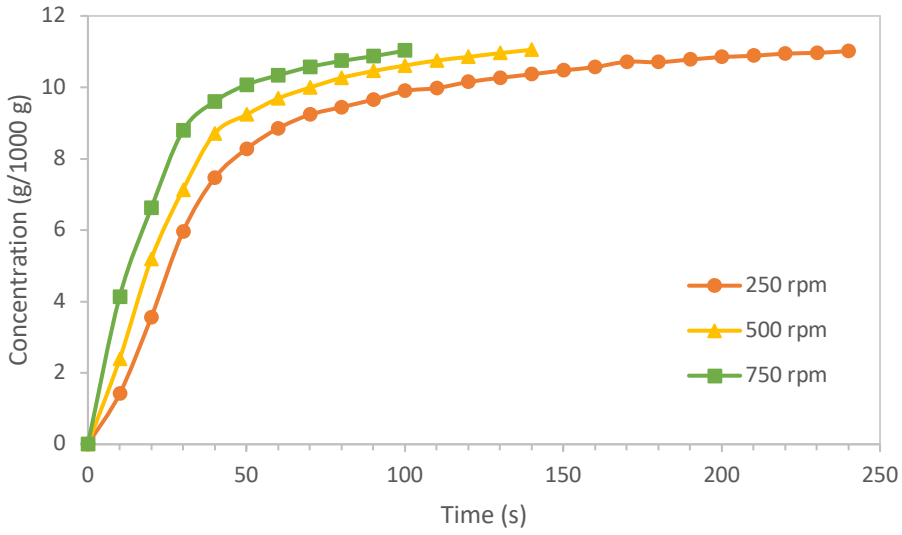

Figure 3.16 Dissolution history of paracetamol powder in water in a stirred tank vessel (Temperature = 20°C)

Table 3.9 Dissolution rate constants at varying mixing intensities in a stirred tank vessel

Agitator Speed	k (s^{-1})
250 rpm	0.022
500 rpm	0.034
750 rpm	0.059

At low agitation speeds the particles are only just suspended and are moving slower than at high agitation speeds where more collisions are taking place. Therefore at higher agitation speed the solute particles have an increased number of states available to occupy within the system and a greater opportunity to come into contact with fresh solvent resulting in more surface renewal with solvent, hence stirring rate influences the transport rate of species in solution. The transport to and from the surface depends on the hydrodynamics of the system under investigation. In the case of a well-stirred solution near the particle surface, the transport is determined by a diffusion gradient through which diffusion takes place according to Fick's second law of diffusion (Fick, 1855) (see Equation. (2.11)). The diffusion of material is caused by the concentration gradient between the bulk and the surface. The thickness of the diffusion layer can be changed, for instance, by changing the stirring rate.

When dissolution histories from Figure 3.16 are compared to the dissolution history with no mixing (see Figure 3.17), it can be seen that dissolution is very slow (minutes), whereas dissolution with stirring took seconds. This emphasises diffusion limiting dissolution rather surface limiting.

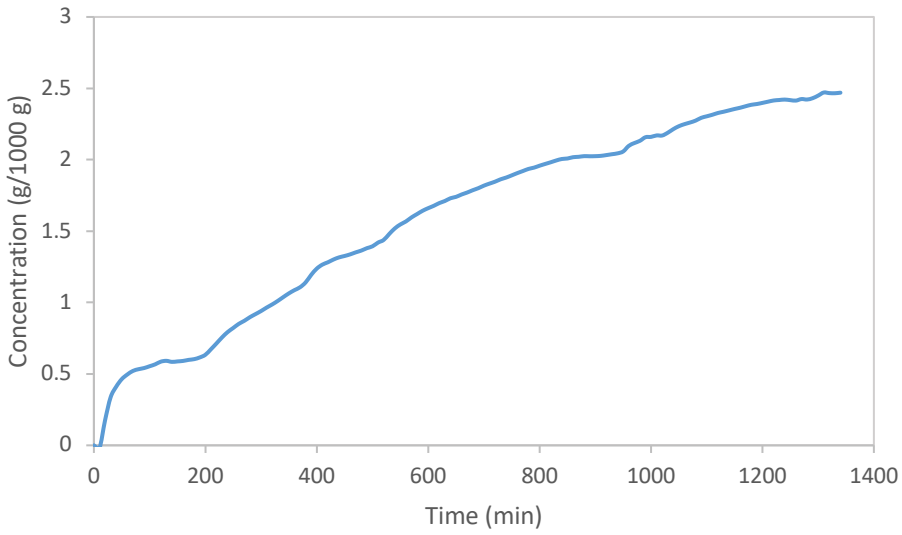

Figure 3.17 Dissolution history of paracetamol powder in water in a vessel with no mixing *(Temperature = 20°C)*

Although stirring rate at the experimental conditions studied (250 rpm, 500 rpm, 750 rpm) did not illustrate mixing as a major factor, Figure 3.17 clearly demonstrates that mixing significantly increases dissolution rate and therefore must be incorporated into the design of a continuous dissolution system. In fact, dissolution kinetic studies performed at different stirring rates showed that the dissolution rate increases linearly with the stirring rate (r^2 = 0.995) which relates stirring rate with depletion of the diffusion layer. Therefore, the combined analysis of temperature and stirring rate effects indicates that the mechanism of the dissolution kinetics under our experimental conditions is predominantly transport controlled.

DOE factors influencing dissolution rate

A full factorial model of 2^3 screening design experiments was employed to determine and prioritise the effects of temperature (A), mixing intensity (B) and solvent composition (C) on the dissolution rate using granular paracetamol. The main effects of A, B, C and

the interaction effects of AB, AC, BC, and ABC were calculated using JMP Software and are shown in Figure 3.18. The temperature, solvent composition, and mixing intensity are all statistically significant parameters, as indicated by the p-value < 0.05.

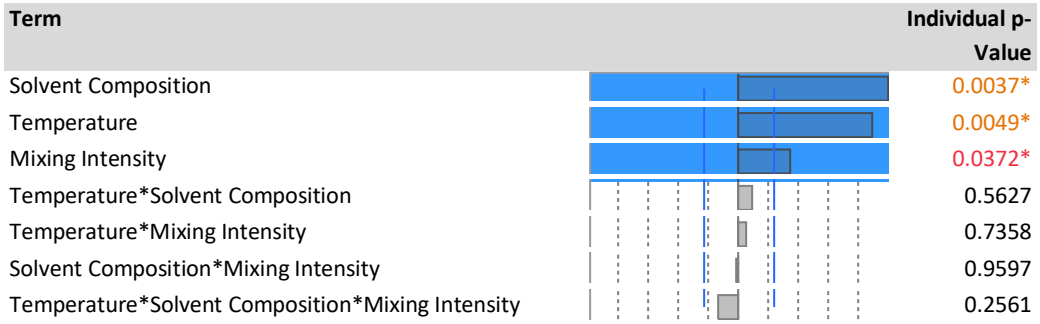

Figure 3.18 Parameter effects on dissolution rates using JMP design of experiments software

Statistical analysis of the experimental design using JMP software confirms that the model is a good fit, indicated by the summary of fit data, i.e. the coefficient of correlation (R^2 value) equal to 0.9840. The prediction profiler in the JMP software can be used to determine the maximum dissolution rate for each parameter setting using this model for paracetamol dissolution in water-IPA mixtures in a stirred tank reactor. The responses are all linear, no quadratic responses were seen, and therefore no further fitting of the model was required.

Solvent Composition and **Temperature** are the main factors affecting dissolution rate, mixing intensity to a lesser extent. The interaction effects are **not** statistically significant in this model.

3.4 Conclusions

This work focuses on a parametric study of the effects of temperature, solvent composition, mixing intensity and particle size on dissolution rates in a stirred tank vessel (STV) with paracetamol in water/ IPA mixtures as the model system. Solute concentration was measured using an in situ ATR-UV probe, dissolution histories were generated and used to extract dissolution kinetics.

Some critical factors impacting the dissolution rate in a batch system are realised through this initial study. For the same type of particles, solvent composition (solubility) is the major parameter when dissolving bulk solids in a batch system, temperature is the second contributing factor, while mixing has less effect on dissolution rates for this type of solvent-solute systems. For the same solvent and temperature, the smallest particle size has the fastest dissolution rate. The mechanism for dissolution of paracetamol in the stirred tank vessel is attributed to mixed controlled processes (both surface and transport) with transport processes being the rate limiting step. The only exception to this was the very fast dissolution of micronised particles where surface reactions were attributed to the dissolution mechanism.

Although micronised solids vastly increased the dissolution rate, the flowability of such material would have a negative impact in a continuous flow system, potentially leading to bridging, blockages for instance. The learning from this work has been applied to the investigation of solid dissolution in a continuous flow system. The temperature and solvent composition were fixed to give optimum dissolution within a continuous flow system with focus being on increasing mixing rate to optimise dissolution.

Chapter 4 **On the use of a twin screw extruder for continuous solid feeding and dissolution for continuous flow processes**

Following on from the successful identification of the major parameters affecting dissolution rate, this chapter investigates the potential of continuous dissolution of paracetamol within a twin screw extruder (TSE). This chapter was also published in the journal of Organic Process Research & Development **2018**, 22**,** 1373-1382.

4.1 Introduction

In this study, the feasibility of a 16mm TSE as a continuous solid feeder is investigated and dissolution within the residence time of the TSE is targeted. The TSE enables the decoupling of liquid from the solid feed, thus eliminating any potential fouled solid feeding. The liquid flow rates have been limited to a maximum of 40 g min^{-1} in this study to prevent potentially flooding the barrel of the TSE. This has restricted the solid feed rates that can be utilised without exceeding the solubility limits of the solvent composition and thereby thwarting complete dissolution.

Paracetamol has low solubility in water, to be able to keep the liquid flow rates less than 40 g min^{-1} (thereby preventing leaks from the barrel) this would require solid feed rates below 1 g min^{-1}, which are unattainable using the available equipment. Whereas the dissolution rate of paracetamol in a 20:80 mixture of water and IPA is very fast making it difficult to extract dissolution kinetics within the short residence time of the TSE. The solubility of paracetamol in an 80:20 mixture of water and IPA allows for solid feed rates up to 4.3 g min^{-1}, this has been chosen as the solvent composition in this study.

Three grades of paracetamol which were used in this project are micronised, powder and granular. This allows a range of bulk properties to be measured, which are typical for raw material input to a solid dosing feeder.

The concentrations of paracetamol during dissolution experiments are monitored using an in-line UV-ATR probe connected to a spectrometer, and dissolution kinetics are extracted. A methodology of estimating the power density for the TSE is proposed, thus enabling a fair comparison of dissolution rates between this continuous system and a batch stirred tank.

4.2 Experimental Preparation and Procedures

4.2.1 Materials

Three grades of paracetamol were used through this work: micronised, powdered and granulated. These come from the same stock material as used in Chapter 3.

4.2.2 Methods

4.2.2.1 Flow Properties

FT4 Powder Rheometer (Freeman Technology Ltd., Tewkesbury, UK) was used in the testing of solid materials to measure bulk properties and dynamic flow for each of the grades of paracetamol, The rheometer measures the resistance of the powder to flow whilst the powder is in motion. By testing samples in consolidated, moderately stressed, aerated or fluidised state gives a simulation of the powder processing conditions.

Five tests were carried out on each material: 1) Stability and Variable Flow, 2) Permeability, 3) Aeration, 4) Compressibility and 5) Shear Cell 9kPa. All tests were conducted in 25mm cells. Data was collected using the FT4 Powder Rheometer software version 4.0 (Freeman Technology Ltd., Tewkesbury, UK) and analysed with FT4 Data Analysis software version 3.01.0057 (Freeman Technology Ltd., Tewkesbury, UK).

4.2.2.2 Dissolution Studies in Continuous Twin Screw Extruder

A 16mm diameter twin screw extruder (TSE) (Eurolab 16, Thermo Fisher Scientific, Stone, UK) is shown schematically in Figure 4.1. The barrel has a length of 400 mm with a length to diameter ratio of 25:1. Liquids are dispensed into the barrel using a peristaltic pump (Watson Marlow, Falmouth, UK) and solids added via a loss in weight (LIW) gravimetric feeder. Two types of feeders were used in this work including a Brabender MT-S LIW Feeder and a Brabender FW-18 Flexwall Classic LIW Feeder (see Figure 4.2). The former is a rigid frame laboratory scale feeder with twin concave screws suitable for low feed rates (< 10 g min^{-1}) of high bulk density materials (e.g. granular paracetamol), while the latter is a universal flexible wall feeder with a single spiral screw suitable for materials with poor flowability and low bulk density (e.g. powder paracetamol).

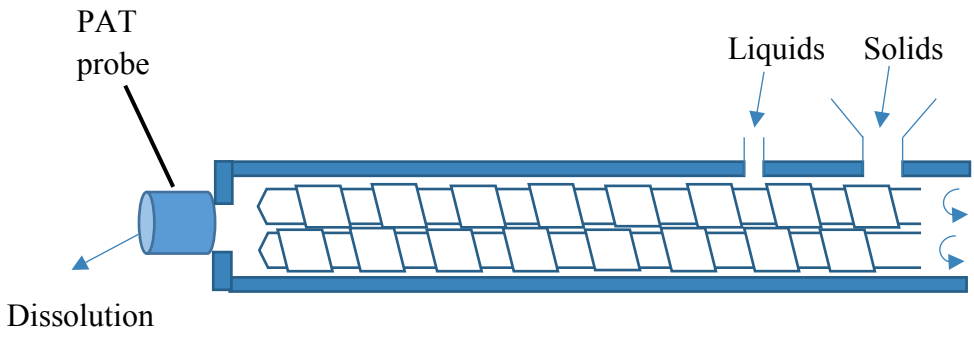

Figure 4.1 Schematic of continuous twin screw extruder

The extruder is connected to a central control unit where temperature and screw speed can be varied. The temperatures of different sections along the barrel are controlled by electrical heating bands and monitored by thermocouples. A bespoke discharge coupling, and tubing was connected to the exit of the twin screw to provide downward output of material. This prevented build-up of material at the extruder exit. The UV probe was mounted on a retort stand and inserted into the tubing. Absorbance data is collected continuously using a UV-ATR probe inserted at the flow exit, interfaced with a Carl Zeiss MC600 Spectrometer and a PC for real-time display, logging and data analysis.

The residence time of liquid within the barrel was measured to aid the determination of dissolution kinetics. A dye was injected at liquid entry ports and minimum residence times of the dye were recorded. When liquid enters the barrel at port 6, the residence time is merely 3 seconds, which is the same as the UV probe capture time, hence the UV probe is insufficient to allow direct measurement for this case, a digital stopwatch was used instead. The variations obtained were $\pm$ 0.2 seconds for five measurements.

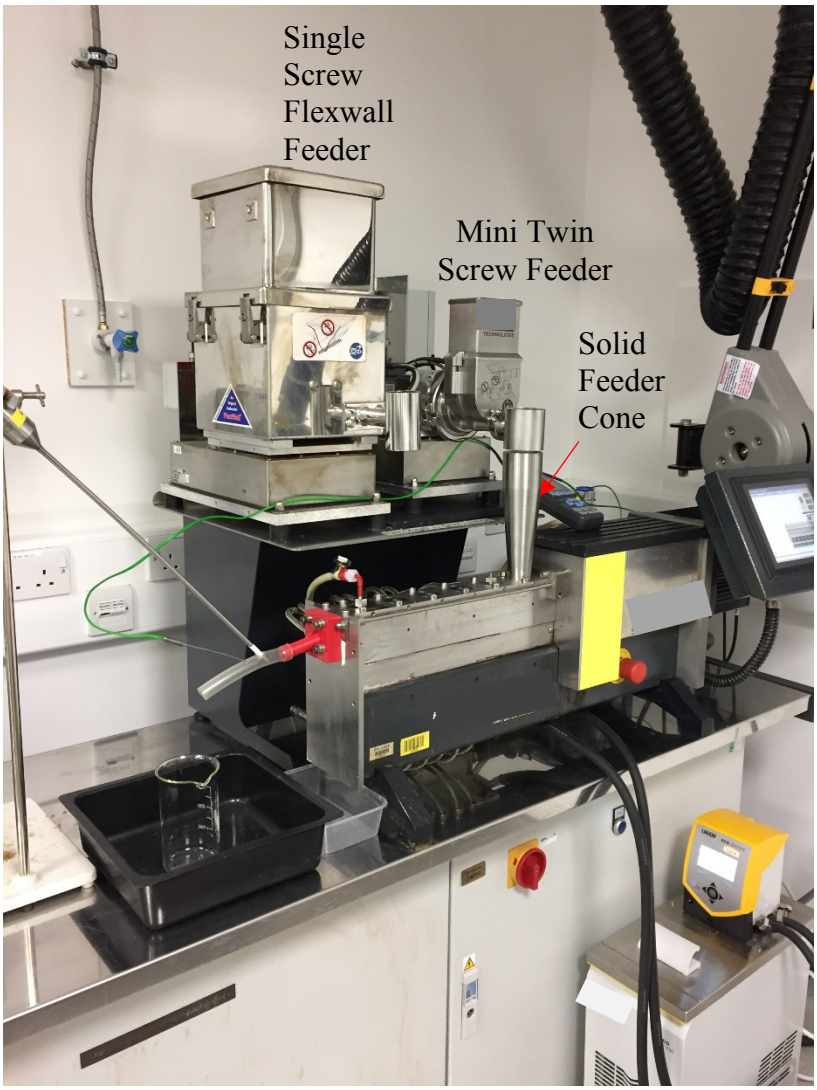

Figure 4.2 Set up of continuous twin screw extruder with LIW gravimetric feeders for dissolution experiments

In dissolution work, solids are dosed at Port 1 of the barrel as shown in Figure 4.3; liquid flows from the right to left and can be pumped in at any of the Ports from 2 to 6 (see Figure 4.3). In this way, the decoupling of the dry solids from the wet liquid is achieved, preventing solids from sticking around the feeder. Liquid coming at Port 2 has

the longest residence time of 13 seconds within the barrel whereas liquid at Port 6 the shortest residence time of 3 seconds.

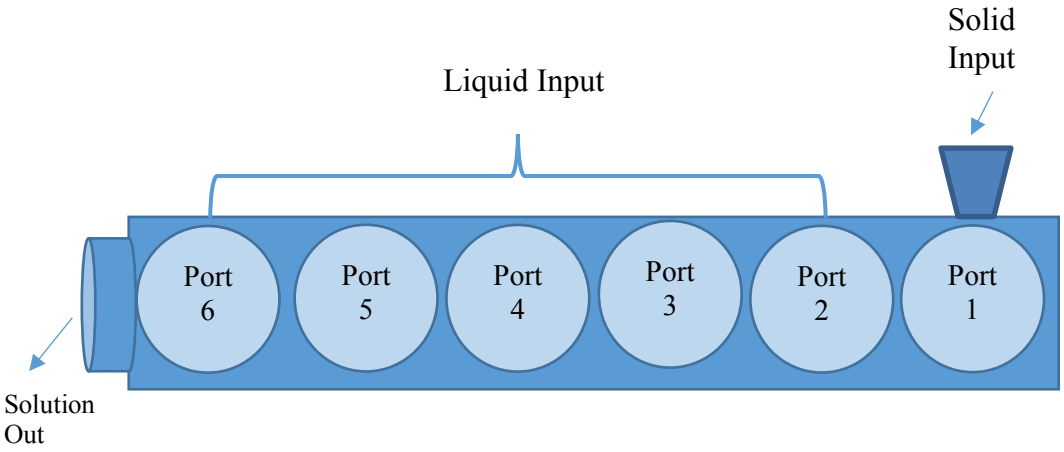

Figure 4.3 Schematic of barrel of twin screw extruder showing solid/liquid input port positions

In order to obtain a concentration-time history, calibration curves of absorbance versus concentration were generated from known amounts of paracetamol in the Water/IPA (80:20) solvent system, with a maximum absorbance peak at 248nm. A complete set of sequential runs were then undertaken at each port, e.g. Run 1 at Port 6, Run 2 at Port 5, Run 3 at Port 4, and so on. This enabled monitoring of the dissolution process along the length of the barrel. The absorbance measurements were recorded using the in-line UV-ATR probe positioned at the TSE exit. Compiling the output concentrations at each port, a dissolution history was finally assembled.

4.3 Results and Discussion

4.3.1 Material Characterisation

To feed solids consistently and accurately in continuous manufacturing processes even at small flow rates (< 5 g min^{-1}), the choice of feeder is of utmost importance. This is because a feeder's performance is strongly dependent upon flow properties of materials

(Wang et al., 2017). For instance, the use of LIW feeders improved the ability to control feed rates for powders with high cohesion and electrostatics (William E. Engisch, 2012); the use of flexible frame LIW feeders with a single spiral screw was good for materials with low bulk density and poor flow ability (Cartwright et al., 2013). For materials with higher values of bulk density (0.5 g ml^{-1}), a rigid frame LIW feeder with concave twin screws worked well.

Prior to the decision of feeder and screw used in this study, the flow properties of powder, micronised and granular paracetamol were determined using the FT4 Powder Rheometer as listed in Table 4.1. See Appendix A 7.1.4 for graphs.

Table 4.1 Particle flow properties of three grades of paracetamol (granular, powder, and micronised) in a FT4 Rheometer

	Mean Particle Size (μm)	Bulk Density (g ml^{-1})	Permeability (cm^2)	Basic Flowability Energy (mJ)	Compressibility (% @ 15kPa)	Cohesion (kPa)
Granular	374	0.728	6.6 x 10^{-5}	630.2	29.1	0.49
Powder	45	0.357	4.1 x 10^{-6}	150.3	51.7	1.68
Micronised	26	0.217	2.6 x 10-6	159.9	65.5	2.58

To assess how the material behaves, a blade is rotated and moved vertical through the powder to establish a flow pattern. The particles flow and the resistance experienced by the blade represents the difficulty of the particle movement i.e. the bulk flow properties. It is clear from Table 4.1 that micronised and powder has lower bulk density and poorer

flow properties (indicated by the numbers of the Basic Flowability Energy) than granular. The bulk properties of all powders are affected by air to some extent since the space between the particles is filled with air. The amount of air present influences how the particles interact with each other and this impacts directly upon the flow properties. Powder and micronised were readily aeratable and only require a small amount of energy to produce flow. In contrast, granular material is the most permeable and has a lower compressibility than powdered material, suggesting that it is a non-cohesive material which is less likely to compact on the feeder. Permeability is of interest when trying to understand the effects of process environments such as storage in and flow out of hoppers, the tests show that granular material has better flow properties than powder or micronised particles. The stability and variable flow tests indicated that three grades of the paracetamol did not show any signs of de-agglomeration or segregation and were stable during flow indicating these materials could be stored in a hopper without significant changes over time. The micronised and powder were more sensitive to changes in flow rate, presumably as a result of higher air content in the cohesive material. Flow output measurements were made on the different feeders and in combination with the FT4, and are in agreement with previous work (Cartwright et al., 2013, Wang et al., 2017, William E. Engisch, 2012).

Dosing trials at a solid feed rate of 3.33 g min^{-1} confirmed the above selections as the other combinations caused significant problems. For example, the single spiral screw was unable to convey granular paracetamol due to an increase in the frictional resistance to flow that results from entrainment. Likewise, the powder presented challenges in the rigid frame feeder due to the increase in torque that has compacted powder within and between the screws, as well as the barrel housing.

Micronised material is difficult to dose due to static therefore the plastic 3D printed fitting for the end of the barrel housing had to be replaced with a stainless-steel fitting. The trials for this grade of material were unsuccessful in both types of feeders. The feeder

output was variable, and the material quickly compacted in the feed hopper causing the feeder to alarm due to increased motor torque. This is a very cohesive powder which has low bulk density and therefore contains a lot of air that is difficult to remove due to the low permeability, causing a high resistance to flow. In comparison to granular material, micronised material requires almost twice the size of storage vessel to contain the same mass of material. The high compressibility was evident as the material compacted very quickly in both the feed hopper and the barrel housing.

Micronisation of powders has been shown to induce surface energetic changes which can be related to important secondary processing properties such as powder flow (Feeley et al., 1998). As such micronised powders are blended with excipients to enhance flow properties. The dissolution studies in this work focused on dosing unadulterated raw materials i.e. material that is not blended.

Micronised material had proved very promising during dissolution studies in a stirred tank vessel (see Table 3.5), when dosed as a single shot with the dissolution rate being five times faster than for granular material. Since micronised material is very difficult to flow, it is not recommended for dissolution work in a continuous system.

4.3.2 Dissolution Studies in TSE

4.3.2.1 Dissolution Tests

The results from the previous chapter show that the optimal dissolution rate for the temperatures investigated was achieved at 40˚C. Therefore to optimise the dissolution rate within the short residence time of the TSE, all dissolution tests were ran with the solvent temperature set at 40˚C. The solubility for paracetamol in water/IPA (80:20) at 40˚C is 11g paracetamol in 100g of solvent (Rohani, 2006a), i.e. a solid: liquid ratio of

1:9. To ensure complete dissolution could be attainable, the dissolution tests were carried out at a lower solid loading than the solubility limit i.e. solid: liquid ratio of 1:11. Paracetamol powder was continuously dosed into the TSE using the single screw flexible wall LIW feeder at a feed rate of 3.33 g min^{-1} and the solvent (Water/IPA 80:20) at a flow rate of 37 g min^{-1} (1:11 ratio), giving a target output concentration of 9.0 g per 100 g solvent. Figure 4.4 shows that complete dissolution was obtained within the residence time of the barrel (13 seconds) where the concentration of paracetamol at the exit was consistently 9.0 g $\pm$ 0.1 g per 100 g solvent.

The same tests were carried out for granular paracetamol using a twin screw rigid wall LIW feeder at the same feed rates. Complete dissolution was not achieved within the residence time of the barrel (see Figure 4.4) with some undissolved paracetamol being observed at the exit. This was expected when comparing to dissolution kinetics in Chapter 3, granular has a slower dissolution rate than powder. The concentration of paracetamol at the exit remained at 7.7 $\pm$ 0.3 g per 100 g solvent for 3000 seconds. The first 160 seconds run time for granular paracetamol is plotted for the purpose of comparison with that for powder paracetamol.

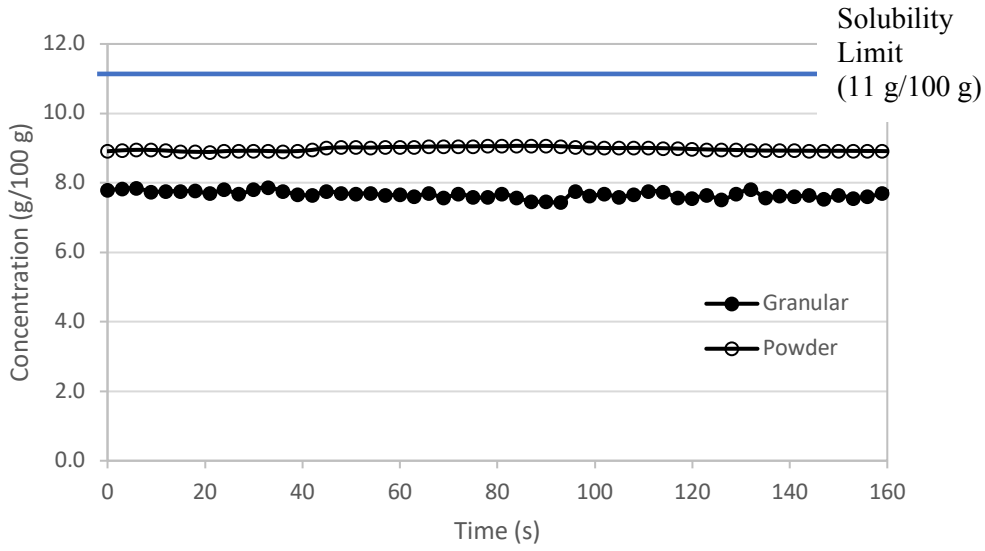

Figure 4.4 Concentration-time history post TSE for dissolution of paracetamol (Temperature = 40˚C, solid feed rate = 3.33 g min^{-1}, liquid flow rate = 37 g min^{-1})

The dissolution tests were ran using the maximum length of the barrel available for dissolution i.e. liquid enters at Port 2 however only the final concentration of solution can be measured on exit. To determine the dissolution rate kinetics required further experiments to be ran consecutively with the liquid entering a separate port for each run, starting at Port 6, ending at Port 2. These dissolution tests were carried out at a solid feed rate of 2.5 g min^{-1} and a liquid flow rate of 29 g min^{-1}, giving a target output concentration of 8.6 g per 100 g solvent. The feed rates were reduced to ensure consistent concentration output could be achieved at low feed rates where the feeder output could be more variable. Dissolution histories were compiled from the concentrations at exit of the TSE for liquid input at each port as shown in Figure 4.5. Note that each concentration measurement was repeated 3 times and the data in Figure 4.5 are the averaged value from three repeats. Error bars are not shown on the graph as they are too small to see clearly. The variation obtained for the runs at each port are given for granular paracetamol - standard error 0.2, 0.3, 0.2, 0.2, and 0.1.

Both grades gradually dissolve along the barrel of the TSE with more rapid and complete dissolution obtained for powder material than for granular grade. This is consistent with what has been shown in Figure 4.4 as well as the work in a stirred tank vessel discussed in Chapter 3.

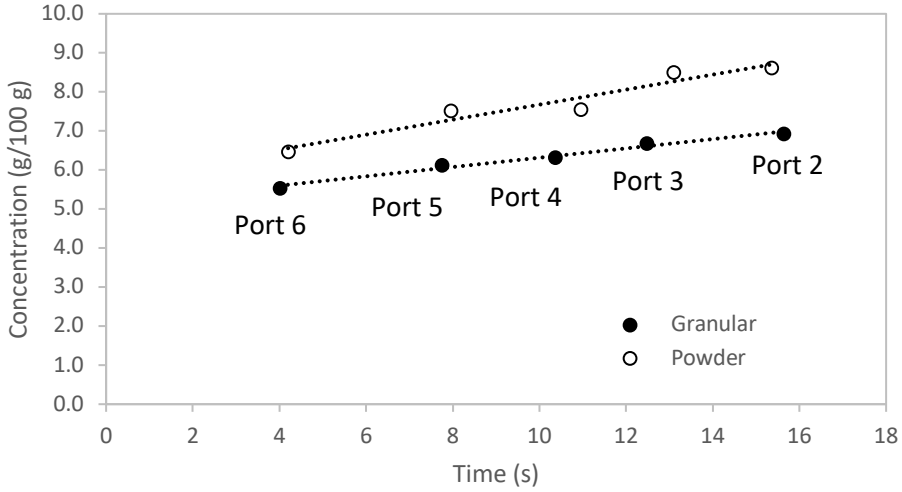

Figure 4.5 Dissolution history for paracetamol dissolution post TSE at each port(Temperature = 40˚C, solid feed rate = 2.5 g min^{-1}, liquid flow rate = 29 g min^{-1})

4.3.2.2 Dissolution Kinetics

The dissolution kinetics were determined using Equation (2.8). Fitting the first order kinetics, Figure 4.6 plots of ln (C2/C1) vs time where C2 and C1 are the concentrations of paracetamol (g 100g^{-1}) at the starting and dissolution times. The fit confirms the first order kinetics and the slope of which gives the rate constant of dissolution k = 0.0162 s^{-1} and 0.0211 s^{-1} for granular and powder respectively. First order is linear with time, hence suggests it can be used to extrapolate dissolution history to completion and then design reactor to fit dissolution kinetics.

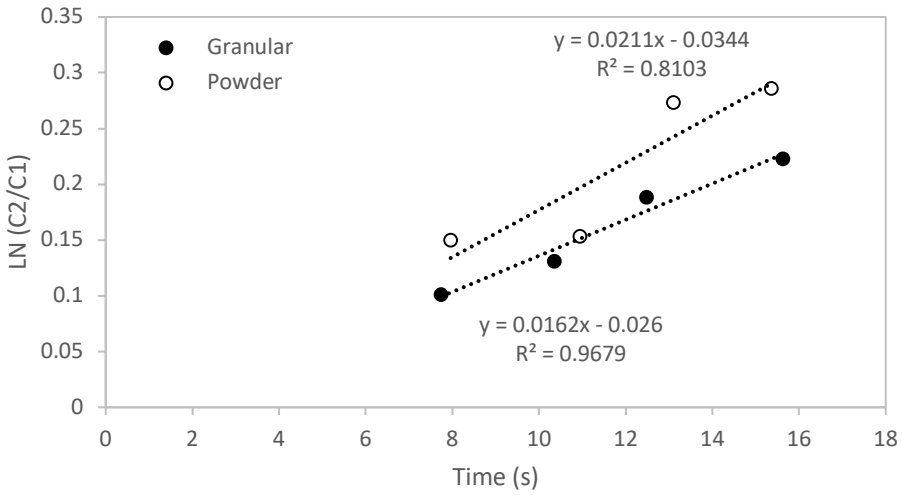

Figure 4.6 Dissolution kinetic plots of ln (C2/C1) vs time for granular and powder paracetamol in a twin screw extruder

Achieving full dissolution

From Figure 4.5, it is seen that the granular paracetamol does not fully dissolve within the residence time of the barrel. The target concentration for full dissolution at the set feed rates (2.5 g min^{-1} solid and 29 g min^{-1} liquid) is 8.6 g (paracetamol)/100 g (solvent). This was achieved for powder grade but not for granular where only 6.9 g (paracetamol)/100 g (solvent) was dissolved. The dissolution rate constant for granular is lower than powdered material – so need longer residence time. Several operational parameters in the TSE can however be manipulated to afford full dissolution, including liquid flow rate, solid feed rate, screw speed, screw configuration and barrel temperature. These parameters are investigated in turn.

4.3.2.3 Effect of Liquid Flow Rate

The solid feed rate was fixed at 2.5 g min^{-1} as this feed rate provided a consistent output concentration from the feeder. The solution temperature was fixed at 40˚C, this highest

temperature which would allow the fastest dissolution rate and still be comparable with the dissolution experiments in the STV. Figure 4.7 shows the dissolution concentrations for various liquid flow rates from 15 to 35 g min^{-1}. Increasing liquid flow rates to achieve sink conditions results in a higher driving force for dissolution but reduces the residence time for mixing within the barrel as the degree of screw fill is higher. Increasing the liquid feed rate decreases the concentration of the output solution and does not achieve full dissolution of the solute. Solvent flow affects the dissolution process by physical abrasion of the solid, thereby reducing the diffusion layer thickness around each particle (Tingstad and Riegelman, 1970). The decrease of liquid flow rate increases the residence time within the barrel from 11 to 15 seconds allowing more time for dissolution. Table 4.2 shows the correlations between the solid/liquid feed rates and concentrations.

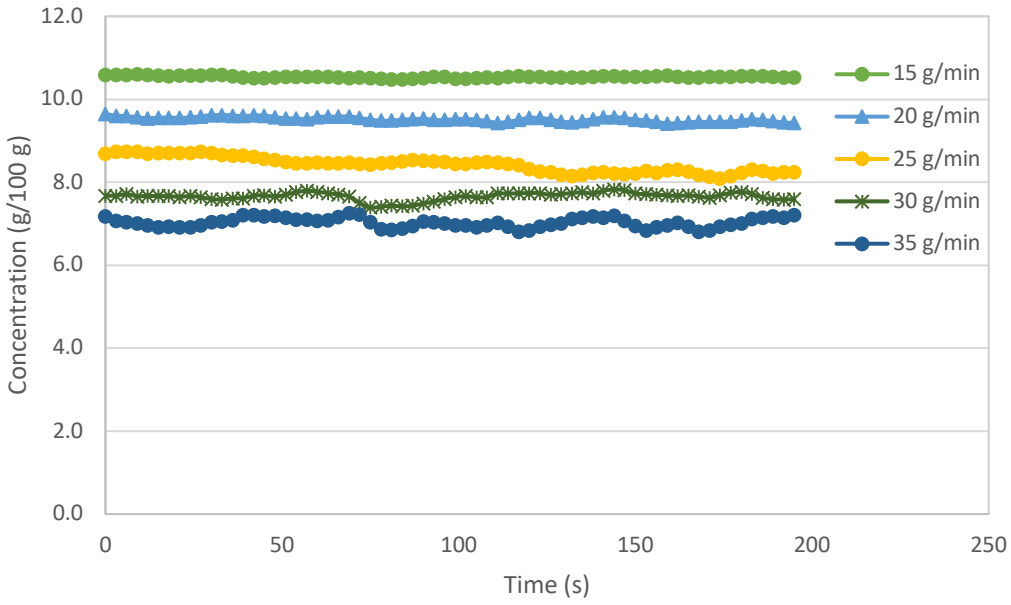

Figure 4.7 Concentration-time history of granular paracetamol in water/IPA (80:20)post TSE at varying liquid flow rates (Temp=40°C, solid feed rate = 2.5 g min^{-1}).

Table 4.2 Correlations between concentrations and liquid flow rate at fixed solid feed rates for dissolution in a twin screw extruder

Solid flow rate (g/min)	**Liquid flow rate (g/min)**	**Target Concentration at full dissolution (g solute/100 g solvent)**	**Actual Concentration (g solute/100 g solvent)**	**Maximum Dissolution Achieved**	**% Dissolved**
2.5	15	10.7 (saturated)	10.6	Yes	99
2.5	20	10.7 (saturated)	9.6	No	90
2.5	25	10.0	8.4	No	84
2.5	30	8.3	7.7	No	93
2.5	35	7.1	6.5	No	92

In a batch system, the dissolution rate is higher at low concentration levels of undersaturation (sink conditions). However, in a continuous system, higher liquid flow rates are required to achieve sink conditions, but as this reduces the residence time, the dissolution rate does not increase in the same way as in a batch system. Therefore, when designing a continuous dissolution system lower liquid flow rates are desired.

4.3.2.4 Effect of Solid Feed Rates

At a fixed liquid flow rate of 30 g min^{-1} (at which full dissolution was not achievable) and at a fixed solution temperature of 40 ˚C, Figure 4.8 shows the effect of varying solid feed rates on the dissolution concentration. Increasing the solid feed rate increases the concentration of the output solution but does not achieve full dissolution of the solute. The free volume of the extruder is reduced as the solid feed rate is increased due to the pitch of the screws being filled with a greater volume of material. This decreases the mas transfer and the available volume for contact between solute and solvent molecules. Decreasing the solid feed rate from 3.33 g min^{-1} to 1.05 g min^{-1} decreases the saturation level of the solution and the degree of screw fill. The TSE is a starve fed system hence when the throughput is decreased at constant rpm more mixing occurs as the materials being processed have a longer residence time in the mixing elements. Full dissolution was achieved at 1.67 g min^{-1}. Table 4.3 shows the correlations between the solid/liquid feed rates and concentrations.

Drug development studies are often carried out with limited amount of materials, the lowest feed rate of solids is thus of significant interest for this type of work. The present results show that the lowest feed rate of solids for the TSE producing consistent concentrations measurements at the exit was 1.67 g min^{-1}. Observations in this study indicate more variability in the exit concentration with decreasing feed rate.

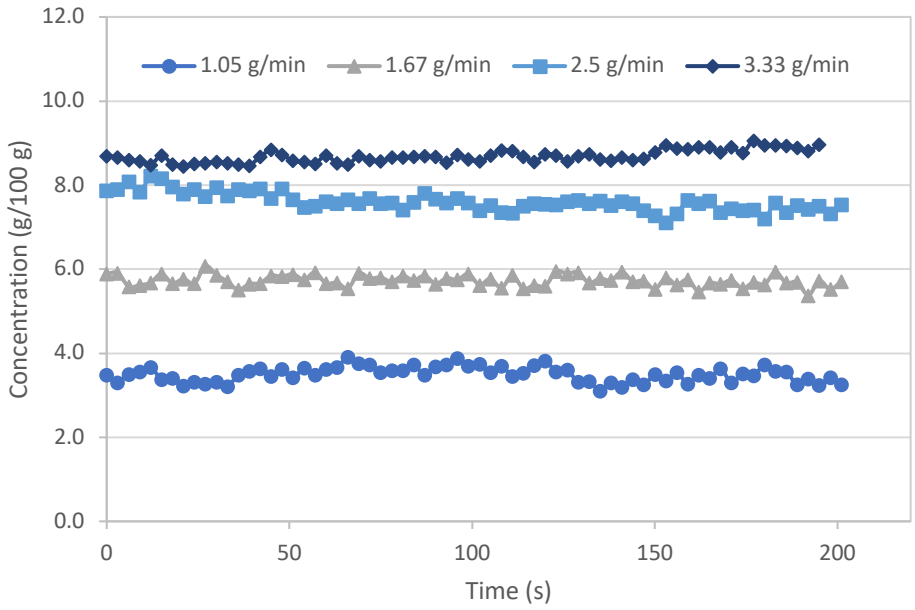

Figure 4.8 Concentration-time history of granular paracetamol in water/IPA (80:20)post TSE at varying solid feed rates (Temp=40°C, liquid flow rate = 30 g min^{-1})

Table 4.3 Correlations between concentrations and solid feed rate at fixed liquid flow rates for dissolution in a twin screw extruder

Solid feed rate (g/min)	Liquid flow rate (g/min)	Target Concentration at full dissolution (g solute/100 g solvent)	Actual Concentration (g solute/100 g solvent)	Maximum Dissolution Achieved	% Dissolved
3.33	30	10.7 (saturated)	8.7	No	81
2.5	30	8.3	7.6	No	92
1.67	30	5.6	5.7	Yes	100
1.05	30	3.5	3.5	Yes	100

When designing a continuous dissolution system, it is desirable to have low solid feed rates as this optimises mixing and residence time within the barrel hence enhances the dissolution rate.

4.3.2.5 Effect of Screw Speed

The screw in the TSE conveys the solids forward and the speed of which can affect dissolution rate. The investigations were carried out for the screw speed from 100 to

500rpm (50 rpm resulted in accumulation of solids at the input port) at a fixed liquid flow rate of 30 g min^{-1}, a fixed solid feed rate of 2.5 g min^{-1} and a solution temperature of 40˚C. The target concentration for full dissolution at the set feed rates is 8.3 g (paracetamol)/100 g (solvent). Complete dissolution was not achieved in the previous tests at these feed rates therefore the effect of screw speed can be identified using these same settings. While shear mixing, and power consumption intensify with the increase of the screw speed, allowing solute molecules to encounter fresh solvent molecules faster, dissolution rate does not change significantly, and complete dissolution of granular paracetamol was not achieved by increasing the screw speed alone. This is due to the fact that the residence time of the solute within the barrel is reduced as the screw speed is increased (see Table 4.4). The screws are configured using conveying elements which forward material along the barrel, preventing material build up and blockages. When the screw speed is increased, the material is conveyed forward along the length of the screws at a faster rate thus the material exits the barrel within a shorter time, which reduces the time available for dissolution. Therefore higher screw speeds are counterproductive when the TSE is used for dissolution processes.

Table 4.4 Effect of screw speed on residence time of dissolution in a twin screw extruder

Screw Speed (rpm)	Mean Concentration of Paracetamol in Solution (g 100 g^{-1})	Residence Time (s)
100	7.9	13.2
200	7.1	8.8
300	7.5	6.9
400	7.8	6.7
500	8.1	6.0

Continuous dissolution systems are optimised at low screw speeds due to maximum residence time.

4.3.2.6 Effect of screw configuration

The twin screws in the TSE are made up of individual elements of either concave conveying or bi-lobe mixing (see Figure 4.9a), delivering different shear energy to the materials. The effect of the screw configuration on dissolution was investigated by using one, two and three mixing elements at the discharge (left) end of the screws (Figure 4.9b), i.e. at Ports 5 and 6 (Figure 4.3). The dissolution history is shown in Figure 4.10. Adding mixing elements to the screw configuration increases dissolution, more for Ports 6-5 than the earlier ones, due to the increase in shear mixing. The impact on residence time of

solute within the barrel was < 2 seconds. Complete dissolution of the granular paracetamol was not attained for any mixing elements, however more consistent concentration of solution is obtained with more mixing elements.

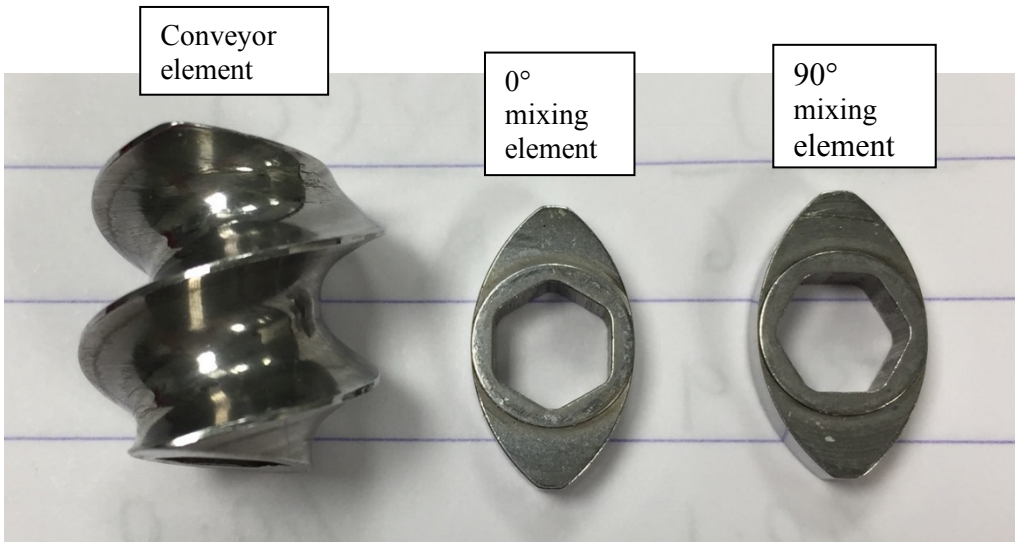

(a)

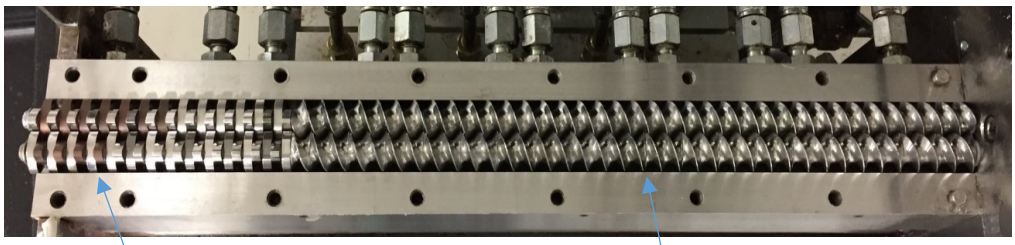

(b)

Figure 4.9(a) - Conveying and Mixing Elements, (b) twin screws within the barrel

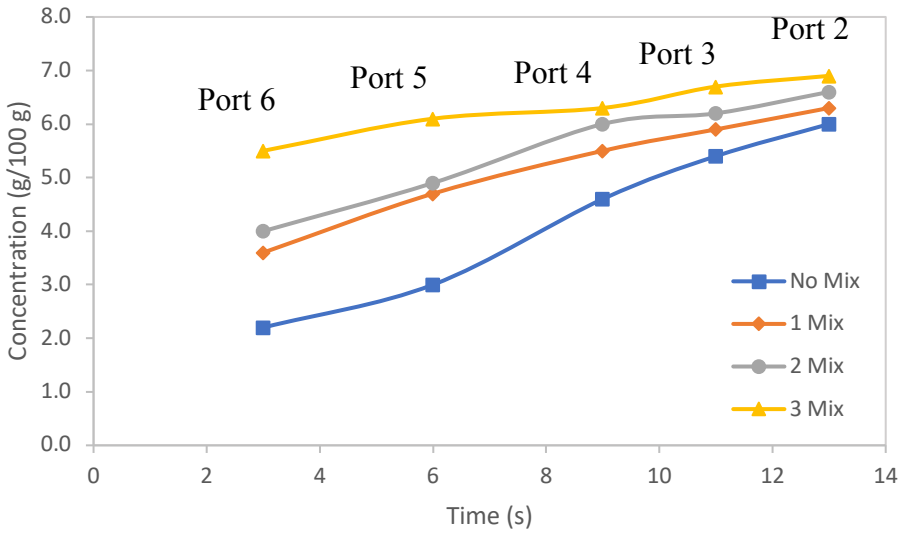

Figure 4.10 Effect of adding mixing elements on dissolution history post TSE at each port (Temperature = 40˚C, solid feed rate = 2.5 g min^{-1}, liquid flow rate = 30 g min^{-1}, screw speed = 100 rpm)

Overall, adding mixing elements in the screw configuration will increase dissolution within the barrel, as can be seen at Port 2 in Figure 4.10. The impact of the mixing section is more notable at Port 6 where these elements were located. Thereby for larger particle material it is beneficial to include mixing sections within the screw configuration. The size and location of these sections is a recommendation for future work.

4.3.2.7 Effect of Barrel Temperature

The barrel is effectively a heating jacket and temperatures in each of the sections (Port 2 to Port 6) can individually or collectively be controlled. Figure 4.11 shows the effect of barrel temperature on dissolution from room temperature to 75°C. It is expected that an increase in barrel temperature enhances dissolution and full dissolution of the granular paracetamol was achieved when the barrel temperature reached 60°C.

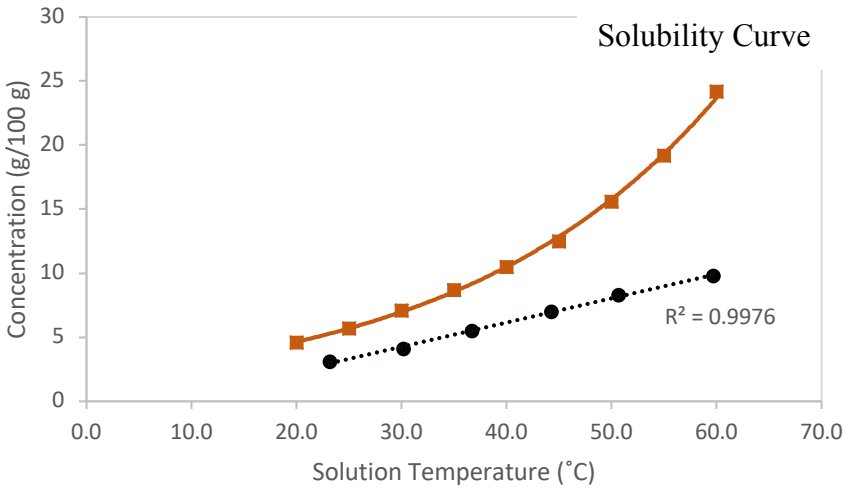

Figure 4.11 Effect of barrel temperature on dissolution of paracetamol post TSE (solid feed rate = 2.5 g min^{-1}, liquid flow rate = 30 g min^{-1}, screw speed = 100 rpm), Solubility curve overlaid

In summary, the flow rates of either liquid or solid together with the barrel temperature can lead to complete dissolution of granular paracetamol. Hence when designing a continuous processing system, the temperature and residence time should be optimised. Solubility curves can be used to predict the temperature of heating barrel.

4.3.2.8 Batch v Continuous Dissolution

Dissolution of solid materials in a batch vessel is the current norm for feeding in the pharmaceutical industry, the same dissolution experiments were carried out in a stirred tank (temp = 40 ˚C, agitation rate = 750 rpm, mass of solute = 83 g, mass of solvent = 1000 g) and compared to the dissolution histories in Figure 4.12. It is clear that dissolution is much faster in the TSE than that in the stirred tank vessel, e.g. 13 seconds to dissolve 83g of paracetamol vs. 126 seconds to dissolve the same. The increase in the dissolution rate in the TSE is due to much more aggressive local shear mixing and higher thermal energy generated by the rotation of the screws (Thiry et al., 2015). This also delivers good uniformity of the solute in the solution.

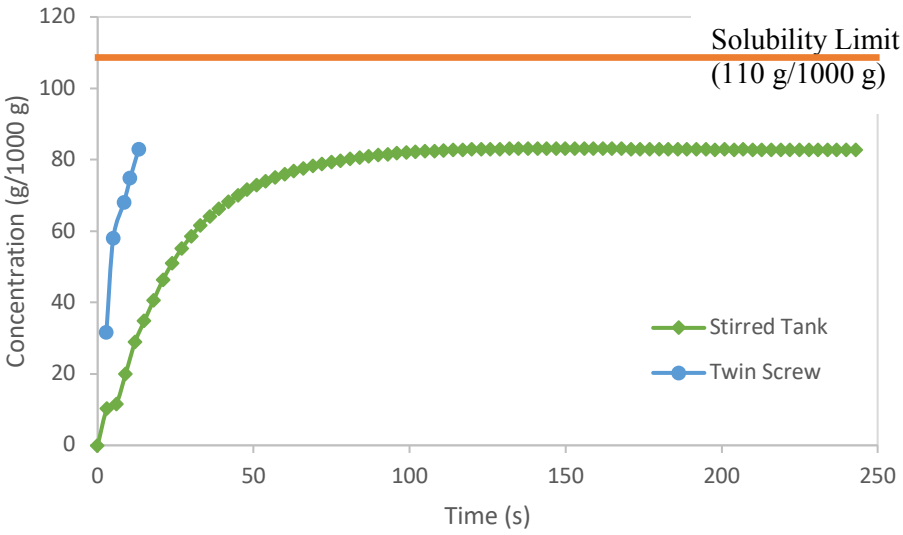

Figure 4.12 Dissolution history of granular paracetamol in water/IPA (80:20) at 40˚C according to two methods(stirred tank vessel and twin screw extruder)

Table 4.5 Dissolution rate constants from a stirred tank vessel and a twin screw extruder

	Dissolution Rate constant, k (s^{-1})	**Dissolution rate constant per power density ($m^3\ W^{-1}\ s^{-1}$)**
Stirred Tank	0.0175	5.48×10^{-6}
Twin Screw Extruder	0.0441	7.39×10^{-6}

The dissolution rate constants are given in Table 4.5 for both devices, however power density should be the basis for such a comparison. The power density of stirred tanks is well reported (Sinnott, 1999, Garside and Davey, 1980) as Equation (4.1):

$$\frac{P}{V} = \frac{P_O \rho {N_s}^3 D_S^5}{V_L} \tag{4.1}$$

where P/V is the power density (W m^{-3}), ρ the fluid density (kg m^{-3} at 40 °C), N_s the speed of the stirrer (rps), D_S the diameter of the stirrer (m), V_L the volume of liquid in the STV (m^3) and P_O the dimensionless power number of the agitator, which was estimated as 2.3 based on data presented by Nienow and Miles (Nienow and Miles, 1971) for the type of impellor used in our work.

Previous estimations of power density in a twin screw extruder (Meijer and Elemans, 1988, Kruijt et al., 2001) were based on a non-isothermal melt and a non-Newtonian fluid, covering various conditions including melt temperatures, feed rates and scale of equipment. However, the definition of power density from previous work differs from this work in that here it is the power dissipated into the liquid or power experienced by the liquid that is estimated, not the power input by the motor as in previous power consumption calculations. By treating the twin screw extruder as a stirred tank working horizontally, we could estimate the power dissipation as follows. The diameter of the stirrer in Equation (4.1) becomes the diameter of the screw, while the rotational speed remains the same. There is no similar power number for the twin screw, but the helical screw impellor is the closest. In terms of the liquid volume, only half of the liquid in the TSE is experiencing the effect of shearing imposed by the twin screws at any given time, as the screw pitch is only 45% filled (see Appendix B 7.2.4) (Martin, 2013).

Applying these values to Equation (4.1), the power density for the stirred tank and the TSE are 3196 and 5968 W m^{-3} respectively. It is observed that faster dissolution rate is

achieved in the TSE and cannot be explained by consideration of the power density alone. Other factors influencing the dissolution rate include the short mass transfer distances and the efficient shear mixing in the TSE.

Start up and shut down losses encountered in this work were low. It took approximately 90 seconds to reach steady state on starting the equipment from empty which equates to losses of approximately 3 g solid and 50 ml solvent. On shutdown the material remaining in the barrel equates to losses of approximately 1g of solid and 8 ml of solvent.

4.4 Conclusions

In this work, it has been demonstrated that the twin screw extruder enables the decoupling of liquid from the solid feed, thus eliminating any potential fouled solid feeding even at low solid feed, e.g. 1.05 g min^{-1}. It also allows the controlled and synchronised input flows, together with intense mixing, to deliver either a dissolved solution or suspension of controlled composition ready for the next unit operation in the process train. These are the novelties of this work, they fill the gap for continuous reaction and crystallisation in the pharmaceutical industry. This study also highlights the flexibility of the TSE to cope with different raw material feed stocks; achieving full dissolution of powder paracetamol within the residence time of the TSE and achieving full dissolution of granular paracetamol by altering key variables such as solid or liquid feed rates and barrel temperature.

For the first time, an alternative method has been proposed of estimating the power density for the TSE when used as a continuous dissolution feed stream. This enables a fair comparison of the dissolution rates between two devices, i.e. TSE and stirred tank. The faster dissolution rate in the TSE is associated with higher power dissipation

generated by the aggressive shear mixing and thermal energy within the barrel. The dissolution rate constant per power density in the TSE is slightly more favourable than that in the stirred tank. In addition, the variability in the output concentration in the former (1%) is much less than that in the latter (up to 10%) (Faanes and Skogestad, 2003).

The general conclusions made are the TSE is a feasible set up for continuous dissolution of solid material of varying particle size and particle size distribution. Design of a dissolution system should incorporate screw configuration with defined mixing elements for large particles, low solid and liquid feed rates, and low screw speed to maximise residence time. Barrel temperatures can be determined from predictions using solubility curves.

Chapter 5 **Investigation of dissolution rates of acetylsalicylic acid, benzoic acid, nicotinic acid, and paracetamol in a stirred tank vessel and a twin screw extruder**

Previous chapters have investigated the dissolution of paracetamol in both a batch and a continuous system and shown how the TSE can be successfully used to continuously dosed solids with complete dissolution within the residence time of the barrel. In the following chapter the feasibility of using the TSE for a range of solubilities is examined. This chapter is submitted to the Journal of Pharmaceutical Development and Technology in January 2019.

5.1 Introduction

Four materials (acetylsalicylic acid, benzoic acid, nicotinic acid, and paracetamol) have been chosen with varying physical and chemical properties including particle size, density, and solubility, which contribute to the flowability and dissolution rate of the material. Chemical structures are shown in Figure 5.1.

This work examines how fast different classes of materials dissolve and the impact on the dissolution rate of these classes of material when comparing batch with continuous dissolution.

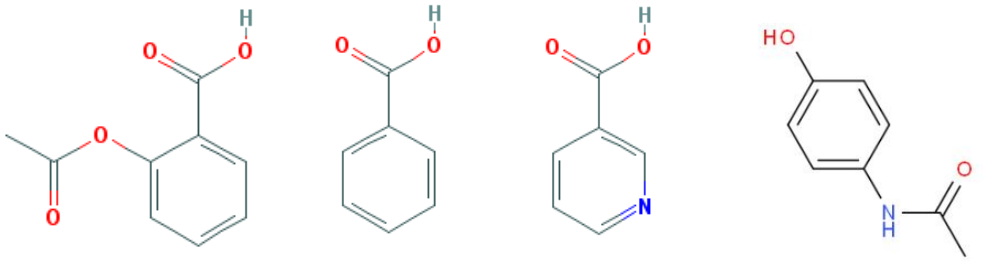

(a) (b) (c) (d)

Figure 5.1 Chemical Structure of (a) Acetylsalicylic Acid, (b) Benzoic Acid, (c) Nicotinic Acid, (d) Paracetamol

5.2 Experimental Preparation and Procedures

5.2.1 Materials

The solvent composition used in this study was a water/IPA (80:20) mixture. Acetylsalicylic acid (white powder with purity ≥99.0%), benzoic acid (white crystalline powder with purity ≥99.5%) and nicotinic acid (3-pyridinecarboxylicacid) (white powder with purity ≥98%) were supplied by Merck. Paracetamol (white powder of 99% purity) was supplied by Mallinckrodt Chemical Limited (UK).

The mean particle size and particle size distributions (see Figure 5.2) were analysed by a Mastersizer (HYDRO, Malvern 3000) and given in Table 5.1. The samples were dispersed in hexane and added directly to the particle sizer. Benzoic acid has the largest mean size, while nicotinic acid the smallest.

Table 5.1 Particle sizes of acetylsalicylic acid, benzoic acid, nicotinic acid and paracetamol using laser diffraction

	Dx (10) (µm)	Dx (50) (µm)	Dx (90) (µm)
Benzoic Acid	813	1460	2510
Acetylsalicylic Acid	338	700	1550
Paracetamol Powder	12.6	44.9	124
Nicotinic Acid	11.6	30.9	72

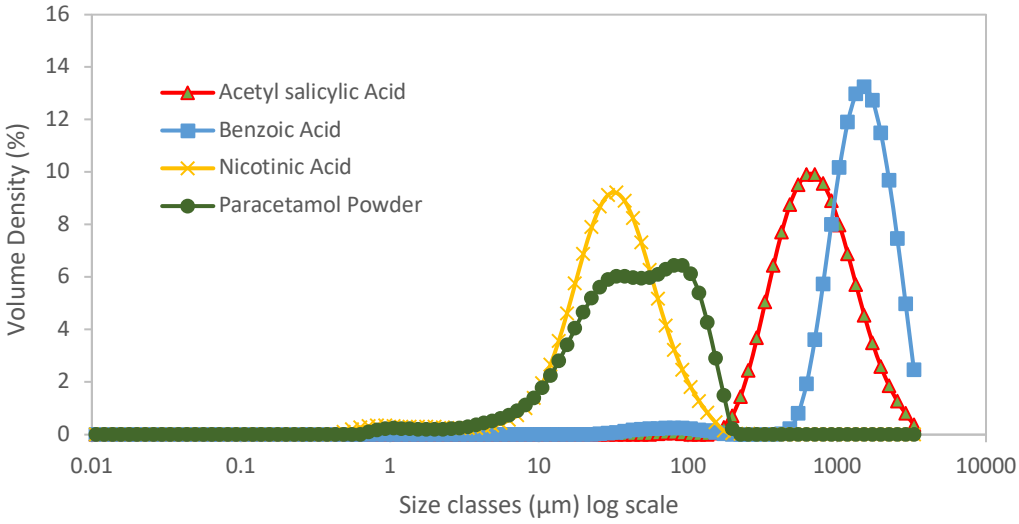

Figure 5.2 Particle size distribution of acetylsalicylic acid, benzoic acid, nicotinic acid and paracetamol using laser diffraction

Scanning Electron Microscopy (SEM) Analysis

SEM analysis was carried out for each API using a Quanta 3D FEG and is presented in Figure 5.3, where benzoic acid is off flake shape, while acetylsalicylic acid is the column shaped.

These materials have a range of polarity, hydrogen bonding ability and solubility as shown in Table 5.2.

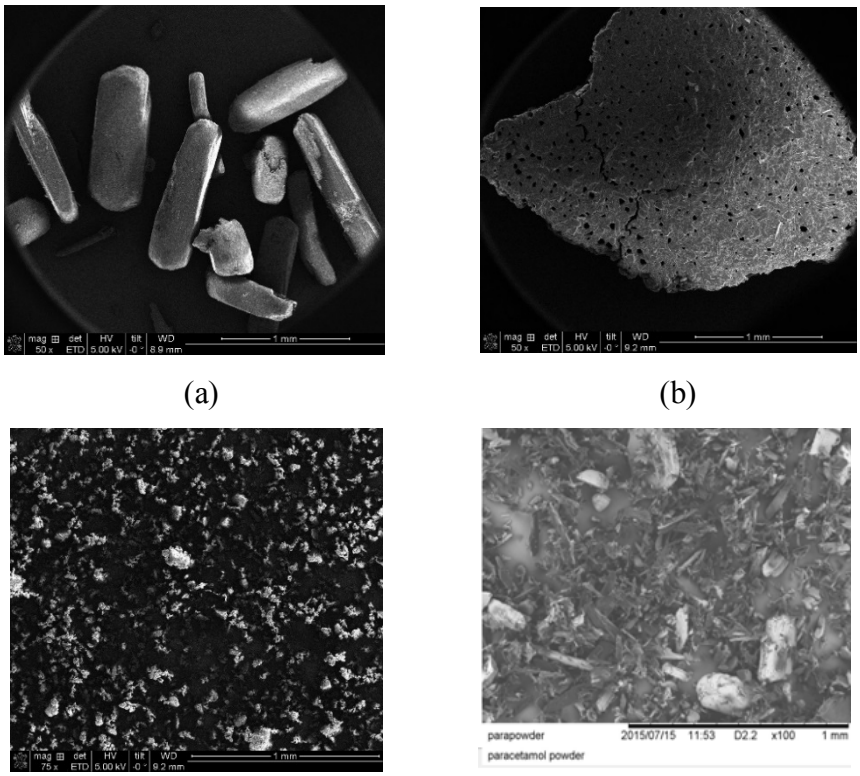

Figure 5.3 SEM images of (a) Acetylsalicylic Acid (x50 magnification), (b) Benzoic Acid (x50 magnification), (c) Nicotinic Acid (x75 magnification), (d) Paracetamol powder (x100 magnification) using 1mm scale

Table 5.2 Chemical and physical properties of acetylsalicylic acid, benzoic acid, nicotinic acid and paracetamol

	Acetylsalicylic Acid	Benzoic Acid	Nicotinic Acid	Paracetamol
Hydrogen Bond Donor Count	1	1	1	2
Hydrogen Bond Acceptor Count	4	2	3	2
Topological Polar Surface Area (A^2)	63.6	37.3	50.2	49.3
Solubility in water at 25°C (mg ml^{-1})	4.6	2.9	18	15

5.2.2 Methods

5.2.2.1 Solubility

Solubility of each API in a water/IPA (80:20) mixture has been determined by a gravimetric method. A known weight of API was added to a conical flask containing 100g of solvent mixture. The flask was placed in a water bath to maintain the temperature and stirred until all solids had dissolved. Further known weights of API were added until no further dissolution had occurred. The excess solid was filtered off, dried and weighed to determine the saturation concentration.

5.2.2.2 Dissolution Studies in Stirred Tank Vessel

The methodology for dissolution in a stirred tank vessel is described in Chapter 3. For each experimental run, 1000g of solvent was added to the STV and heated/cooled to the desired temperature (40°C), 63g of API was weighed using an electronic balance and was poured into the vessel using a funnel, to minimise loss, giving a target solution concentration of 6.3 g (solute)/100 g (solvent). The solution was held at temperature and stirred under a fixed rotational speed (500 rpm) until dissolution was complete isothermally. Solute concentration was measured, and dissolution rates determined.

5.2.2.3 Dissolution Studies in Twin Screw Extruder

The methodology for dissolution in a twin screw extruder is described in Chapter 4. A rigid frame laboratory scale feeder with twin concave screws suitable for low feed rates of high bulk density materials was used to dose benzoic acid and acetylsalicylic acid, while a universal flexible wall feeder with a single spiral screw suitable for materials with poor flowability and low bulk density was used to dose powder paracetamol and nicotinic acid.

The API was continuously dosed into the TSE using the LIW feeder at a feed rate of 2.5 g min^{-1} and the solvent (Water/IPA 80:20) at a flow rate of 40 g min^{-1}, giving a target solution concentration of 6.3 g (solute)/100 g (solvent). This is equivalent to the target concentration in the STV.

5.3 Results and Discussion

5.3.1 Solubility

Benzoic acid and acetylsalicylic acid are aromatic carboxylic acids, nicotinic acid is a pyridine carboxylic acid and paracetamol is a phenol (4-aminophenol) as shown in Figure 5.1. The aromatic carboxylic acids have the lowest solubility in water (see Table 5.2), while the pyridine carboxylic acid and the amino phenol classes have greater solubility due to the nitrogen atom in their chemical structure. The increased hydrogen bonding ability of acetylsalicylic acid which has 4 hydrogen bond acceptors enables greater solubility in water than benzoic acid which has 2 hydrogen bond acceptors. This is also the case for nicotinic acid which has 3 hydrogen bond acceptors whereas paracetamol has only 2, with lower solubility in water than nicotinic acid. These are reflected in the solubility graph in Figure 5.4 where a water/IPA (80:20) mixture is used as solvent. Paracetamol has the highest solubility, with nicotinic acid having the lowest solubility.

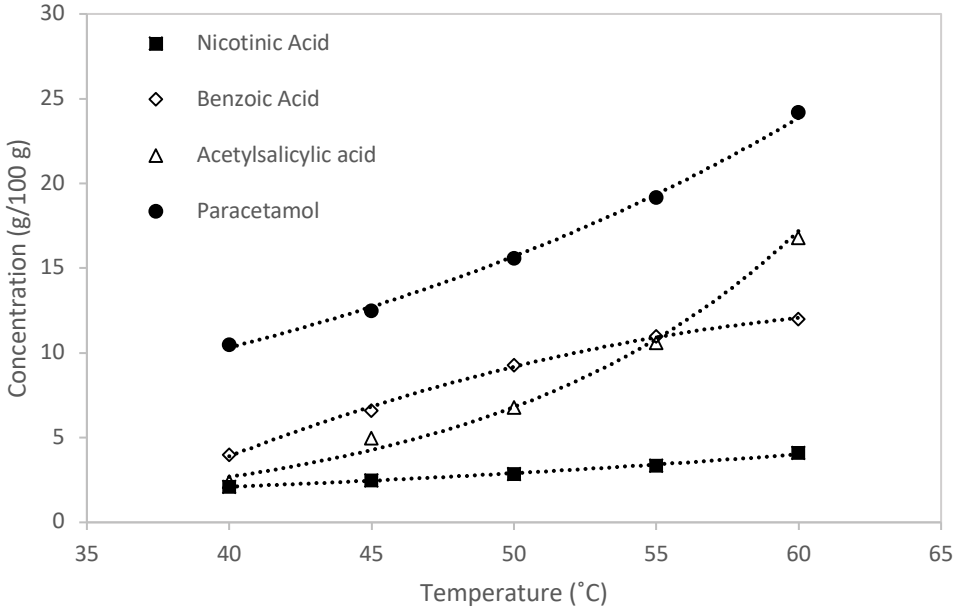

Figure 5.4 Solubility of acetylsalicylic acid, benzoic acid, nicotinic acid and paracetamol in water/IPA (80:20)

Figure 5.4 also shows the effect of temperature on solubility for each API. The solution process absorbs energy and the solubility increases as the temperature increases, for benzoic acid however, the solubility history is rather different from the rest, which is consistent with previously published work by Humayun (Humayun et al., 2016).

5.3.2 Calibrations

Calibration curves were generated by measuring the absorbance of known amounts of each API in water/IPA (80:20) at 40˚C, as seen in Figure 5.8; these were subsequently used to determine the concentration of solute in solution for each dissolution test. Maximum absorbance peak was 248 nm for paracetamol, 197 nm for benzoic acid, 199 nm for acetylsalicylic acid, and 193 nm for nicotinic acid.

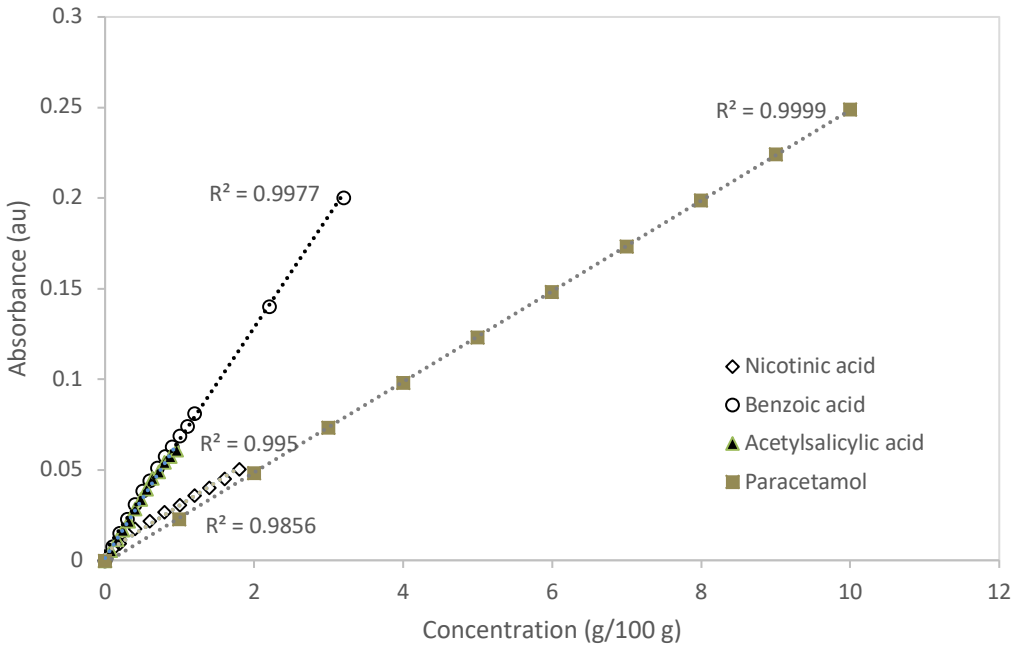

Figure 5.5 Calibration curves of acetylsalicylic acid, benzoic acid, nicotinic acid and paracetamol in water/IPA (80:20)(Temperature = 40 ˚C)

5.3.3 Dissolution Tests

Dissolution tests were carried out firstly in the STV and then in the TSE using the four APIs.

5.3.3.1 Dissolution in STV

Figure 5.6 shows the dissolution history for paracetamol, benzoic acid, acetylsalicylic acid and nicotinic acid. Three runs were carried out for each API in the dissolution tests to ensure good repeatability. Equilibrium solubility at 40˚C is given in Table 5.3.

Table 5.3 Solubility of acetylsalicylic acid, benzoic acid, nicotinic acid and paracetamol in water/IPA (80:20) at 40˚C

	Solubility (g/100 g)
Paracetamol	10.5
Benzoic acid	4.0
Acetylsalicylic acid	2.4
Nicotinic acid	2.1

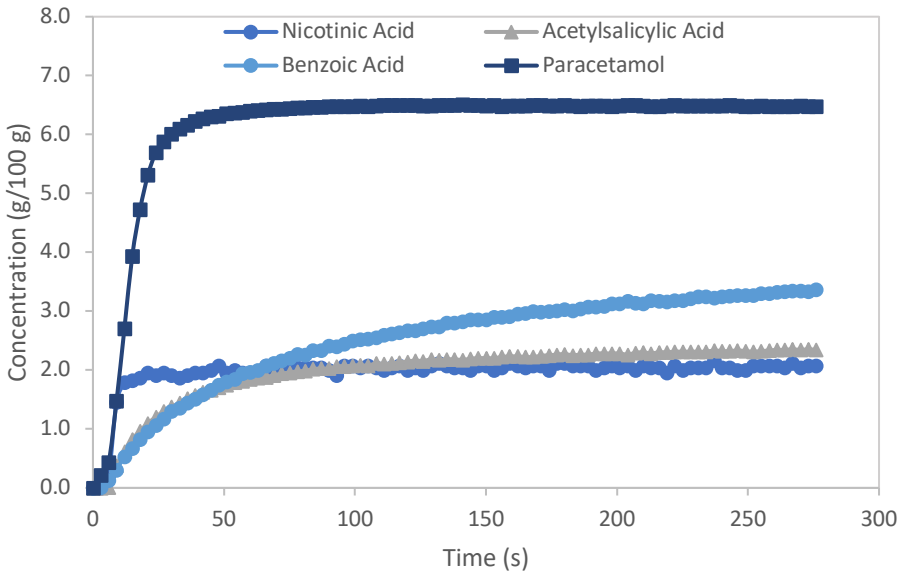

Figure 5.6 Dissolution history of acetylsalicylic acid, benzoic acid, nicotinic acid and paracetamol in water/IPA (80:20) at 40˚C in a stirred tank vessel

It can be seen that complete dissolution was obtained for paracetamol while a supersaturated solution was obtained for benzoic acid, acetylsalicylic acid and nicotinic acid. The initial concentrations from the dissolution historiess (up to the plateau) were used to extract the dissolution kinetics. Fitting each dissolution history to first order kinetics, Equation (2.8) confirms the same kinetic mechanism exists for all APIs. This suggests that the mechanism of dissolution for all APIs is largely the same in aqueous solution. The respective dissolution rate constants are given in Table 5.4.

These materials have different wetting characteristics which affects both the time to wet the material and the time to achieve dissolution. The time to wet was 3 seconds for paracetamol, 6 seconds for nicotinic acid, 6 seconds for benzoic acid and 9 seconds for acetylsalicylic acid; the subsequent dissolution time is 42 seconds for paracetamol, 21 seconds for nicotinic acid, 93 seconds for acetylsalicylic acid and 189 seconds for benzoic acid. This suggests that wetting characteristics are not a dominant factor in bulk solid dissolution. The faster dissolution rates for paracetamol and nicotinic acid are comparable to work in previous chapters where powders with narrow particle size distribution (see Figure 5.2) and small particle size (see Table 5.1) enhanced the dissolution rate due to larger surface area. Conversely, benzoic acid and acetylsalicylic acid have broad particle size distribution and larger particles which contribute their slower dissolution rates.

5.3.3.2 Twin Screw Extruder

A complete set of sequential runs were undertaken for liquid entering at each port, e.g. Run 1 at Port 6, Run 2 at Port 5, Run 3 at Port 4, (see Figure 4.3) and so on. Compiling the output concentrations at each port (see Appendix A 7.1.5), the dissolution histories were assembled, Figure 5.7. Note that each concentration measurement was repeated 3 times and the data in Figure 5.7 are the averaged value from three repeats. Error bars are

not shown on the graph as they are too small to see clearly. The averaged standard error was 0.1.

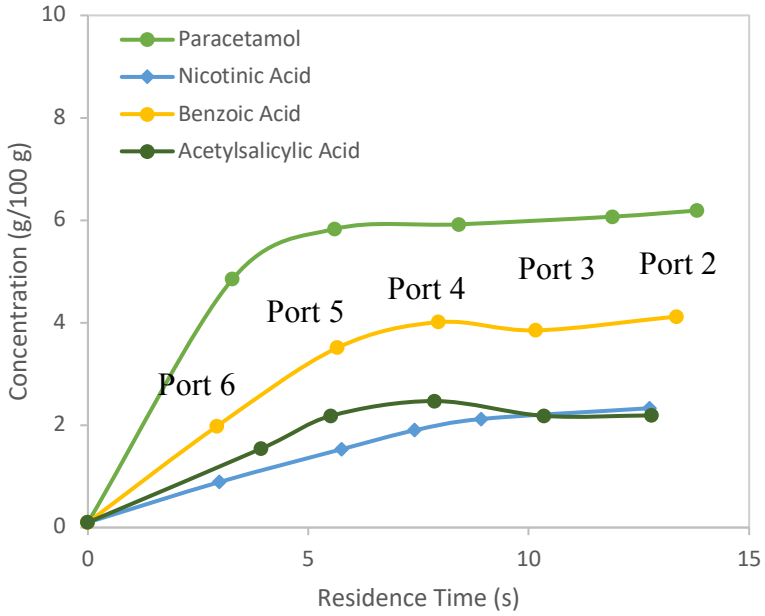

Figure 5.7 Concentration-time history for acetylsalicylic acid, benzoic acid, nicotinic acid and paracetamol dissolution at exit of a twin screw extruder (Temperature = 40˚C, solid flow rate = 2.5 g min-1, liquid flow rate = 40 g min-1)

Figure 5.7 shows that complete dissolution was obtained within the residence time of the barrel (14 seconds) for paracetamol where the concentration at the exit was 6.2 g per 100 g solvent. Benzoic acid, acetylsalicylic acid and nicotinic acid did not fully dissolve within the residence time of the barrel with the concentration at exit of 4.1 g, 2.2 g, and 2.3 g per 100 g solvent, respectively. This is consistent with the dissolution tests in the STV however the dissolution is faster in the TSE as the time taken to wet and dissolve particles is overcome by mechanical forces in the TSE.

5.3.4 Dissolution Kinetics

The rate constant of dissolution *k* was determined using the same methodology as used in STV, the comparison of the dissolution rate constants is given in Table 5.4.

Table 5.4 Dissolution rate constants for acetylsalicylic acid, benzoic acid, nicotinic acid and paracetamol in water/IPA (80:20) at 40˚C in a stirred tank vessel and a twin screw extruder

	Dissolution Rate constant, k (s^{-1})	**Dissolution Rate constant, k (s^{-1})**
	STV	**TSE**
Paracetamol	0.037	0.119
Nicotinic Acid	0.031	0.037
Benzoic Acid	0.018	0.072
Acetylsalicylic Acid	0.014	0.073

63 g of API in 1000 g of solvent was used as the basis for comparison because this was the lowest solid flow rate for the TSE. At these fixed solid and liquid feed rates and based on the solubilities of the APIs, it resulted an undersaturated solution for paracetamol and supersaturated solutions for benzoic acid, acetylsalicylic acid and nicotinic acid, as shown in Table 5.4. These would affect the dissolution rates and the degree of saturation was taken into account; the dissolution rate constants of benzoic acid, acetylsalicylic acid and nicotinic acid were recalculated by extrapolation with respect to

the same undersaturation of paracetamol assuming a linear relationship in solubilities and re-tabulated in Table 5.5 (see Appendix B 7.2.2).

Table 5.5 Dissolution rate constants at fixed saturation level for acetylsalicylic acid, benzoic acid, nicotinic acid and paracetamol in water/IPA (80:20) at 40˚C in a stirred tank vessel and a twin screw extruder

			STV	**TSE**
	Saturation Level	% Saturation	Dissolution Rate constant, k (s^{-1})	Dissolution Rate constant, k (s^{-1})
Paracetamol	Undersaturated	67	0.037	0.119
Nicotinic Acid	Supersaturated	200	0.041	0.049
Benzoic Acid	Supersaturated	58	0.039	0.155
Acetylsalicylic Acid	Supersaturated	163	0.020	0.103

It is now seen that the dissolution rates are similar for each material in the stirred tank. However the more aggressive local shear mixing and higher thermal energy generated by the rotation of the screws (Thiry et al., 2015) had a greater impact on disintegrating the particles and enhancing the dissolution rates in the TSE. This also delivers good uniformity of the solute in the solution. In terms of dissolution time, it took 14 seconds to dissolve 62g of paracetamol in the TSE vs 42 seconds in the stirred tank vessel to dissolve the same amount of API. Dissolution within the short residence time of the TSE is

feasible for slowly dissolving materials. The dissolution rate can be enhanced by increasing the barrel temperature using predictions from the solubility curves.

5.3.5 Achieving complete Dissolution

From Figure 5.7, we see that complete dissolution was not achievable at these solid feed rates for benzoic acid, acetylsalicylic acid and nicotinic acid. From the solubility graph in Figure 5.4, increasing the solution temperature enables fuller dissolution. Complete dissolution was attained for benzoic acid and acetylsalicylic acid when the temperature of the output solution increased from 40 to 50 ˚C, by increasing the barrel temperature, as shown in Figure 5.8.

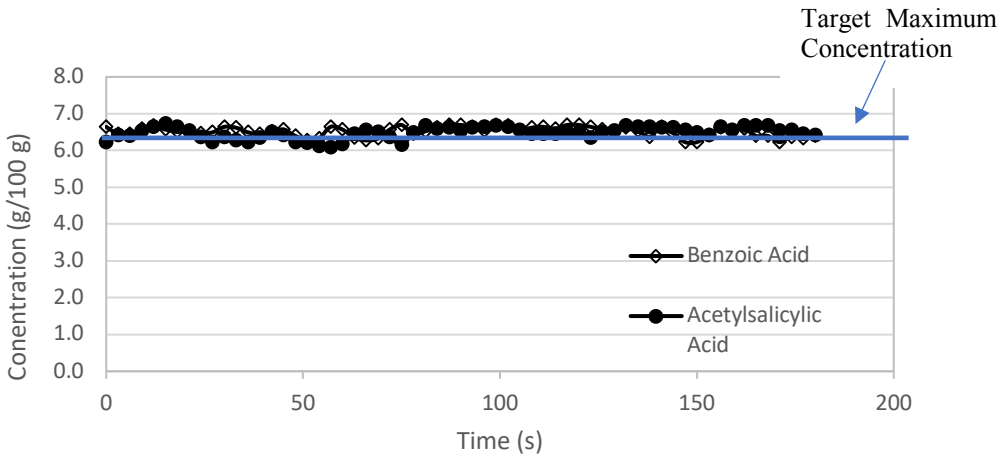

Figure 5.8 Dissolution history of benzoic acid and acetylsalicylic acid in water/IPA (80:20) at exit of a twin screw extruder (Temperature = 50˚C, solid flow rate = 2.5 g min^{-1}, liquid flow rate = 40 g min^{-1})

At the solution temperature of 50 ˚C, however, complete dissolution of nicotinic acid was still not reachable. It was demonstrated in Chapter 4 that operational parameters, including liquid flow rate, solid feed rate, screw speed, screw configuration and barrel temperature, can also affect dissolution rate within the TSE, but none of the above resulted in complete dissolution within the residence time of the barrel, instead a slurry

was obtained with good homogeneity, e.g. the error of mass balance between the input and exit was 0.49 % RSD.

The solubility of nicotinic acid was investigated in a selection of solvent systems (see Table 5.6) to determine if 6.3g of nicotinic acid could dissolve in 100g solvent to match the concentration required at the exit of the TSE. A solvent screen prediction provided from COSMOtherm software ranks the solvent by solubility. This predicted that nicotinic acid is more soluble in dimethyl sulfoxide (DMSO) than in IPA, which is consistent with previously published work by Gonçalves on the solubility of nicotinic acid (Gonçalves and Minas da Piedade, 2012).

Table 5.6 Solubility of nicotinic acid in water, IPA, and DMSO mixtures at 40˚C

Solvent System	
Water	Insoluble
Water/IPA (80:20)	Insoluble
Water/IPA (50:50)	Insoluble
IPA	Insoluble
Water/DMSO (80:20)	Insoluble
Water/DMSO (50:50)	Insoluble
DMSO	Soluble

Water and IPA are polar protic solvents which can participate in hydrogen bonding. DMSO is a dipolar aprotic solvent which has a large dielectric constant and large dipole moments but does not participate in hydrogen bonding. Its high polarity allows DMSO to dissolve charged species such as various anions used as nucleophiles. As charges attract there is a tendency to get quite strong clusters of charged (permanent dipole) particles in solution.

The current experimental set up of the TSE is suitable for aqueous systems and not pure solvents which would require the relocation of the equipment into a safe environment. This has been identified as further work required to achieve full dissolution of nicotinic acid.

5.3.6 Slurry Homogeneity

Constraints of the TSE are the flow rates required to feed downstream processes which may result in incomplete dissolution within the residence time of the barrel. Limitations on the lowest feed rates of the feeders can result in the solution being oversaturated, when the solubility of the solute in the solvent system is low. In such cases a homogeneous slurry is obtained at the exit. In current batch system when a slurry is being fed from the vessel the concentration varies over feeding time as solids adhere to the vessel walls when the volume level drops. On refill there can be significant variations in the concentration of the slurry when solids from the previous batch remain in the vessel.

When the output from the TSE is a slurry the concentration remains uniform. This was further demonstrated by investigation of the mass balance in and out of the TSE. The mass balance was determined from five consecutive catch and weigh samples from the exit at one minute intervals for each API (see Appendix A 7.1.6). The error of mass

balance between the input and exit varied from 0.27 % RSD to 0.86 % RSD, demonstrating a slurry was obtained with good homogeneity.

This shows that a consistent output is achieved when both a solution and a slurry exit the TSE highlighting the feasibility of a TSE as a feed system with accurate, continuous delivery of solids.

5.3.7 Dual solid continuous feeding

The TSE has six entry ports for solid and liquid input. When the desired output is a solution for feeding downstream continuous flow processes then the maximum residence time for dissolution is chosen to ensure full dissolution. This is achieved when the solid is input at port position 1 and liquid at port 2 (see Section 4.2.2.2). A further solid feed can be dosed into the TSE at another port.

The addition of a second solid may not result in full dissolution of both solids depending on the solubility of the solids in the solvent at the set flow rates. However, when an insoluble catalyst or a reaction quench such as a sulphur addition is required this would be achieved in a batch system by addition of a second feed separate feed stream and often large amounts of solvent are necessary to ensure flow into the reactor. The TSE can provide a continuous flow of both solids simultaneously or the second solid intermittently, depending on the mass required for the second solid. The resultant output from the TSE is a heterogeneous slurry, eliminating the requirement for a second feed stream and additional solvent.

Dual solid feeding has been demonstrated using full dissolution of paracetamol powder (2.5 g min^{-1}) in water/IPA (80:20) at 40˚C (40 g min^{-1}) with solid entering the TSE at port

1 and liquid at port 2. Sand was chosen as the second solid feed (0.8 g min-1) and dosed into the TSE at port 6 (see Figure 5.9).

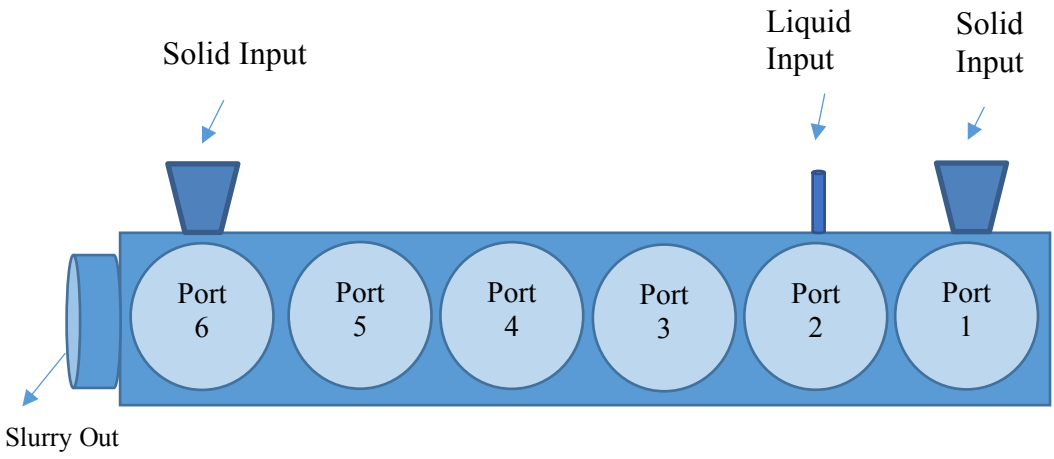

Figure 5.9 Schematic of barrel showing input port positions for liquid and solid dual feeding

The mass balance was determined from five consecutive catch and weigh samples from the exit at one minute intervals. The addition of a second solid did not adversely impact the resulting consistency of the output as the % RSD did not change significantly for samples collected with one or two solids dosed (See Appendix A 7.1.6).

5.3.8 Intermittent continuous feeding

Further investigation of continuous feeding probed the suitability of the TSE for intermittent continuous feeding. Technology platforms may have to be put on hold when there is a fault due to blockages, leakage or equipment failure in a unit operation further downstream in the processing train. In addition, the output flow rates from the feed stream may be higher than required for input into the next stage of manufacturing. These

situations would benefit from the ability to feed intermittently from the TSE, as and when required.

Several tests were carried out, stopping and starting the solid feeder, the liquid pump, and the screw rotation. The equipment was left switched off for periods of one hour between test runs. This resulted in solvent vapour reaching the solid input port causing blockages due to wet material build up inside the solids feeder cone.

Further tests where the screws were left running with the solid feeder and liquid pump off, showed no signs of material build up as the solvent vapour was continually conveyed along the twin screws to the extruder exit.

For longer stoppage times, an airline was attached at port 2 with the liquid input at port 3 thus ensuring decoupling of the solvent vapour from the solids at port 1. The screws were left running with the air flow on overnight and no material build up was visible on restarting the equipment.

The TSE can be operated intermittently with the screws running during short stoppage times and with the addition of airflow on for longer stoppages. This allows semi-continuous feed streams into low volume flow processes.

5.4 Conclusions

In this work, the feasibility of using the twin screw extruder for continuous delivery of solids was examined using four example APIs. Full dissolution of powder paracetamol was attained within the residence time of the TSE, while full dissolution of benzoic acid and acetylsalicylic acid was achievable by having higher barrel temperature. These subsequent solutions can then be fed into any pharmaceutical downstream processes. Full

dissolution of nicotinic acid was not achievable in the TSE under the experimental conditions, a slurry of good homogeneity was resulted. The solubility curves can be used to predict the operating parameters of the TSE.

The dissolution rate in the TSE is faster than that in the STV, associating with higher power dissipation generated by the aggressive shear mixing and thermal energy within the barrel.

The major advantages of using the TSE for a solid dosing system include the decoupling of solid from liquid feed, hence preventing solids from clogging feed nozzles, and the ability of using low solid feed rates, 2.5 g min^{-1}, with consistent dissolution concentration.

Chapter 6 **Conclusion and recommendation for future work**

The summaries of conclusions from this PhD work are as follows:

Critical factors impacting the dissolution rate in a batch system have been identified. For the same type of particles, solvent composition (solubility) is the major parameter when dissolving bulk solids in a batch system, temperature is the second contributing factor, while mixing has less effect on dissolution rates. For the same solvent, temperature, and mixing rate, the smallest particle size has the fastest dissolution rate.

When designing a continuous dissolution system, the solvent chosen for dissolution should have the maximum solubility at the processing temperature conditions. This can be determined from solubility curves of the solute in the solvent composition. Where possible the highest processing temperature should be chosen for the solvent temperature, within the confines of the flash point and boiling point temperature limitations of the solvent, to prevent vapour losses. Any solvent losses during processing will introduce variation in the concentration of the output solution. Mixing should be incorporated into the design as no mixing vastly reduces the dissolution rate.

Micronised solids increased the dissolution rate, however the flowability of such material would have a negative impact in a continuous flow system, potentially leading to bridging or blockages. Larger particles have good flowability and can be dispensed more accurately however they require a longer residence time to achieve a solution.

The twin screw extruder is a feasible set up for continuous dissolution of solid material for delivering solids to flow processes. TSE enables the decoupling of liquid from the solid feed thus eliminating any potential fouled solid feeding. The significance of this is that there is a reduced potential of variations in solution quality and the continuous equipment is less likely to stop the flow of materials in and out due to blockages.

TSE design allows for the controlled and synchronised input flows, together with intense mixing, to deliver either a dissolved solution or suspension of controlled composition ready for the next unit operation in the process train, e.g. 4-aminophenol and IPA to feed a reactor vessel in the synthesis of paracetamol, or paracetamol in solvent to feed a crystalliser vessel during the purification of paracetamol. More than one solid material can be dispensed simultaneously or intermittently during manufacture. This can be advantageous when more than one solid starting material is required to be fed into a reaction vessel or when adding small volumes of catalyst or reaction quench material.

TSE has the flexibility to cope with different raw material feed stocks; achieving full dissolution of powder paracetamol within the residence time of the TSE and achieving full dissolution of granular paracetamol by altering key variables such as solid or liquid feed rates, screw configuration and barrel temperature. Raw materials and intermediates will have a range of bulk properties, prior knowledge of particle size and particle size distribution can be utilised to determine choice of screw selection in the feeder. Granular material flows better using twin concave screws whilst powders flow is better using single spiral screws. Other screw designs for the feeder e.g. auger screws were not investigated in this study.

The variability in the output concentration in the twin screw extruder is much less than the batch to batch variation in the stirred tank thereby enhanced product quality has been observed when dissolution is carried out in the continuous system.

Overall the start-up and shut down losses are small for running a continuous operation and especially if the twin screw extruder were to be linked with a continuous crystalliser, which currently may need some hours to bring to a true steady state.

An alternative method has been determined for estimating the power density for the twin screw extruder when used as a continuous dissolution feed stream. This enables a fair comparison of the dissolution rates between two devices, i.e. twin screw extruder and stirred tank. The faster dissolution rate in the TSE is associated with higher power dissipation generated by the aggressive shear mixing and thermal energy within the barrel. The dissolution rate constant per power density in the TSE is slightly more favourable than that in the stirred tank.

Design of a continuous dissolution system should incorporate screw configuration with defined mixing elements for large particles, low solid and liquid feed rates, and low screw speed to maximise residence time. Barrel temperatures can be determined from predictions using solubility curves.

Four APIs with varying solubility were continuously dosed into the TSE. These subsequent solutions can then be fed into pharmaceutical downstream processes e.g. crystallisation. Full dissolution of powder paracetamol is attained within the residence time of the TSE, while full dissolution of benzoic acid and acetylsalicylic acid is achievable by having higher barrel temperature. Nicotinic acid exits the TSE as a consistent slurry.

Use of the TSE provides the ability to dissolve and charge hot solutions into continuous flow chemistry, thereby enhancing the chemist's toolbox for drug development and synthesis using alternative reaction schemes. Enables the charging of slurries with consistent output at the exit thereby maintaining slurry homogeneity in flow. Both

soluble and insoluble particles can be dosed simultaneously eliminating the requirement for separate feed streams and reducing the volume of solvent required in the feed streams. This can improve the environmental impact and cost of production.

The feasibility of a twin screw extruder for continuous solid dosing and dissolution has been demonstrated by the work in this PhD project. However, there are areas which would require further study of both science and technology for the development of the TSE into a platform for use in continuous manufacturing.

6.1 Scientific developments

- Four example APIs were analysed in this work, future work would involve a broader range of API and chemical materials covering a wider range of viscosities, densities and surface characteristics.

- Broader range of solvents. The solubility and dissolution kinetics vary depending on the solvent system used. A fuller spectrum of solvents will determine whether dissolution can be achieved within the residence time of the barrel.

- Longer continuous runs to determine the variation in output concentration when refilling the solid feed hopper and the liquid feed vessel. The build-up of material in the extruder may not have been evident during the short runs executed in this work (maximum run time was 80 minutes). Vapour reaching the solid input may increase over long run times.

- Incorporate dissolution to continuous crystallisation to verify the consistency of materials input. The crystallisation process can be monitored real time using an FBRM probe to identify fluctuations in material received from the TSE.

- Residence Time Distribution modelling to characterise the mixing and flow in the TSE would enhance process understanding.

- Incorporate camera for particle imaging – to visualise how aggregates are broken down and particle sizes reduced prior to dissolution which can be used to enhance screw configuration to maximise dissolution kinetics.

- The real time trajectory of the particle can be visualised and measured accurately in a twin screw extruder by tracing a radioactive particle using a Positron Emission Particle Tracking technique. The speed at which the material flows along the mixing and conveying zones can be traced to maximise residence time distribution.

- Positron Emission Tomography allows the observation of the liquid phase. A quantity of radioactive water can be injected into the TSE in order to observe the spread of the liquid in different sections.

- Further experiments at varying screw speeds and feed rates to investigate the impact of degree of screw fill has on shear mixing and therefore on dissolution kinetics.

6.2 Technological developments

- The best choice of feeder from the two available options used in this study has been documented. The configuration of the Flexwall feeder can be changed from the single spiral screw used in this work in order to improve the flow of feed stock of larger particles. A broad selection of screw sizes of varying pitch and diameter are available. Further work on the feeder screw selection has been identified to ensure compatibility with a broader range of raw materials, including micronised powder.

- For larger particle material it is beneficial to include mixing sections within the screw configuration. The size and location of these sections is a recommendation for future work.

- Quality by Design (QbD) concepts emphasise that the quality should be built into the products through the understanding of the product and process. This can be achieved by integrating a process control monitoring system to optimise the process and reduce variation.

- An automated feedback control system to the solids feeder can smooth the variation in output concentration. Setting up a diversion waste stream will enable monitoring during start up and shutdown processes.

- Design and build TSE that can accommodate longer residence times for slow dissolution kinetics systems. Adding a recycle loop back into the barrel will increase the residence time until full dissolution is achieved.

- Scale up and scale down of operation by using a 24 mm and an 11 mm Twin Screw Extruder to achieve flow rates which suit a broader range of continuous processing requirements.

- Using a smaller motor than required for current extrusion equipment as dissolution within the TSE is operated at lower pressures and temperatures than required for extrusion or granulation processes. This would thereby reduce the power input of the system.

- Progress towards End-to-End continuous manufacturing by connecting the output stream from the TSE to other unit operations. Feeding into duty/standby catch pots will allow for continuous monitoring and provide a feed stream into a continuous process.

- Start up and shutdown losses. The losses in this TSE work are just facts based on what was done. These could be further managed now that there is an understanding of what they are and what the contributing factors are to start up/shut down. Tilting the barrel would allow to drain at shutdown.

- Incorporating a clean in place (CIP) system by introducing a solvent flush at the end of the dissolution run would improve the cleaning process. The output concentration from the TSE can be measured using the PAT probe to indicate cleaning effectiveness. Cleaning validation could then be incorporated into the process.

Chapter 7 **Appendices**

7.1 Appendix A Experimental Data

7.1.1 Solids Loading

The solids loading in each solvent system during the dissolution experiments in the STV (see Chapter 3.2.2.5) were determined from the solubility. The weight of paracetamol used for the experiments is documented in Table 7.1.

Table 7.1 Solid Loading for paracetamol in one litre of solvent at 95% Solubility

	Solid Loading (g/L)		
Solvent System	20˚C	30˚C	40˚C
Water	11.61	16.49	23.51
Water/IPA (80:20)	43.41	66.93	102.29
Water/IPA (20:80)	213.70	260.31	315.13

7.1.2 Calibration Curves

The calibration curves at different temperatures (see Chapter 3.3.2.1) for paracetamol in water at 20, 30 and 40˚C are shown in figures 7.1, 7.2, and 7.3.

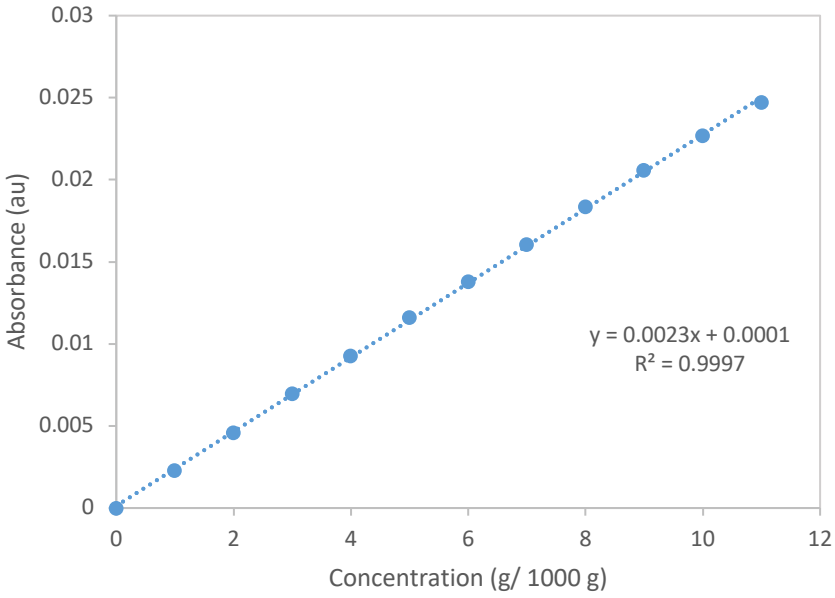

Figure 7.1 Calibration of Paracetamol in Water at 20˚C

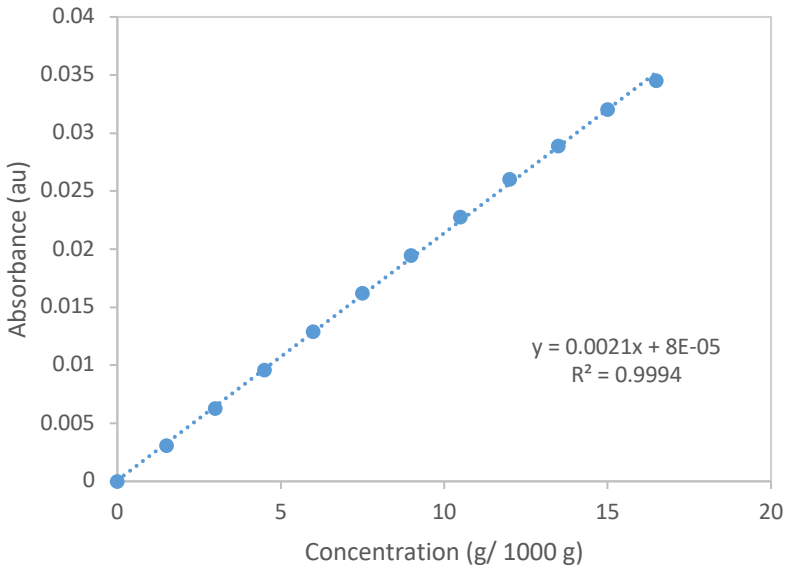

Figure 7.2 Calibration of Paracetamol in Water at 30˚C

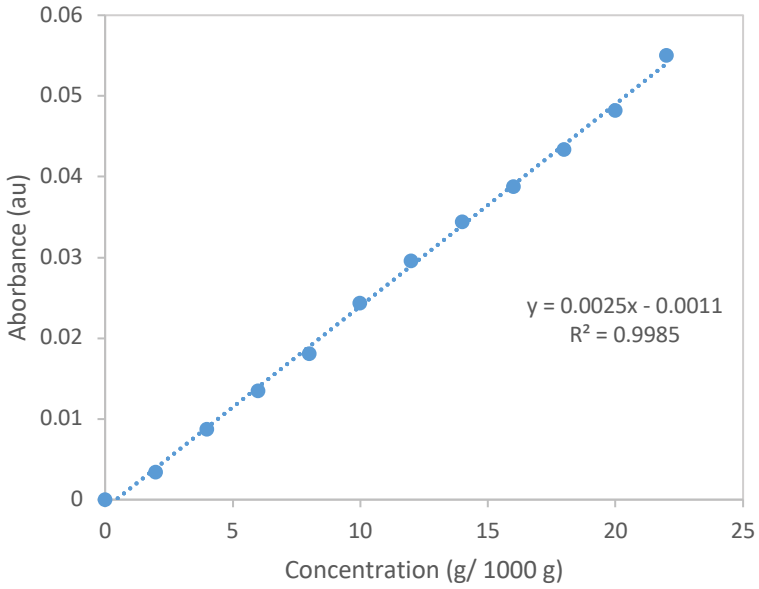

Figure 7.3 Calibration of Paracetamol in Water at 40˚C

Dissolution experiments were ran three times to confirm precision of experiments as illustrated in Figure 7.4.

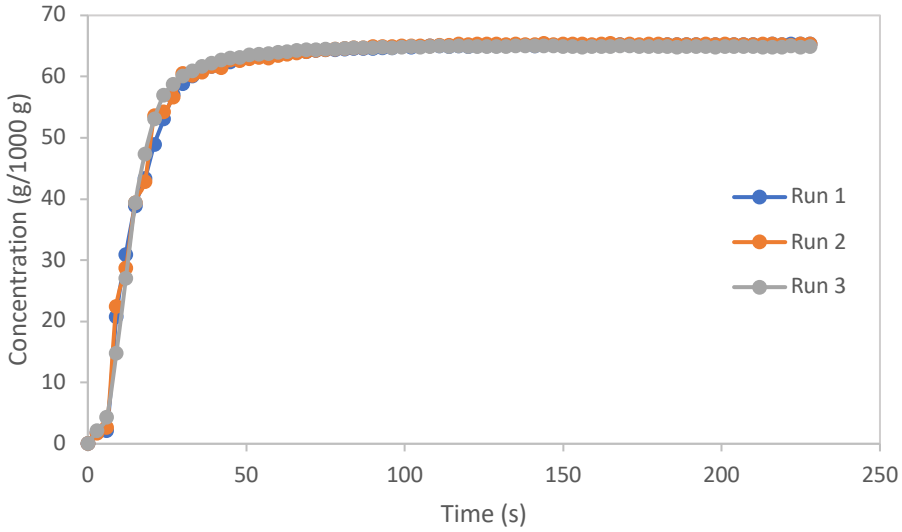

Figure 7.4 Dissolution history of three experimental runs of powder paracetamol in water/IPA (80:20) in a stirred tank vessel (Temperature = 40°C, Mixing Speed = 750 rpm)

7.1.3 Surface Energy

Surface energy (see Chapter 3.3.3, Table 3.4) is directly related to the thermodynamic work of adhesion between two materials. Thermodynamic work of adhesion is the work required to reversibly separate an interface between two bulk phases. Work of cohesion is between like bodies and work of adhesion is between unlike bodies. When irreversible chemical interactions are neglected, and only physical interactions are present, the total work of cohesion (and adhesion) can be determined according to geometric mean method.

$$W = W^{d} + W^{ab} \tag{7.1}$$

where W^d is the dispersive contribution and the W^{ab} is the specific contribution to the work of cohesion/adhesion.

$$W_{Coh}^{Total} = 2\left[\left(\gamma_s^d\right) + \left(\gamma_s^- \cdot \gamma_s^+\right)^{1/2} + \left(\gamma_s^+ \cdot \gamma_s^-\right)^{1/2}\right]$$

$$W_{Adh}^{Total} = W_{adh}^{d} + W_{adh}^{ab} = 2(\gamma_{s1}^{d} \cdot \gamma_{s2}^{d})^{1/2} + 2\left[\left(\gamma_{s1}^- \cdot \gamma_{s2}^+\right)^{1/2} + \left(\gamma_{s1}^+ \cdot \gamma_{s2}^-\right)^{1/2}\right] =$$
$$= 2\left[\left(\gamma_{s1}^d \cdot \gamma_{s2}^d\right)^{1/2} + \left(\gamma_{s1}^- \cdot \gamma_{s2}^+\right)^{1/2} + \left(\gamma_{s1}^+ \cdot \gamma_{s2}^-\right)^{1/2}\right]$$

(Ref: iGC-SEA User manual Version 1)

Higher work of cohesion values shows higher tendency of aggregation in the sample. The higher the work of adhesion, the more wettable the material becomes. The significant increase in specific surface energy in granular material in comparison to both micronised and powder results in higher work of adhesion and therefore signifies that granular material is the higher wettability grade material.

7.1.4 FT4 Rheometer Graphs

Five tests were carried out on each grade of paracetamol (granular, powder, micronised) using the FT4 Rheometer: 1) Stability and Variable Flow, 2) Permeability, 3) Aeration, 4) Compressibility and 5) Shear Cell 9kPa (see Chapter 4.3.1).

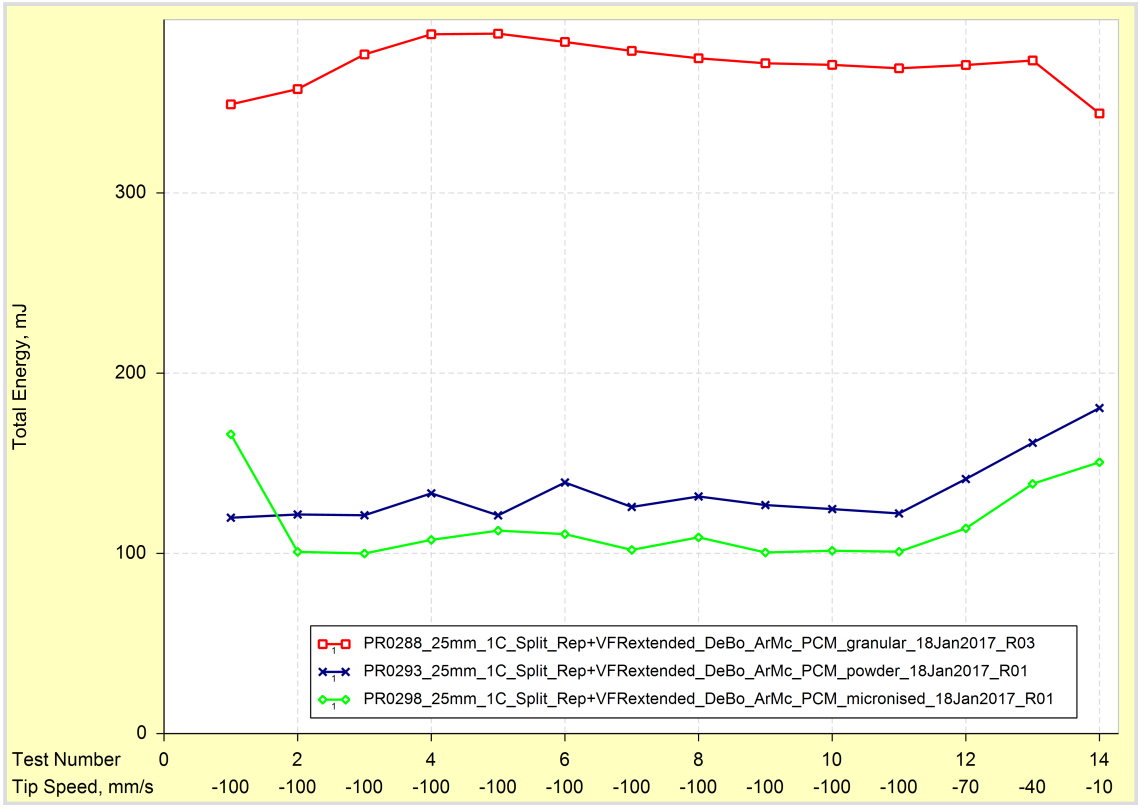

Figure 7.5 FT4 Rheometer test for stability and variable flow using three grades of paracetamol (granular, powder and micronised)

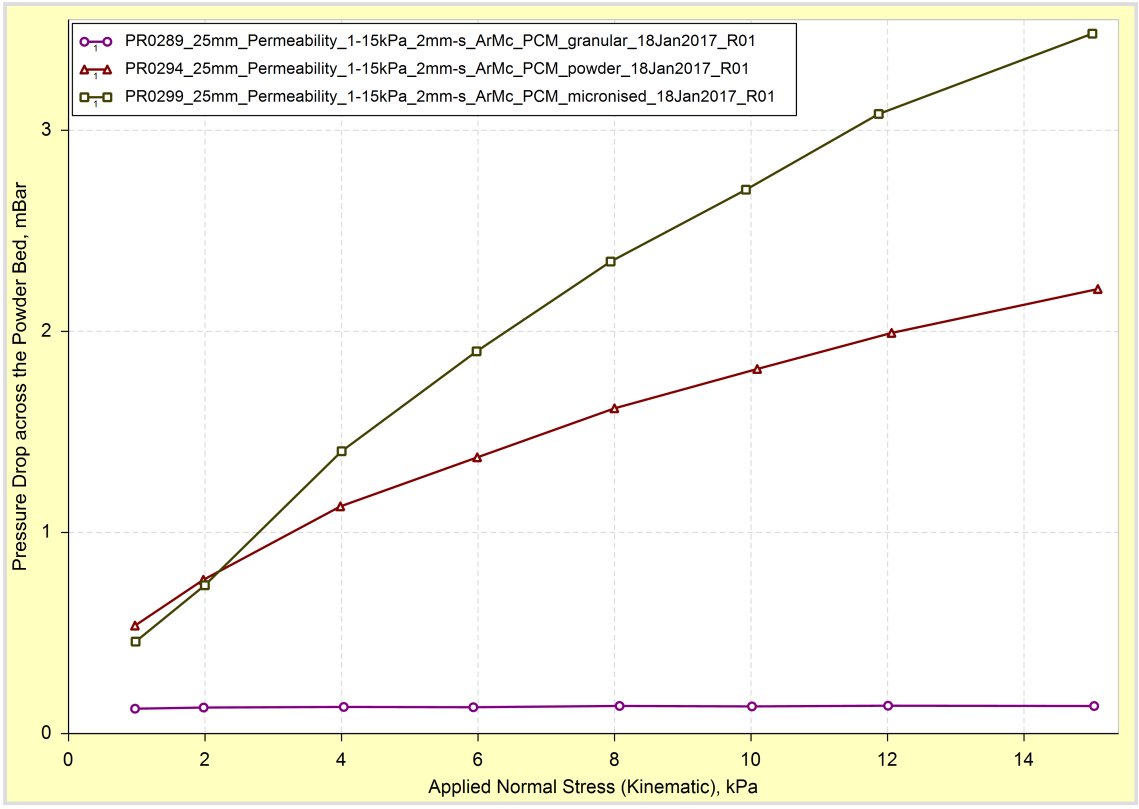

Figure 7.6 FT4 Rheometer test for permeability using three grades of paracetamol (granular, powder and micronised)

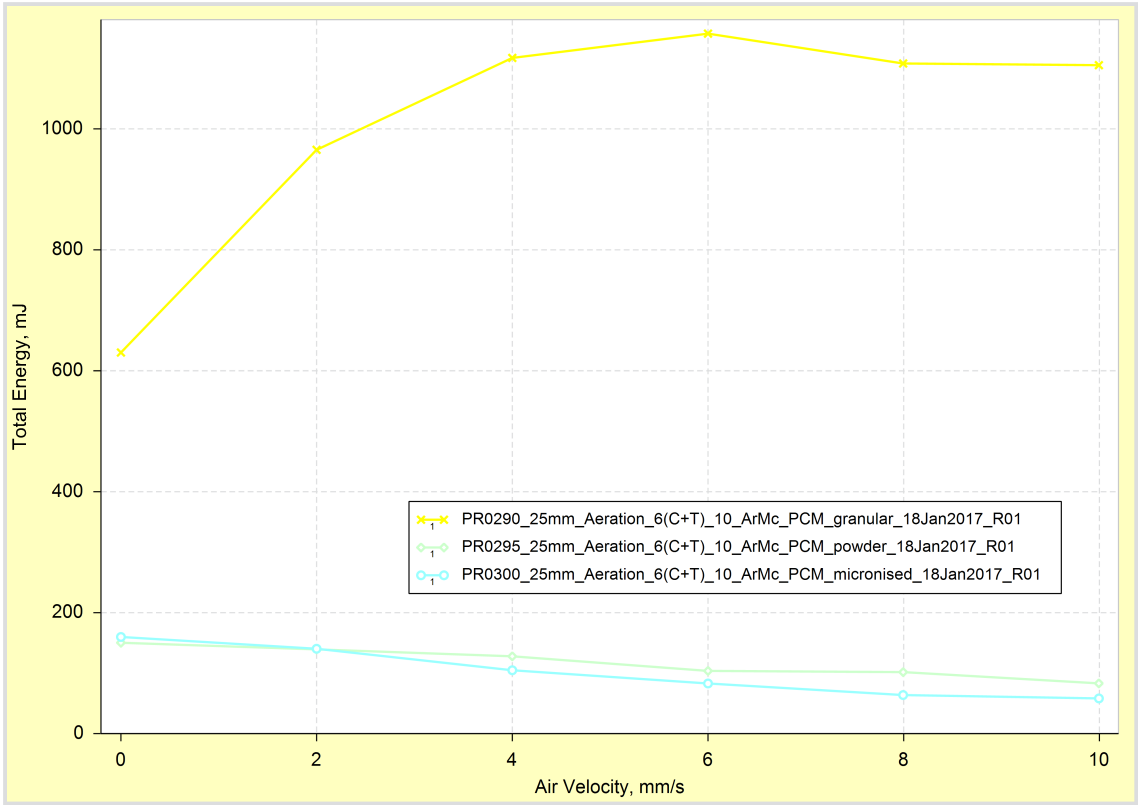

Figure 7.7 FT4 Rheometer test for aeration using three grades of paracetamol (granular, powder and micronised)

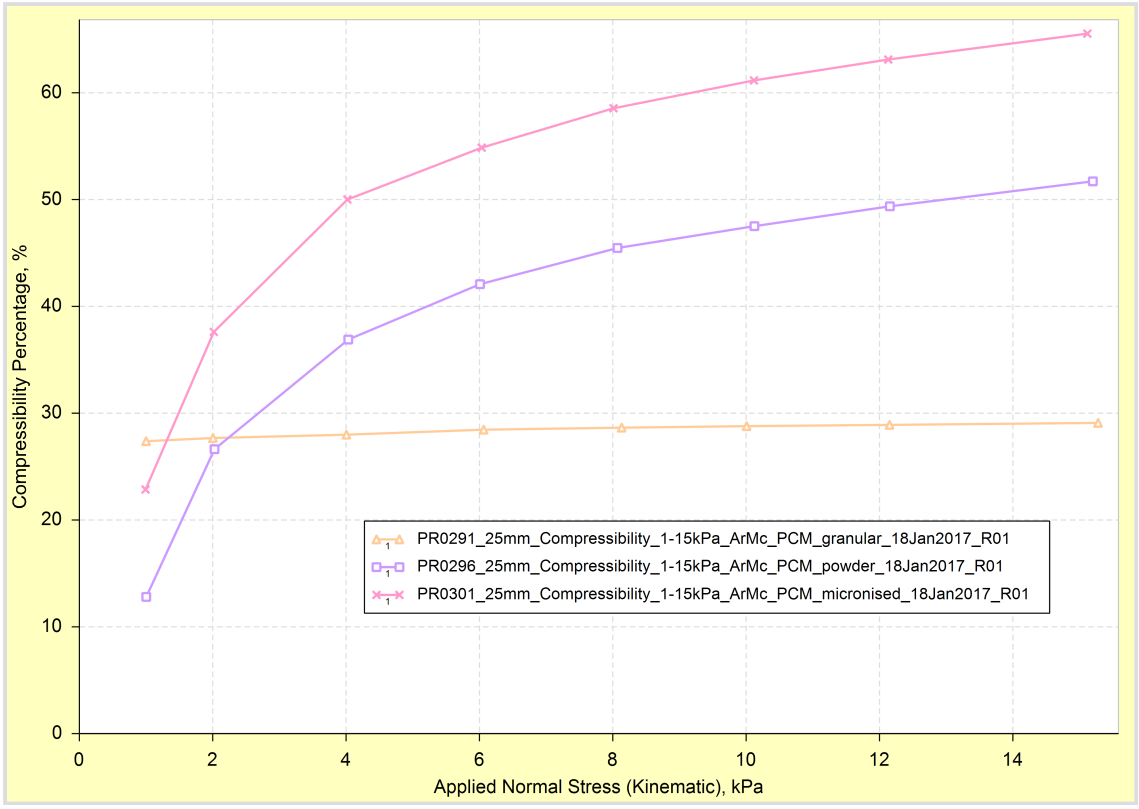

Figure 7.8 FT4 Rheometer test for compressibility using three grades of paracetamol (granular, powder and micronised)

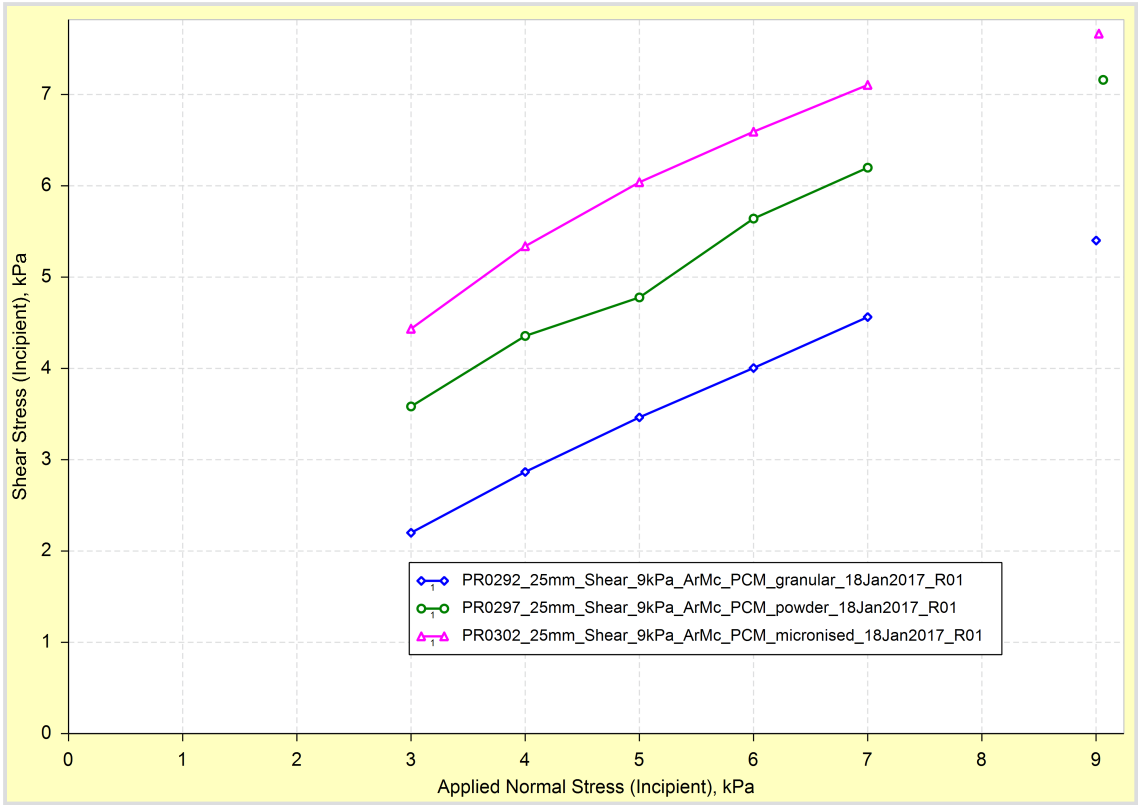

Figure 7.9 FT4 Rheometer test for compressibility using three grades of paracetamol (granular, powder and micronised)

7.1.5 Concentration data at each port

A complete set of sequential runs were undertaken for liquid entering at each port, e.g. Run 1 at Port 6, Run 2 at Port 5, Run 3 at Port 4, and so on (see Chapter 5.3.3.2). The absorbance data measured at the exit from the TSE was used to compile the output concentrations at each port (see Tables 7.2, 7.3, 7.4 and 7.5).

Table 7.2 Concentration data for paracetamol at each port

Std Dev	2.9	2.1	2.0	5.8	6.2
Std Err	0.4	0.2	0.2	0.6	0.8
Mean	48.5	58.3	59.2	60.7	61.9
Time (s)	Port 6 Concentration (g/100g)	Port 5 Concentration (g/100g)	Port 4 Concentration (g/100g)	Port 3 Concentration (g/100g)	Port 2 Concentration (g/100g)
0	47.2	56.8	56.3	63.9	54.3
3	47.4	55.8	57.6	62.9	56.6
6	46.4	55.3	59.7	60.0	59.1
9	47.6	54.9	59.2	58.9	64.9
12	47.2	53.0	57.9	57.4	71.4
15	47.7	54.7	58.3	56.1	63.6
18	46.9	55.2	61.2	58.2	57.3
21	45.7	56.9	58.1	60.1	60.4
24	46.5	59.5	55.4	60.0	66.9
27	46.6	60.3	54.8	57.4	63.8

30	46.2	58.9	57.9	58.0	69.3
33	45.9	56.3	58.6	59.8	64.1
36	44.8	55.1	57.7	58.7	57.9
39	45.1	54.8	55.8	57.7	59.0
42	44.3	56.4	56.1	59.1	69.8
45	45.5	58.4	58.8	64.8	71.0
48	46.1	60.8	59.0	67.0	62.1
51	45.0	61.5	57.3	70.5	63.2
54	45.2	60.8	58.3	71.6	63.4
57	46.7	60.9	60.5	67.1	58.6
60	46.1	61.4	61.2	63.4	55.1
63	43.7	61.7	60.9	60.5	60.1
66	44.6	60.6	61.4	62.8	65.0
69	46.2	60.3	60.4	65.0	64.2
72	45.8	60.6	59.7	66.8	58.0

75	45.4	60.3	61.9	64.3	70.9
78	46.6	61.5	60.9	59.3	78.9
81	47.8	60.4	59.7	61.0	67.6
84	47.7	60.9	61.8	66.9	59.2
87	48.3	60.4	61.5	69.4	69.0
90	48.1	58.4	59.7	66.5	70.9
93	49.2	56.9	57.3	63.0	60.1
96	47.6	59.5	57.5	63.4	53.3
99	48.8	60.2	60.4	67.0	59.1
102	49.2	59.4	63.6	65.9	70.6
105	48.6	58.5	62.1	60.5	64.7
108	51.5	56.7	58.3	57.9	54.9
111	53.5	56.9	59.3	61.0	59.5
114	53.7	57.1	59.8	61.9	70.8
117	52.2	58.2	59.1	59.1	71.0

120	51.6	56.0	60.2	54.4	63.1
123	51.3	55.9	60.4	52.7	54.4
126	51.5	55.9	60.7	55.1	52.1
129	52.4	57.4	61.3	55.6	55.2
132	52.7	60.1	62.0	59.1	57.0
135	53.1	59.2	63.3	62.3	63.9
138	51.8	60.6	61.7	62.9	65.5
141	52.1	57.9	59.7	66.2	65.2
144	51.6	57.1	61.2	66.6	60.9
147	52.3	56.5	61.2	68.5	57.5
150	53.3	56.2	60.0	71.1	57.3
153	51.9	56.7	58.6	70.2	58.7
156	50.1	58.6	61.7	69.1	69.7
159	51.0	56.0	61.8	66.8	64.5
162	52.1	55.9	57.6	65.2	57.4

165		57.7	57.7	61.4	57.7
168		60.6	59.0	56.6	52.3
171		60.1	57.9	57.1	49.0
174		60.2	58.2	60.4	49.4
177		59.2	59.6	59.9	60.2
180		59.0	58.2	57.0	70.5
183		59.8	57.1	60.6	72.5
186		60.6	57.7	65.4	60.3
189		61.2	57.1	65.7	60.6
192		60.1	57.1	65.0	66.5
195		58.7	56.1	60.2	58.0
198		56.4	55.1	55.6	52.8
201		57.2	58.7	57.7	59.1
204		56.7	60.9	61.3	59.9
207		57.9		55.3	

210		59.1		47.1	
213		58.5		46.1	
216		58.6		53.8	
219				58.6	
222				53.4	
225				48.1	
228				48.7	
231				48.0	
234				50.2	
237				65.2	

Table 7.3 Concentration data for benzoic acid at each port

Std Dev	0.4	0.6	0.6	1.1	0.5
Std Err	0.1	0.1	0.1	0.2	0.1

Mean	30.3	35.1	40.1	38.5	41.2
Time (s)	Port 6 Concentration (g/1000g)	Port 5 Concentration (g/1000g)	Port 4 Concentration (g/1000g)	Port 3 Concentration (g/1000g)	Port 2 Concentration (g/1000g)
0	30.0	35.3	40.0	40.0	41.5
3	30.6	35.3	40.6	38.6	40.9
6	30.3	35.5	41.1	38.7	41.2
9	30.3	34.9	40.6	38.6	41.1
12	30.3	35.2	41.5	37.7	40.9
15	30.3	34.9	40.9	37.4	42.0
18	30.3	35.8	40.1	37.7	41.5
21	30.3	36.2	41.2	38.9	41.7
24	30.4	35.8	40.9	38.1	41.9
27	30.0	36.1	40.3	37.8	41.5
30	30.6	35.5	40.1	36.5	41.9
33	30.6	35.8	40.1	35.8	41.4
36	30.4	35.3	40.4	36.3	40.9

39	30.7	35.2	40.3	37.1	40.7
42	30.7	34.2	39.8	38.3	41.4
45	30.8	34.3	39.8	37.7	41.7
48	30.6	34.5	40.1	38.1	41.7
51	30.3	34.3	40.3	38.0	41.7
54	30.2	34.3	40.0	37.8	41.4
57	30.7	34.3	40.0	38.1	40.3
60	30.4	35.0	40.3	38.9	40.4
63	30.0	34.7	40.3	37.8	40.6
66	30.0	35.3	40.1	36.9	40.4
69	30.3	35.5	40.3	37.5	40.4
72	30.0	34.7	40.4	38.3	40.0
75	29.6	34.7	41.2	39.5	40.6
78	30.4	34.6	41.4	40.3	41.1
81	29.9	34.2	41.2	39.7	40.9

84	29.9	33.9	40.7	38.7	41.4
87	30.0	35.5	39.8	39.2	41.5
90	29.7	34.9	40.1	40.1	41.1
93	29.3	34.6	40.7	40.0	40.3
96	29.9	35.2	40.0	39.4	40.3
99	29.6	35.0	39.2	39.0	41.2
102	30.2	34.2	39.5	39.0	41.2
105	30.2	34.0	40.0	39.5	41.5
108	30.0	34.0	39.7	39.7	41.4
111	30.4	34.2	39.4	39.5	41.9
114	30.8	33.9	39.0	38.9	41.7
117	31.2	34.7	39.4	39.4	41.1
120	31.0	35.0	39.4	39.2	40.3
123	30.4	34.3	39.4	39.5	41.1
126	30.2	34.5	39.5		41.7

129	30.6	34.6	39.4		41.2
132		35.0	39.8		41.9
135		35.0	39.7		41.4
138		35.5	39.2		41.2
141		35.5	39.7		
144		35.5	39.7		
147		35.8	39.7		
150		35.8	40.0		
153		35.6	40.1		
156		35.9	39.8		
159		35.3			
162		35.0			
165		34.6			
168		35.8			
171		35.6			

174		35.2			
177		34.5			
180		34.7			
183		35.8			
186		36.1			
189		36.5			
192		36.1			
195		35.2			
198		35.8			
201		35.8			
204		35.3			
207		35.5			
210		35.0			
213		35.6			
216		35.6			

219		35.8			
222		35.8			
225		35.0			

Table 7.4 Concentration data for nicotinic acid at each port

Std Dev	0.4	0.6	0.4	0.4	1.6
Std Err	0.1	0.1	0.0	0.1	0.2
Mean	8.9	15.3	19.0	21.2	23.3
Time (s)	Port 6 Concentration (g/100g)	Port 5 Concentration (g/100g)	Port 4 Concentration (g/100g)	Port 3 Concentration (g/100g)	Port 2 Concentration (g/100g)
0	9.5	15.8	19.4	22.3	24.1
3	9.0	15.0	19.9	21.7	23.9
6	9.2	14.8	19.7	22.1	22.5
9	9.4	14.3	19.6	21.9	20.7
12	9.4	14.3	19.2	22.1	19.7

15	9.5	15.0	19.6	21.1	22.1
18	9.2	16.0	19.4	20.5	24.3
21	9.5	16.0	18.8	20.1	24.5
24	9.5	16.3	19.0	21.7	24.8
27	9.4	16.3	19.4	21.3	24.8
30	9.5	16.5	19.7	21.5	24.5
33	9.4	16.1	19.6	21.3	24.5
36	9.4	15.8	19.6	21.7	24.5
39	9.4	16.0	19.0	21.3	23.9
42	9.5	15.6	19.0	21.5	22.1
45	9.2	15.6	19.2	21.5	20.9
48	9.0	15.2	19.7	20.9	19.6
51	9.5	14.7	19.6	21.3	21.1
54	8.8	14.8	19.9	21.5	24.3
57	8.8	14.8	19.7	20.5	24.3

60	8.8	14.7	19.6	21.3	24.5
63	8.5	14.5	19.7	21.3	24.3
66	8.2	14.3	19.6	21.3	24.3
69	8.5	14.1	19.6	21.1	24.8
72	8.2	14.1	19.2	20.7	24.3
75	8.5	14.3	19.2	21.3	24.5
78	8.2	14.8	19.2	21.1	24.3
81	8.8	15.8	19.2	21.1	23.5
84	9.0	15.6	19.4	21.3	22.1
87	8.7	15.8	18.8	20.9	20.5
90	8.8	15.8	18.6	20.7	21.9
93	9.2	15.2	18.6	21.1	24.1
96	8.7	15.0	18.4	20.9	24.3
99	8.8	15.2	18.6	20.9	24.5
102	8.7	15.4	18.4	21.1	24.3

105	8.7	15.4	19.0	21.3	24.5
108	8.7	15.6	19.0	21.1	23.9
111	8.5	15.2	18.8	20.5	23.7
114	8.7	15.2	19.0	21.1	22.7
117	8.7	15.0	19.2	21.1	20.7
120	8.7	14.5	19.6	21.1	19.2
123	8.7	14.5	19.4	21.1	21.3
126	9.0	15.0	19.4	21.5	24.3
129	9.0	15.4	19.4	21.3	24.3
132	8.8	15.0	19.4	21.3	24.1
135	8.8	15.2	19.4	20.5	23.9
138	9.2	15.8	19.4	20.7	24.1
141	9.0	15.8	19.4	21.3	23.9
144	9.0	15.8	18.8	21.1	23.3
147	8.5	15.4	18.8	20.5	

150	8.3	15.4	18.6	21.3	
153	8.7	15.6	18.6		
156	8.3	15.4	18.6		
159	8.3		19.0		
162			18.8		
165			19.2		
168			19.0		
171			18.4		
174			19.0		
177			19.0		
180			19.0		
183			19.0		
186			19.0		
189			19.4		
192			18.6		

195			19.0		
198			18.8		
201			18.6		
204			18.6		
207			18.6		
210			18.6		
213			19.0		
216			19.2		
219			18.8		
222			18.8		
225			19.0		
228			18.8		
231			19.2		
234			18.8		
237			18.4		

240			19.0		
243			19.0		
246			18.8		
249			18.4		
252			18.4		
255			18.4		
258			18.4		

Table 7.5 Concentration data for acetylsalicylic acid at each port

Std Dev	0.7	0.3	0.2	0.6	0.6
Std Err	0.1	0.0	0.0	0.1	0.1
Mean	15.4	21.8	24.7	21.8	21.9
Time (s)	Port 6 Concentration (g/100g)	Port 5 Concentration (g/100g)	Port 4 Concentration (g/100g)	Port 3 Concentration (g/100g)	Port 2 Concentration (g/100g)
0	14.5	22.1	24.0	22.7	22.5

3	14.1	22.1	23.9	23.0	22.4
6	14.3	21.9	24.3	22.8	22.3
9	14.5	21.9	24.6	23.0	21.9
12	15.0	22.3	24.4	23.1	22.2
15	15.0	22.1	24.8	22.8	22.5
18	14.8	22.4	24.6	22.7	23.5
21	14.9	22.6	24.4	22.5	23.0
24	14.9	22.2	25.1	22.1	21.9
27	14.6	22.4	24.7	22.2	21.8
30	14.5	22.6	24.8	22.2	21.8
33	14.4	22.4	24.9	21.6	21.9
36	14.7	22.0	25.0	21.2	22.2
39	15.1	22.2	24.9	21.1	22.8
42	15.2	22.0	24.9	21.2	22.9
45	14.8	22.1	24.9	21.0	22.8

48	14.5	22.0	25.1	21.4	23.1
51	14.8	21.8	25.0	21.5	22.8
54	15.0	21.8	24.7	21.4	22.1
57	15.5	21.8	24.9	21.0	21.9
60	15.7	22.1	24.9	21.4	22.0
63	15.6	21.8	25.1	21.5	22.2
66	15.4	21.3	24.9	21.9	22.3
69	15.6	21.6	24.9	21.9	22.1
72	15.3	21.8	25.0	21.9	21.6
75	15.3	21.8	25.0	21.7	21.7
78	15.5	21.8	24.8	21.8	21.5
81	15.4	21.7	24.9	21.8	21.5
84	15.7	21.5	24.7	22.0	21.7
87	15.5	21.5	24.5	22.0	21.8
90	15.9	21.6	24.6	22.0	21.6

93	16.0	21.5	24.6	22.4	21.5
96	16.0	21.5	24.8	22.3	22.0
99	16.0	21.8	24.8	21.9	22.2
102	16.1	21.7	24.7	21.8	22.3
105	16.1	21.8	24.8	21.9	22.4
108	16.0	21.8	24.8	21.9	22.2
111	15.8	21.2	24.8	21.7	21.9
114	15.6	21.5	24.7	21.4	21.6
117	15.9	21.4	24.6	22.1	21.1
120	16.1	21.4	24.7	22.7	21.0
123	16.3	21.8	24.7	22.7	20.9
126	16.4	21.5	24.7	22.5	21.0
129	16.5	21.4	24.6	21.7	21.0
132	16.1	21.1	24.6	21.5	21.0
135	16.3	21.5	24.4	21.4	21.3

138	16.6	21.7	24.5	21.6	21.1
141	16.6	21.7	24.5	21.6	20.9
144		21.8	24.4	21.8	21.1
147		21.8	24.5	21.7	21.6
150		21.7	24.8	21.6	21.5
153		21.8	24.7	21.1	21.3
156		21.5	25.0	21.3	21.2
159		21.6	24.9	21.1	21.2
162		21.7	24.5	21.2	21.0
165		21.6	24.8	21.0	21.1
168		21.8	24.7	21.5	21.1
171		21.7	24.7	21.8	21.6
174		21.6	24.6	21.6	21.4
177		21.7	24.9	21.1	21.8
180		21.8	24.5		22.1

183			24.5		22.4
186			24.4		22.4
189			24.9		21.7
192			24.8		22.4
195			24.8		21.9
198			24.6		21.9
201			24.3		22.0
204			24.4		22.1
207			24.3		22.7
210			24.2		22.4
213					21.9
216					21.8
219					21.8
222					21.8

7.1.6 Mass Balance of TSE

The mass balance (see Chapter 5.3.6 and Chapter 5.3.7) was determined from five consecutive catch and weigh samples from the exit at one minute intervals for each API (see Tables 7.6 and 7.7).

Table 7.6 Mass balance for acetylsalicylic acid, benzoic acid, nicotinic acid and paracetamol in water/IPA (80:20) at 40˚C in a twin screw extruder

	Paracetamol powder		**Nicotinic Acid**		**Benzoic Acid**		**Acetylsalicylic Acid**	
Output	Dissolved	Dissolved	Slurry	Slurry	Slurry	Slurry	Slurry	Slurry
Mass of Solid In (g/min)	2.5	2.5	2.5	2.5	2.5	2.5	2.5	2.5
Mass of Liquid In (g/min)	38.08	38.08	38.08	38.08	38.08	38.08	38.08	38.08
Total Mass In (g/min)	40.58	40.58	40.58	40.58	40.58	40.58	40.58	40.58
Predicted Mass Out (g/min)	40.58	40.58	40.58	40.58	40.58	40.58	40.58	40.58
Actual Mass	40.4	40.3	40.4	39.8	40	39.6	40.3	40.4

Out 1 (g/min)								
Actual Mass Out 2 (g/min)	40.3	40.5	40.1	40.1	39.8	40.5	40.4	40.4
Actual Mass Out 3 (g/min)	40.2	40.1	39.9	40.4	39.7	40.1	40.2	40.5
Actual Mass Out 4 (g/min)	40.1	40	40.2	40.3	40.2	40.3	40.3	40.4
Actual Mass Out 5 (g/min)	40.4	40.4	39.9	39.9	39.9	40.3	40.5	40.2
Mass Balance 1 (%)	99.6	99.3	99.6	98.1	98.6	97.6	99.3	99.6
Mass Balance 2 (%)	99.3	99.8	98.8	98.8	98.1	99.8	99.6	99.6
Mass Balance 3 (%)	99.1	98.8	98.3	99.6	97.8	98.8	99.1	99.8

Mass Balance 4 (%)	98.8	98.6	99.1	99.3	99.1	99.3	99.3	99.6
Mass Balance 5 (%)	99.6	99.6	98.3	98.3	98.3	99.3	99.8	99.1
% RSD	0.32	0.52	0.53	0.64	0.48	0.86	0.28	0.27

Table 7.7 Mass balance for paracetamol, and paracetamol/sand in water/IPA (80:20) at 40˚C in a twin screw extruder

	Paracetamol powder	**Sand/ Paracetamol powder**
Output	Dissolved	Slurry
Mass of Solid In (g/min)	2.5	3.3
Mass of Liquid In (g/min)	38.08	38.08
Total Mass In (g/min)	40.58	41.38
Predicted Mass Out (g/min)	40.58	41.38
Actual Mass Out 1 (g/min)	40.4	41

Actual Mass Out 2 (g/min)	40.3	41.3
Actual Mass Out 3 (g/min)	40.2	41.2
Actual Mass Out 4 (g/min)	40.1	41
Actual Mass Out 5 (g/min)	40.4	40.8
Mass Balance 1 (%)	99.6	99.1
Mass Balance 2 (%)	99.3	99.8
Mass Balance 3 (%)	99.1	99.6
Mass Balance 4 (%)	98.8	99.1
Mass Balance 5 (%)	99.6	98.6
% RSD	0.32	0.47

7.2 Appendix B Calculations

7.2.1 Normalisation of dissolution data

Both the micronised and powder particles were difficult to dose due to static force and prone to stick to the walls of the dispensing funnel and sides of the vessel when dispensing in one shot, while dosing granular material was trouble free without loss of material, as such the total concentration of paracetamol dissolved was slightly less for micronised and powder than for granular particles. The data has therefore been normalised (see Chapter 3.3.3, Figure 3.11) prior to analysis of the dissolution kinetics as follows:

Granular concentration (g 1000 g^{-1} (solvent)) = (concentration/15.68) * 100

Powder concentration (g 1000 g^{-1} (solvent)) = (concentration/14.87) * 100

Micronised concentration (g 1000 g^{-1} (solvent)) = (concentration/14.78) * 100

7.2.2 Degree of Saturation

The dissolution rate constants of benzoic acid, acetylsalicylic acid and nicotinic acid were recalculated by extrapolation with respect to the same undersaturation of paracetamol assuming a linear relationship in solubilities and re-tabulated in (see Chapter 5.3.4, Table 5.5) using Equation (7.2).

$$ks = \left(\frac{(\%\, Sx + \%\, Sp)}{\%\, Sx} \right) * k \qquad (7.2)$$

where ks = dissolution rate constant at equivalent saturation (s^{-1}), % Sx = percentage saturation level of benzoic acid, nicotinic acid or acetylsalicylic acid, % Sp = percentage saturation level of paracetamol, k = dissolution rate constant (s^{-1})

7.2.3 Permeability Calculation

Pressure drop data from the FT4 Rheometer was converted to permeability data (see Chapter 4.3.1, Table 4.1). Permeability is calculated using the Darcy's Law (see Equation (7.3)):

$$Q = \frac{kA}{\mu} \frac{Pa-Pb}{L} \quad (7.3)$$

where Q= Air volume per unit time ($cm^3\ s^{-1}$), k = Permeability (cm^2), A = Cross-sectional area of powder bed (cm^2), Pa – Pb = Pressure drop across powder bed (Pa), μ = Air viscosity (Pas), L= Length of powder bed (cm)

Rearranging and dividing by area gives: -

$$k = \frac{q\mu L}{\Delta P} \quad (7.4)$$

where q = Flux, or air flow rate ($cm\ s^{-1}$), ΔP = Pressure drop across powder bed (mbar).

7.2.4 Screw Fill Calculation

The screw pitch % fill (see Chapter 4.3.2.8) is calculated using Equation (7.5).

$$\% fill = (Q \times .2777) / (SV \times rpm/60) \times (SG \times Ef) \quad (7.5)$$

where Q=Flow rate in kg hr^{-1}, SV=Specific volume of extruder in cc/diameter of length, rpm=Screw rpm, SG=Specific gravity of the material being processed, Ef=Average forwarding efficiency (approx. 35% for a screw with 1/3 mixers and 2/3 flighted elements).

Specific Volume (SV) represents the approximate volume for one Length/Diameter of the process section = 0.94 x (outside screw $diameter^2$ - Inside screw $diameter^2$) x Outer diameter/1000

References

A. FORSTER, J. H., I. TUCKER, T. RADES 2001. Selection of excipients for melt extrusion with two poorlybwater-soluble drugs by solubility parameter calculation and thermal analysis. *International Journal of Pharmaceutics,* 226**,** 147–161.

ABOLGHASEM JOUYBAN, O. A., SHAHLA MIRZAEI, DAVOUD HASSANZADEH, TARAVAT GHAFOURIAN, WILLIAM EUGENE ACREE,JR., AND ALI NOKHODCHI 2008. Solubility Prediction of Paracetamol in Water–Ethanol–Propylene Glycol Mixtures at 25 and 30 °C Using Practical Approaches. *Chem. Pharm. Bull.,* 56**,** 602-606.

AGNEW, L. R., CRUICKSHANK, D. L., MCGLONE, T. & WILSON, C. C. 2016. Controlled production of the elusive metastable form II of acetaminophen (paracetamol): a fully scalable templating approach in a cooling environment. *Chemical Communications,* 52**,** 7368-7371.

AGNEW, L. R., MCGLONE, T., WHEATCROFT, H. P., ROBERTSON, A., PARSONS, A. R. & WILSON, C. C. 2017. Continuous Crystallization of Paracetamol (Acetaminophen) Form II: Selective Access to a Metastable Solid Form. *Crystal Growth & Design,* 17**,** 2418-2427.

AHO, J., BOETKER, J. P., BALDURSDOTTIR, S. & RANTANEN, J. 2015. Rheology as a tool for evaluation of melt processability of innovative dosage forms. *Int J Pharm,* 494**,** 623-42.

ALSENZ, J. 2011. PowderPicking: An inexpensive, manual, medium-throughput method for powder dispensing. *Powder Technology,* 209**,** 152-157.

AMIT SURI, M. H. 2009. A novel cartridge type powder feeder. *Powder Technology,* 189**,** 497–507.

ANDREWS, G. P. & JONES, D. S. 2014. Hot melt extrusion - processing solid solutions? *J Pharm Pharmacol,* 66**,** 145-7.

ATIEMO-OBENG, V. A., PENNEY, W. R. & ARMENANTE, P. 2004. Solid–Liquid Mixing. *Handbook of Industrial Mixing.* John Wiley & Sons, Inc.

BAKA, E., COMER, J. E. & TAKACS-NOVAK, K. 2008. Study of equilibrium solubility measurement by saturation shake-flask method using hydrochlorothiazide as model compound. *J Pharm Biomed Anal,* 46**,** 335-41.

BAKER, J. R. 1991. Motionless mixers stir up new uses. *Chemical Engineering Progress,* 87**,** 32-38.

BARRA, J., LESCURE, F., DOELKER, E. & BUSTAMANTE, P. 1997. The Expanded Hansen Approach to Solubility Parameters. Paracetamol and Citric Acid in Individual Solvents. *Journal of Pharmacy and Pharmacology,* 49**,** 644-651.

BARRETT, P. & GLENNON, B. 2002. Characterizing the Metastable Zone Width and Solubility Curve Using Lasentec FBRM and PVM. *Chemical Engineering Research and Design,* 80**,** 799-805.

BAUMANN, M. & BAXENDALE, I. R. 2015. The synthesis of active pharmaceutical ingredients (APIs) using continuous flow chemistry. *Beilstein Journal of Organic Chemistry,* 11**,** 1194-1219.

BAXENDALE, I. R., BRAATZ, R. D., HODNETT, B. K., JENSEN, K. F., JOHNSON, M. D., SHARRATT, P., SHERLOCK, J.-P. & FLORENCE, A. J. 2015. Achieving

Continuous Manufacturing: Technologies and Approaches for Synthesis, Workup, and Isolation of Drug Substance. May 20–21, 2014 Continuous Manufacturing Symposium. *Journal of Pharmaceutical Sciences,* 104**,** 781-791.

BERNHARD, G., DAVID, C. & OLIVER, K. C. 2015. Continuous‐Flow Technology−A Tool for the Safe Manufacturing of Active Pharmaceutical Ingredients. *Angewandte Chemie International Edition,* 54**,** 6688-6728.

BERTHELSEN, R., HOLM, R., JACOBSEN, J., KRISTENSEN, J., ABRAHAMSSON, B. & MÜLLERTZ, A. 2016. Dissolution model development: Formulation effects and filter complications. *Dissolution Technologies,* 23**,** 1-12.

BESENHARD, M. O., NEUGEBAUER, P., SCHEIBELHOFER, O. & KHINAST, J. G. 2017. Crystal Engineering in Continuous Plug-Flow Crystallizers. *Crystal Growth & Design,* 17**,** 6432-6444.

BLAGDEN, N. D. M., M. GAVAN, P. T. YORK, P. 2007. Crystal engineering of active pharmaceutical ingredients to improve solubility and dissolution rates. *Advanced Drug Delivery Reviews,* 59**,** 617-630.

BREON, T. L. & PARUTA, A. N. 1970. Solubility Profiles for Several Barbiturates in Hydroalcoholic Mixtures. *Journal of Pharmaceutical Sciences,* 59**,** 1306-1313.

BRIENS, C., BERRUTI, F., FELLI, V. & CHAN, E. 2008. Solids entrainment into gas, liquid, and gas–liquid spray jets in fluidized beds. *Powder Technology,* 184**,** 52-57.

BROWN, C. J. & NI, X.-W. 2011. Evaluation of growth kinetics of antisolvent crystallization of paracetamol in an oscillatory baffled crystallizer utilizing video imaging. *Crystal Growth & Design,* 11**,** 3994-4000.

BUMBRAH, G. S. & SHARMA, R. M. 2015. Raman spectroscopy – Basic principle, instrumentation and selected applications for the characterization of drugs of abuse. *Egyptian Journal of Forensic Sciences*.

CABASSI, G., CAVALLI, D., FUCCELLA, R. & MARINO GALLINA, P. 2015. Evaluation of four NIR spectrometers in the analysis of cattle slurry. *Biosystems Engineering,* 133**,** 1-13.

CALVO, N. L., KAUFMAN, T. S. & MAGGIO, R. M. 2015. A PCA-based chemometrics-assisted ATR-FTIR approach for the classification of polymorphs of cimetidine: Application to physical mixtures and tablets. *Journal of Pharmaceutical and Biomedical Analysis,* 107**,** 419-425.

CARTWRIGHT, J. J., ROBERTSON, J., D'HAENE, D., BURKE, M. D. & HENNENKAMP, J. R. 2013. Twin screw wet granulation: Loss in weight feeding of a poorly flowing active pharmaceutical ingredient. *Powder Technology,* 238**,** 116-121.

CHEN, X., SEYFANG, K. & STECKEL, H. 2012. Development of a micro dosing system for fine powder using a vibrating capillary. Part 1: the investigation of factors influencing on the dosing performance. *Int J Pharm,* 433**,** 34-41.

CHENG, W.-P., HSIEH, Y.-J., YU, R.-F., HUANG, Y.-W., WU, S.-Y. & CHEN, S.-M. 2010a. Characterizing polyaluminum chloride (PACl) coagulation floc using an on-line continuous turbidity monitoring system. *Journal of the Taiwan Institute of Chemical Engineers,* 41**,** 547-552.

CHENG, W. P., KAO, Y. P. & YU, R. F. 2010b. Comparison of three coagulants by online turbidity monitoring. *Proceedings of the Institution of Civil Engineers: Water Management,* 163**,** 89-94.

COLE, K. P. & JOHNSON, M. D. 2018. Continuous flow technology vs. the batch-by-batch approach to produce pharmaceutical compounds. *Expert Review of Clinical Pharmacology,* 11**,** 5-13.

CROWLEY, M. M., ZHANG, F., REPKA, M. A., THUMMA, S., UPADHYE, S. B., BATTU, S. K., MCGINITY, J. W. & MARTIN, C. 2007. Pharmaceutical applications of hot-melt extrusion: part I. *Drug Dev Ind Pharm,* 33**,** 909-26.

D.J.W. GRANT, M. M., AH-L. CHOW AND J.E. FAIRBROTHER 1984. Non-linear van't Hoff solubility-temperature plots and their pharmaceutical interpretation. *International Journal of Pharmaceutics,* 18**,** 25-38.

DAVÉ, R. N., BILGILI, E., CUITIÑO, A. & JALLO, L. 2013. Special issue on pharmaceutical powders: Towards developing understanding of the influence of materials and processes on product performance. *Powder Technology,* 236**,** 1-4.

DHENGE, R. M., CARTWRIGHT, J. J., DOUGHTY, D. G., HOUNSLOW, M. J. & SALMAN, A. D. 2011. Twin screw wet granulation: Effect of powder feed rate. *Advanced Powder Technology,* 22**,** 162-166.

DHENGE, R. M., CARTWRIGHT, J. J., HOUNSLOW, M. J. & SALMAN, A. D. 2012. Twin screw wet granulation: Effects of properties of granulation liquid. *Powder Technology,* 229**,** 126-136.

DIMIAN, A. C., BILDEA, C. S. & KISS, A. A. 2014. Chapter 11 - Batch Processes. *In:* ALEXANDRE C. DIMIAN, C. S. B. & ANTON, A. K. (eds.) *Computer Aided Chemical Engineering.* Elsevier.

DORRIS, G. M. & GRAY, D. G. 1980. Adsorption of n-alkanes at zero surface coverage on cellulose paper and wood fibers. *Journal of Colloid and Interface Science,* 77**,** 353-362.

EBRAHIMI, A., SAFFARI, M., DEHGHANI, F. & LANGRISH, T. 2016. Incorporation of acetaminophen as an active pharmaceutical ingredient into porous lactose. *International Journal of Pharmaceutics,* 499**,** 217-227.

EGGERS, R., VON SCHNITZLER, J., KEMPE, T. 2002. Continuous dosing of solids in high pressure systems.

ENGISCH, W. E. & MUZZIO, F. J. 2012. Method for characterization of loss-in-weight feeder equipment. *Powder Technology,* 228**,** 395-403.

ENGISCH, W. E. & MUZZIO, F. J. 2015. Feedrate deviations caused by hopper refill of loss-in-weight feeders. *Powder Technology,* 283**,** 389-400.

ERIC GARCIA, C. H., STEPHANE VEESLER 2002. Dissolution and phase transition of pharmaceutical compounds. *Journal of Crystal Growth* 237-239**,** 2233-2239.

ERIC GARCIA, S. V., ROLAND BOISTELLE, CHRISTIAN HOFF 1999. Crystallization and dissolution of pharmaceutical compounds An experimental approach. *Journal of Crystal Growth* 198/199**,** 1360-1364.

ESCRIBÀ-GELONCH, M., HESSEL, V., MAIER, M. C., NOËL, T., NEIRA D'ANGELO, M. F. & GRUBER-WOELFLER, H. 2017. Continuous-Flow In-Line Solvent-Swap Crystallization of Vitamin D3. *Organic Process Research & Development*.

FAANES, A. & SKOGESTAD, S. 2003. Buffer Tank Design for Acceptable Control Performance. *Industrial & Engineering Chemistry Research,* 42**,** 2198-2208.

FAN, S., ZHANG, B., LI, J., HUANG, W. & WANG, C. 2016. Effect of spectrum measurement position variation on the robustness of NIR spectroscopy models for soluble solids content of apple. *Biosystems Engineering,* 143**,** 9-19.

FEELEY, J. C., YORK, P., SUMBY, B. S. & DICKS, H. 1998. Determination of surface properties and flow characteristics of salbutamol sulphate, before and after micronisation. *International Journal of Pharmaceutics,* 172**,** 89-96.

FERGUSON, S., MORRIS, G., HAO, H., BARRETT, M. & GLENNON, B. 2012. In-situ monitoring and characterization of plug flow crystallizers. *Chemical Engineering Science,* 77**,** 105-111.

FERGUSON, S., MORRIS, G., HAO, H. X., BARRETT, M. & GLENNON, B. 2013. Characterization of the anti-solvent batch, plug flow and MSMPR crystallization of benzoic acid. *Chemical Engineering Science,* 104**,** 44-54.

FICK, A. 1855. V. On liquid diffusion AU - Fick, Adolph. *The London, Edinburgh, and Dublin Philosophical Magazine and Journal of Science,* 10**,** 30-39.

FILGUEIRAS, P. R., SAD, C. M. S., LOUREIRO, A. R., SANTOS, M. F. P., CASTRO, E. V. R., DIAS, J. C. M. & POPPI, R. J. 2014. Determination of API gravity, kinematic viscosity and water content in petroleum by ATR-FTIR spectroscopy and multivariate calibration. *Fuel,* 116**,** 123-130.

FUJIWARA, M., CHOW, P. S., MA, D. L. & BRAATZ, R. D. 2002. Paracetamol Crystallization Using Laser Backscattering and ATR-FTIR Spectroscopy: Metastability, Agglomeration, and Control. *Crystal Growth & Design,* 2**,** 363-370.

GABRIEL I. TARDOS, Q. L. 1996. Precision dosing of powders by vibratory and screw feeders: an experimental study. *Advanced Powder Technology,* 7**,** 51-58.

GARSIDE, J. & DAVEY, R. J. 1980. Invited review secondary contact nucleation: kinetics, growth and scale-up. *Chemical Engineering Communications,* 4**,** 393-424.

GHANEM, A., LEMENAND, T., DELLA VALLE, D. & PEERHOSSAINI, H. 2014. Static mixers: Mechanisms, applications, and characterization methods – A review. *Chemical Engineering Research and Design,* 92**,** 205-228.

GIRARD, J.-M., DESCHÊNES, J.-S., TREMBLAY, R. & GAGNON, J. 2013. FT-IR/ATR univariate and multivariate calibration models for in situ monitoring of sugars in complex microalgal culture media. *Bioresource Technology,* 144**,** 664-668.

GOERTZ, H. H. D., KLIMESCH, R. G. D., LAEMMERHIRT, K. D., LANG, S. D., SANNER, A. D. & SPENGLER, R. D. 1992. Process for the preparation of solid pharmaceutical forms. Google Patents.

GONÇALVES, E. M. & MINAS DA PIEDADE, M. E. 2012. Solubility of nicotinic acid in water, ethanol, acetone, diethyl ether, acetonitrile, and dimethyl sulfoxide. *The Journal of Chemical Thermodynamics,* 47**,** 362-371.

GUIDRY, M. W. & MACKENZIE, F. T. 2003. Experimental study of igneous and sedimentary apatite dissolution: Control of pH, distance from equilibrium, and temperature on dissolution rates. *Geochimica et Cosmochimica Acta,* 67**,** 2949-2963.

GULLETT, B. K. & GILLIS, G. R. 1987. Low flow rate laboratory feeders for agglomerative particles. *Powder Technology,* 52**,** 257-260.

GUNDOGDU, M. Y. 2004. Design improvements on rotary valve particle feeders used for obtaining suspended airflows. *Powder Technology,* 139**,** 76-80.

H.A.CUSHMAN. 1897. *Rubber, Tubing Machine*. 579,938.

HAMLIN, W. E., NORTHAM, J. I. & WAGNER, J. G. 1965. Relationship Between In Vitro Dissolution Rates and Solubilities of Numerous Compounds Representative of Various Chemical Species. *Journal of Pharmaceutical Sciences,* 54**,** 1651-1653.

HANSON, W. A. 1991. *Handbook of Dissolution Testing*, Aster Publishing Corporation.

HAROLD F. GILES JR, E. M. M. I., JOHN R. WAGNER, JR. 2004. *Extrusion: The Definitive Processing Guide and Handbook*, William Andrew.

HATTORI, Y. & OTSUKA, M. 2012. Time-resolved near-infrared spectroscopic study of the dissolution of crystalline lactose. *European Journal of Pharmaceutical Sciences,* 47**,** 884-889.

HEMRAJANI, R. R. & TATTERSON, G. B. 2004. Mechanically Stirred Vessels. *Handbook of Industrial Mixing.* John Wiley & Sons, Inc.

HERNANDEZ, E., PAWAR, P., KEYVAN, G., WANG, Y., VELEZ, N., CALLEGARI, G., CUITINO, A., MICHNIAK-KOHN, B., MUZZIO, F. J. & ROMAÑACH, R. J. 2016. Prediction of dissolution profiles by non-destructive near infrared spectroscopy in tablets subjected to different levels of strain. *Journal of Pharmaceutical and Biomedical Analysis,* 117**,** 568-576.

HOCSMAN, A., DI NEZIO, S., CHARLET, L. & AVENA, M. 2006. On the mechanisms of dissolution of montroydite [HgO(s)]: Dependence of the dissolution rate on pH, temperature, and stirring rate. *Journal of Colloid and Interface Science,* 297**,** 696-704.

HÖRMANN, T., SUZZI, D. & KHINAST, J. G. 2011. Mixing and Dissolution Processes of Pharmaceutical Bulk Materials in Stirred Tanks: Experimental and Numerical Investigations. *Industrial & Engineering Chemistry Research,* 50**,** 12011-12025.

HORST, J. T. 2016. *Solubility: Importance, Measurement and More.* [Online]. Scientific Update UK: Webinar on Solubility: Scientific Update UK. [Accessed 18 March 2016.

HU, Y., WEN, Y. & WANG, X. 2016. Novel method of turbidity compensation for chemical oxygen demand measurements by using UV–vis spectrometry. *Sensors and Actuators B: Chemical,* 227**,** 393-398.

HUANG, W., SHI, Y., WANG, C., YU, K., SUN, F. & LI, Y. 2013. Using spray-dried lactose monohydrate in wet granulation method for a low-dose oral formulation of a paliperidone derivative. *Powder Technology,* 246**,** 379-394.

HUGHES, D. L. 2018. Applications of Flow Chemistry in Drug Development: Highlights of Recent Patent Literature. *Organic Process Research & Development,* 22**,** 13-20.

HUMAYUN, H. Y., SHAARANI, M. N. N. M., WARRIOR, A., ABDULLAH, B. & SALAM, M. A. 2016. The Effect of Co-solvent on the Solubility of a Sparingly Soluble Crystal of Benzoic Acid. *Procedia Engineering,* 148**,** 1320-1325.

ISLAM, M. T., MANIRUZZAMAN, M., HALSEY, S. A., CHOWDHRY, B. Z. & DOUROUMIS, D. 2014. Development of sustained-release formulations processed by hot-melt extrusion by using a quality-by-design approach. *Drug Deliv Transl Res,* 4**,** 377-87.

ISLAM, M. T., SCOUTARIS, N., MANIRUZZAMAN, M., MORADIYA, H. G., HALSEY, S. A., BRADLEY, M. S., CHOWDHRY, B. Z., SNOWDEN, M. J. & DOUROUMIS, D. 2015. Implementation of transmission NIR as a PAT tool for monitoring drug transformation during HME processing. *Eur J Pharm Biopharm,* 96**,** 106-16.

J.A. COVAS, J. M. M., A.V. MACHADO, P. COSTA 2008. On-line rotational rheometry for extrusion and compounding operations. *Jornal of Non-Newtonian Fluid Mechanics,* 148**,** 88–96.

JAMALEDDINE, T. J., SAHA, M., BERRUTI, F. & BRIENS, C. 2015. Effect of interaction between spray and attrition jets in a high temperature fluidized bed. *Powder Technology,* 278**,** 57-64.

JANICKI, S., SZNITOWSKA, M., ZEBROWSKA, W., GABIGA, H. & KUPIEC, M. 2001. Evaluation of paracetamol suppositories by a pharmacopoeial dissolution test – comments on methodology. *European Journal of Pharmaceutics and Biopharmaceutics,* 52**,** 249-254.

JAVADZADEH, Y., DIZAJ, S. M., VAZIFEHASL, Z. & MOKHTARPOUR, M. 2015. Recrystallization of Drugs — Effect on Dissolution Rate. *In:* GLEBOVSKY, V. (ed.) *Recrystallization in Materials Processing.* Rijeka: InTech.

JIA, Z., DAVIS, E., MUZZIO, F. J. & IERAPETRITOU, M. G. 2009. Predictive Modeling for Pharmaceutical Processes Using Kriging and Response Surface. *Journal of Pharmaceutical Innovation,* 4**,** 174-186.

JUHA A. KURKELA, D. P. B., JANNE RAULA, ESKO I. KAUPPINEN 2008. New apparatus for studying powder deagglomeration. *Powder Technology,* 180**,** 164–171.

KAIALY, W., LARHRIB, H., CHIKWANHA, B., SHOJAEE, S. & NOKHODCHI, A. 2014. An approach to engineer paracetamol crystals by antisolvent crystallization technique in presence of various additives for direct compression. *Int J Pharm,* 464**,** 53-64.

KHAN, A., IQBAL, Z., KHAN, A., MUGHAL, M. A., KHAN, A., ULLAH, Z. & KHAN, I. 2016. Modulation of pH-Independent release of a Class II Drug (Domperidone) from a polymeric matrix using acidic excipients. *Dissolution Technologies,* 23**,** 32-40.

KIM, I., MA, X. & ANDREASSEN, J.-P. 2012. Study of the Solid-liquid Solubility in the Piperazine-H2O-CO2 System using FBRM and PVM. *Energy Procedia,* 23**,** 72-81.

KOGANTI, V., CARROLL, F., FERRAINA, R., FALK, R., WAGHMARE, Y., BERRY, M., LIU, Y., NORRIS, K., LEASURE, R. & GAUDIO, J. 2010. Application of Modeling to Scale-up Dissolution in Pharmaceutical Manufacturing. *AAPS PharmSciTech,* 11**,** 1541-1548.

KORLAKUNTE V.R. PRASAD, R. I. R., DAVID B. SHEEN, JOHN N. SHERWOOD 2002. Dissolution kinetics of paracetamol single crystals. *International Journal of Pharmaceutics,* 238 29-41.

KOUICHI NAKAMICHI, T. N., HIROYUKI YASUURA, SHOGO IZUMI, YOSHIAKI KAWASHIMA 2002. The role of the kneading paddle and the effects of screw revolution speed and water content on the preparation of solid dispersions using a twin-screw extruder. *International Journal of Pharmaceutics,* 241**,** 203–211.

KRUIJT, P. G. M., GALAKTIONOV, O. S., PETERS, G. W. M. & MEIJER, H. E. H. 2001. The Mapping Method for Mixing Optimization. *International Polymer Processing,* 16**,** 161-171.

KUMINEK, G., RAUBER, G. S., RIEKES, M. K., CAMPOS, C. E. M. D., MONTI, G. A., BORTOLUZZI, A. J., CUFFINI, S. L. & CARDOSO, S. G. 2013. Single crystal structure, solid state characterization and dissolution rate of terbinafine hydrochloride. *Journal of Pharmaceutical and Biomedical Analysis,* 78–79**,** 105-111.

KWON, J. S.-I., NAYHOUSE, M., CHRISTOFIDES, P. D. & ORKOULAS, G. 2014. Modeling and control of crystal shape in continuous protein crystallization. *Chemical Engineering Science,* 107**,** 47-57.

LAITINEN, R., LAHTINEN, J., SILFSTEN, P., VARTIAINEN, E., JARHO, P. & KETOLAINEN, J. 2010. An optical method for continuous monitoring of the dissolution rate of pharmaceutical powders. *Journal of Pharmaceutical and Biomedical Analysis,* 52**,** 181-189.

LASAGA, A. C. 1997. *Kinetic Theory in the Earth Sciences,* New Jersey, Princeton University Press.

LEBLOND, D., ALTAN, S., NOVICK, S., PETERSON, J., SHEN, Y. & YANG, H. 2016. In vitro dissolution curve comparisons: A critique of current practice. *Dissolution Technologies,* 23**,** 14-23.

LEE, J. 2014. Chapter 1.2 - Surface Tension and Contact Angle A2 - Seetharaman, Seshadri. *Treatise on Process Metallurgy.* Boston: Elsevier.

LEE, S. L., O'CONNOR, T. F., YANG, X., CRUZ, C. N., CHATTERJEE, S., MADURAWE, R. D., MOORE, C. M. V., YU, L. X. & WOODCOCK, J. 2015. Modernizing Pharmaceutical Manufacturing: from Batch to Continuous Production. *Journal of Pharmaceutical Innovation,* 10**,** 191-199.

LEE, T., LIN, H. Y. & LEE, H. L. 2013. Engineering reaction and crystallization and the impact on filtration, drying, and dissolution behaviors: The study of acetaminophen (paracetamol) by in-process controls. *Organic Process Research and Development,* 17**,** 1168-1178.

LEGRAS, A., KONDOR, A., HEITZMANN, M. T. & TRUSS, R. W. 2015. Inverse gas chromatography for natural fibre characterisation: Identification of the critical parameters to determine the Brunauer-Emmett-Teller specific surface area. *J Chromatogr A,* 1425**,** 273-9.

LIU, J. & RASMUSON, Å. C. 2013. Influence of agitation and fluid shear on primary nucleation in solution. *Crystal Growth & Design,* 13**,** 4385-4394.

LU, X., YANG, S. & EVANS, J. R. G. 2007. Dose uniformity of fine powders in ultrasonic microfeeding. *Powder Technology,* 175**,** 63-72.

LU, X., YANG, S. & EVANS, J. R. G. 2009. Microfeeding with different ultrasonic nozzle designs. *Ultrasonics,* 49**,** 514-521.

MANGIN, D., GARCIA, E., GERARD, S., HOFF, C., KLEIN, J. P. & VEESLER, S. 2006. Modeling of the dissolution of a pharmaceutical compound. *Journal of Crystal Growth,* 286**,** 121-125.

MANIRUZZAMAN, M., BOATENG, J. S., SNOWDEN, M. J. & DOUROUMIS, D. 2012. A review of hot-melt extrusion: process technology to pharmaceutical products. *ISRN Pharm,* 2012**,** 436763.

MANIRUZZAMAN, M., ISLAM, M. T., HALSEY, S., AMIN, D. & DOUROUMIS, D. 2016. Novel Controlled Release Polymer-Lipid Formulations Processed by Hot Melt Extrusion. *AAPS PharmSciTech,* 17**,** 191-9.

MARTIN, C. 2013. Melt Extrusion. *In:* REPKA, M. A. L., N. ; DINUNZIO, J. (ed.) *Materials, Technology and Drug Product Design.* Springer: AAPS Advances in the Pharmaceutical Sciences Series 9.

MARTINEZ-MARCOS, L., LAMPROU, D. A., MCBURNEY, R. T. & HALBERT, G. W. 2016. A novel hot-melt extrusion formulation of albendazole for increasing dissolution properties. *International Journal of Pharmaceutics,* 499**,** 175-185.

MATSUDA, H., MORI, K., TOMIOKA, M., KARIYASU, N., FUKAMI, T., KURIHARA, K., TOCHIGI, K. & TOMONO, K. 2015. Determination and prediction of solubilities of active pharmaceutical ingredients in selected organic solvents. *Fluid Phase Equilibria,* 406**,** 116-123.

MAURO, J. C. & ELLISON, A. J. 2011. Breakdown of the fractional Stokes–Einstein relation in silicate liquids. *Journal of Non-Crystalline Solids,* 357**,** 3924-3927.

MCGLONE, T., BRIGGS, N. E. B., CLARK, C. A., BROWN, C. J., SEFCIK, J. & FLORENCE, A. J. 2015. Oscillatory Flow Reactors (OFRs) for Continuous Manufacturing and Crystallization. *Organic Process Research & Development,* 19**,** 1186-1202.

MCMULLEN, J. P., MARTON, C. H., SHERRY, B. D., SPENCER, G., KUKURA, J. & EYKE, N. S. 2018. Development and Scale-Up of a Continuous Reaction for Production of an Active Pharmaceutical Ingredient Intermediate. *Organic Process Research & Development*.

MCWILLIAMS, J. C., ALLIAN, A. D., OPALKA, S. M., MAY, S. A., JOURNET, M. & BRADEN, T. M. 2018. The Evolving State of Continuous Processing in Pharmaceutical API Manufacturing: A Survey of Pharmaceutical Companies and Contract Manufacturing Organizations. *Organic Process Research & Development*.

MEIJER, H. E. H. & ELEMANS, P. H. M. 1988. The modeling of continuous mixers. Part I: The corotating twin‐screw extruder. *Polymer Engineering & Science,* 28**,** 275-290.

MENDEZ TORRECILLAS, C., HALBERT, G. W. & LAMPROU, D. A. 2017. A novel methodology to study polymodal particle size distributions produced during continuous wet granulation. *International Journal of Pharmaceutics,* 519**,** 230-239.

MESSMER, T. D. 2013. Improve the performance of your gravimetric feeder. Gardner Publications, Inc.

MITCHELL, N. A., FRAWLEY, P. J. & Ó'CIARDHÁ, C. T. 2011. Nucleation kinetics of paracetamol–ethanol solutions from induction time experiments using Lasentec FBRM®. *Journal of Crystal Growth,* 321**,** 91-99.

MITSUKO FUJIWARA, P. S. C., DAVID L. MA, AND RICHARD D. BRAATZ 2002. Paracetamol Crystallization Using Laser Backscattering and ATR-FTIR Spectroscopy. *CRYSTAL GROWTH & DESIGN,* 2**,** 363-370.

MOHAMMAD, M. A. 2015. Accuracy verification of surface energy components measured by inverse gas chromatography. *J Chromatogr A,* 1399**,** 88-93.

MORADIYA, H., ISLAM, M. T., WOOLLAM, G. R., SLIPPER, I. J., HALSEY, S., SNOWDEN, M. J. & DOUROUMIS, D. 2014a. Continuous Cocrystallization for Dissolution Rate Optimization of a Poorly Water-Soluble Drug. *Crystal Growth & Design,* 14**,** 189-198.

MORADIYA, H. G., ISLAM, M. T., HALSEY, S., MANIRUZZAMAN, M., CHOWDHRY, B. Z., SNOWDEN, M. J. & DOUROUMIS, D. 2014b. Continuous cocrystallisation of carbamazepine and trans-cinnamic acid via melt extrusion processing. *CrystEngComm,* 16**,** 3573.

MOSHARRAF, M. & NYSTRÖM, C. 1995. The effect of particle size and shape on the surface specific dissolution rate of microsized practically insoluble drugs. *International Journal of Pharmaceutics,* 122**,** 35-47.

MULIADI, A. R., LITSTER, J. D. & WASSGREN, C. R. 2013. Validation of 3-D finite element analysis for predicting the density distribution of roll compacted pharmaceutical powder. *Powder Technology,* 237**,** 386-399.

MURRAY, P. R. D., BROWNE, D. L., PASTRE, J. C., BUTTERS, C., GUTHRIE, D. & LEY, S. V. 2013. Continuous Flow-Processing of Organometallic Reagents Using an Advanced Peristaltic Pumping System and the Telescoped Flow Synthesis of (E/Z)-Tamoxifen. *Organic Process Research & Development,* 17**,** 1192-1208.

MYERSON, A. S. (ed.) 2002. *Handbook of Industrial Crystallisation*: Butterworth-Heinemann.

NAGY, Z. K., FUJIWARA, M., WOO, X. Y. & BRAATZ, R. D. 2008. Determination of the kinetic parameters for the crystallization of paracetamol from water using metastable zone width experiments. *Industrial and Engineering Chemistry Research,* 47**,** 1245-1252.

NI, X. 2006. Continuous Oscillatory Baffled Reactor Technology. *Innovations in Pharmaceutical Technology,* 20**,** 90-96.

NIENOW, A. & MILES, D. 1971. Impellor power numbers in closed vessels. *Ind. Eng. Chem. Process Des. Dev.,* 10**,** 41-43.

NOWAK, S. 2013. Using a gravimetric feeder to dose pharmaceutical bulk solids: loss-in-weight feeders provide high accuracy for batch or continuous processes. Advanstar Communications, Inc.

NUENNERICH, P., DIERKES, H. & BORK, M. 2008. Method for Suspending and Introducing Solid Matter in a High-Pressure Process. Google Patents.

O'CONNOR, T. & LEE, S. 2017. Chapter 37 - Emerging Technology for Modernizing Pharmaceutical Production: Continuous Manufacturing A2 - Qiu, Yihong. *In:* CHEN, Y., ZHANG, G. G. Z., YU, L. & MANTRI, R. V. (eds.) *Developing Solid Oral Dosage Forms (Second Edition)*. Boston: Academic Press.

ØSTERGAARD, J., WU, J. X., NAELAPÄÄ, K., BOETKER, J. P., JENSEN, H. & RANTANEN, J. 2014. Simultaneous UV Imaging and Raman Spectroscopy for the Measurement of Solvent-Mediated Phase Transformations During Dissolution Testing. *Journal of Pharmaceutical Sciences,* 103**,** 1149-1156.

ØSTERGAARDJESPER, J., LENKE, J., JENSEN, S. S., SUN, Y. & YE, F. 2014. UV imaging for in vitro dissolution and release studies: Initial experiences. *Dissolution Technologies,* 21**,** 27-38.

OZTURK, N., KAYNAK, M. S. & SAHIN, S. 2015. Comparison of dissolution profiles of commercially available Lamivudine tablets. *Dissolution Technologies,* 22**,** 38-43.

PAGE, T., DUBINA, H., FILLIPI, G., GUIDAT, R., PATNAIK, S., POECHLAUER, P., SHERING, P., GUINN, M., MCDONNELL, P. & JOHNSTON, C. 2015. Equipment and Analytical Companies Meeting Continuous Challenges. May 20–21, 2014 Continuous Manufacturing Symposium. *Journal of Pharmaceutical Sciences,* 104**,** 821-831.

PANGARKAR, V. G., YAWALKAR, A. A., SHARMA, M. M. & BEENACKERS, A. A. C. M. 2002. Particle−Liquid Mass Transfer Coefficient in Two-/Three-Phase Stirred Tank Reactors. *Industrial & Engineering Chemistry Research,* 41**,** 4141-4167.

PAROJČIĆ, J., VASILJEVIĆ, D., IBRIĆ, S. & DJURIĆ, Z. 2008. Tablet disintegration and drug dissolution in viscous media: Paracetamol IR tablets. *International Journal of Pharmaceutics,* 355**,** 93-99.

PARSONS, A. R., BLACK, S. N. & COLLING, R. 2003. Automated Measurement of Metastable Zones for Pharmaceutical Compounds. *Chemical Engineering Research and Design,* 81**,** 700-704.

PATIL, H., TIWARI, R. V. & REPKA, M. A. 2015. Hot-Melt Extrusion: from Theory to Application in Pharmaceutical Formulation. *AAPS PharmSciTech*.

PAUL, E. L., MIDLER, M. & SUN, Y. 2004. Mixing in the Fine Chemicals and Pharmaceutical Industries. *Handbook of Industrial Mixing.* John Wiley & Sons, Inc.

PAUS, R. & JI, Y. 2016. Modeling and predicting the influence of variable factors on dissolution of crystalline pharmaceuticals. *Chemical Engineering Science,* 145**,** 10-20.

PLUMB, K. 2005. Continuous Processing in the Pharmaceutical Industry Changing the Mind Set. *Chemical Engineering Research and Design,* 83**,** 730-738.

PO, H. N. & SENOZAN, N. M. 2001. The Henderson-Hasselbalch Equation: Its History and Limitations. *Journal of Chemical Education,* 78**,** 1499.

POLITANO, F. & OKSDATH-MANSILLA, G. 2018. Light on the Horizon: Current Research and Future Perspectives in Flow Photochemistry. *Organic Process Research & Development*.

POLSTER, C. S., COLE, K. P., BURCHAM, C. L., CAMPBELL, B. M., FREDERICK, A. L., HANSEN, M. M., HARDING, M., HELLER, M. R., MILLER, M. T., PHILLIPS, J. L., POLLOCK, P. M. & ZABORENKO, N. 2014. Pilot-Scale Continuous Production

of LY2886721: Amide Formation and Reactive Crystallization. *Organic Process Research & Development,* 18**,** 1295-1309.

PONOMAREV, D., RODIER, E., SAUCEAU, M., NIKITINE, C., MIZONOV, V. & FAGES, J. 2012. Modelling non-homogeneous flow and residence time distribution in a single-screw extruder by means of Markov chains. *Journal of Mathematical Chemistry,* 50**,** 2141-2154.

PRASAD, K. V. R., RISTIC, R. I., SHEEN, D. B. & SHERWOOD, J. N. 2002. Dissolution kinetics of paracetamol single crystals. *International Journal of Pharmaceutics,* 238**,** 29-41.

PUDLAS, M., KYEREMATENG, S. O., WILLIAMS, L. A., KIMBER, J. A., VAN LISHAUT, H., KAZARIAN, S. G. & WOEHRLE, G. H. 2015. Analyzing the impact of different excipients on drug release behavior in hot-melt extrusion formulations using FTIR spectroscopic imaging. *Eur J Pharm Sci,* 67**,** 21-31.

RASMUSON, R. A. G. A. A. C. 1999. Solubility of paracetamol in pure solvents. *J. Chem. Eng. Data,* 44**,** 1391-1395.

REPKA, M. A., BATTU, S. K., UPADHYE, S. B., THUMMA, S., CROWLEY, M. M., ZHANG, F., MARTIN, C. & MCGINITY, J. W. 2007. Pharmaceutical applications of hot-melt extrusion: Part II. *Drug Dev Ind Pharm,* 33**,** 1043-57.

RIBEIRO, A. C. F., BARROS, M. C. F., VERÍSSIMO, L. M. P., SANTOS, C. I. A. V., CABRAL, A. M. T. D. P. V., GASPAR, G. D. & ESTESO, M. A. 2012. Diffusion coefficients of paracetamol in aqueous solutions. *The Journal of Chemical Thermodynamics,* 54**,** 97-99.

RICCIARDI, R. J. & LAIDLAW, J. S. 1995. Materials feeding system with level sensing probe and method for automatic bulk density determination. Google Patents.

ROHANI, H. H. A. S. 2006a. Measurement and Prediction of Solubility of Paracetamol in Water-Isopropanol Solution. Part 1. Measurement and Data Analysis. *Organic Process Research & Development,* 10**,** 1101-1109.

ROHANI, H. H. A. S. 2006b. Measurement and Prediction of Solubility of Paracetamol in Water-Isopropanol Solution. Part 2. Prediction. *Organic Process Research & Development,* 10**,** 1110-1118.

RÜCKRIEM, M., ENKE, D. & HAHN, T. 2015. Inverse gas chromatography (IGC) as a tool for an energetic characterisation of porous materials. *Microporous and Mesoporous Materials,* 209**,** 99-104.

SALEEMI, A. N., RIELLY, C. D. & NAGY, Z. K. 2012. Monitoring of the combined cooling and antisolvent crystallisation of mixtures of aminobenzoic acid isomers using ATR-UV/vis spectroscopy and FBRM. *Chemical Engineering Science,* 77**,** 122-129.

SALEH, M. F., DHENGE, R. M., CARTWRIGHT, J. J., HOUNSLOW, M. J. & SALMAN, A. D. 2015. Twin screw wet granulation: Binder delivery. *International Journal of Pharmaceutics,* 487**,** 124-134.

SALVATORE, M., HEIDER. P. L., HAITAO, Z., LAKERVELD, R., BRAHIM, B., BARTON, P. I., BRAATZ, R. D., COONEY, C. L., EVANS, J. M. B., JAMISON, T. F., JENSEN, K. F., MYERSON, A. S., TROUT, B. L. 2013. End‐to‐End Continuous Manufacturing of Pharmaceuticals: Integrated Synthesis, Purification, and Final Dosage Formation. *Angewandte Chemie International Edition,* 52**,** 12359-12363.

SHAH, Z. & LONDHE, V. 2016. Influence of various media on the dissolution profiles of immediate-release quetiapine tablets in India. *Dissolution Technologies,* 23**,** 42-46.

SHEKUNOV, B. & MONTGOMERY, E. R. 2015. Theoretical Analysis of Drug Dissolution: I. Solubility and Intrinsic Dissolution Rate. *Journal of Pharmaceutical Sciences*.

SHIBATA, Y., FUJII, M., SUGAMURA, Y., YOSHIKAWA, R., FUJIMOTO, S., NAKANISHI, S., MOTOSUGI, Y., KOIZUMI, N., YAMADA, M., OUCHI, K. & WATANABE, Y. 2009. The preparation of a solid dispersion powder of indomethacin with crospovidone using a twin-screw extruder or kneader. *Int J Pharm,* 365**,** 53-60.

SIMON LAWTON, G. S., PHIL SHERING 2009,. Continuous Crystallization of Pharmaceuticals Using a Continuous Oscillatory Baffled Crystallizer. *Organic Process Research & Development,* 13**,** 1357–1363.

SIMONETTI, R., OLIVERI, P., HENRY, A., DUPONCHEL, L. & LANTERI, S. 2016. Has your ancient stamp been regummed with synthetic glue? A FT-NIR and FT-Raman study. *Talanta,* 149**,** 250-256.

SINCLAIR, M. J., HART, R. A., POPE, H. M. & CAMPBELL, E. J. M. 1968. The use of the henderson-hasselbalch equation in routine medical practice. *Clinica Chimica Acta,* 19**,** 63-69.

SINNOTT, R. K. 1999. Equipment Selection, Specification and Design. *In:* SINNOTT, R. K. (ed.) *Coulson and Richardson's Chemical Engineering Volume 6 - Chemical Engineering Design.* Third ed. Oxford: Butterworth-Heinemann.

SMIRNOV, V. I. & BADELIN, V. G. 2014. Effect of the composition of a water-alcohol solvent on the thermodynamics of dissolution of DL-α-alanyl-β-alanine at 298.15 K. *Russian Journal of Physical Chemistry A,* 88**,** 2087-2090.

SPARKS, D. L., FENDORF, S. E., TONER, C. V. & CARSKI, T. H. 1996. Kinetic Methods and Measurements. *In:* SPARKS, D. L., PAGE, A. L., HELMKE, P. A. & LOEPPERT, R. H. (eds.) *Methods of Soil Analysis Part 3—Chemical Methods.* Madison, WI: Soil Science Society of America, American Society of Agronomy.

STANKOVIC, M., FRIJLINK, H. W. & HINRICHS, W. L. 2015. Polymeric formulations for drug release prepared by hot melt extrusion: application and characterization. *Drug Discov Today,* 20**,** 812-23.

TANG, L. & CHEN, W.-Y. 1999. Improvements on a particle feeder for experiments requiring low feed rates. *Review of Scientific Instruments,* 70**,** 3143.

TARDOS, G. I. & LU, Q. 1996. Precision dosing of powders by vibratory and screw feeders: an experimental study. *Advanced Powder Technology,* 7**,** 51-58.

THAKUR, R. K., VIAL, C., NIGAM, K. D. P., NAUMAN, E. B. & DJELVEH, G. 2003. Static Mixers in the Process Industries—A Review. *Chemical Engineering Research and Design,* 81**,** 787-826.

THIRY, J., KRIER, F. & EVRARD, B. 2015. A review of pharmaceutical extrusion: critical process parameters and scaling-up. *Int J Pharm,* 479**,** 227-40.

THOMPSON, D. R., KOUGOULOS, E., JONES, A. G. & WOOD-KACZMAR, M. W. 2005. Solute concentration measurement of an important organic compound using ATR-UV spectroscopy. *Journal of Crystal Growth,* 276**,** 230-236.

TIMOKLEIA TOGKALIDOU, M. F., SHEFALI PATEL, RICHARD D. BRAATZ 2001. Solute concentration prediction using chemometrics and ATR-FTIR spectroscopy. *Journal of Crystal Growth,* 231**,** 534-543.

TINGSTAD, J. E. & RIEGELMAN, S. 1970. Dissolution Rate Studies I: Design and Evaluation of a Continuous Flow Apparatus. *Journal of Pharmaceutical Sciences,* 59**,** 692-696.

TODD M. FRANCIS, C. J. G., ALAN W. WEIMER 2006. Spinning wheel powder feeding device — fundamentals and applications. *Powder Technology,* 170**,** 36–44.

TOWLER, G. & SINNOTT, R. 2013. Chapter 15 - Design of Reactors and Mixers. *Chemical Engineering Design (Second Edition)*. Boston: Butterworth-Heinemann.

TRAN, T. T.-D., TRAN, P. H.-L., PARK, J.-B. & LEE, B.-J. 2012. Effects of solvents and crystallization conditions on the polymorphic behaviors and dissolution rates of valsartan. *Archives of Pharmacal Research,* 35**,** 1223-1230.

VASIL'CHENKO, M., SHAKHTSHNEIDER, T., NAUMOV, D. Y. & BOLDYREV, V. 1996. Topochemistry of the initial stages of the dissolution of single crystals of acetaminophen. *Journal of pharmaceutical sciences,* 85**,** 929-934.

VERCRUYSSE, J., CÓRDOBA DÍAZ, D., PEETERS, E., FONTEYNE, M., DELAET, U., VAN ASSCHE, I., DE BEER, T., REMON, J. P. & VERVAET, C. 2012. Continuous twin screw granulation: Influence of process variables on granule and tablet quality. *European Journal of Pharmaceutics and Biopharmaceutics,* 82**,** 205-211.

WAHL, P. R., TREFFER, D., MOHR, S., ROBLEGG, E., KOSCHER, G. & KHINAST, J. G. 2013. Inline monitoring and a PAT strategy for pharmaceutical hot melt extrusion. *International Journal of Pharmaceutics,* 455**,** 159-168.

WANG, P., WANG, J., GONG, J. & ZHANG, M. 2011. Determination of the solubility, dissolution enthalpy and entropy of Deflazacort in different solvents. *Fluid Phase Equilibria,* 306**,** 171-174.

WANG, Y., LI, T., MUZZIO, F. J. & GLASSER, B. J. 2017. Predicting feeder performance based on material flow properties. *Powder Technology,* 308**,** 135-148.

WARREN, F. J., GIDLEY, M. J. & FLANAGAN, B. M. 2016. Infrared spectroscopy as a tool to characterise starch ordered structure—a joint FTIR–ATR, NMR, XRD and DSC study. *Carbohydrate Polymers,* 139**,** 35-42.

WHITNEY, A. A. N. A. W. R. 1897. The Rate of Solution of Solid Substances in their own Solutions. *Journal of the American Chemical Society,* 19**,** 930-934.

WILLIAM E. ENGISCH, F. J. M. 2012. Method for characterization of loss-in-weight feeder equipment. *Powder Technology,* 228**,** 395–403.

WILLIAM L. JORGENSEN, E. M. D. 2002. Prediction of drug solubility from structure. *Advanced Drug Delivery Reviews* 54**,** 355-366.

WOOD, A. 2009. Generic Batch Procedures for Flexible Manufacturing. *Control Engineering,* 56**,** P1-P5.

WOODRUFF, R. B., KREIDER, P. & WEIMER, A. W. 2012. A novel brush feeder for the pneumatic delivery of dispersed small particles at steady feed rates. *Powder Technology,* 229**,** 45-50.

XU, R., WANG, J., HAN, S., DU, C., MENG, L. & ZHAO, H. 2016. Solubility modelling and thermodynamic dissolution functions of phthalimide in ten organic solvents. *The Journal of Chemical Thermodynamics,* 94**,** 160-168.

YANG, S. & EVANS, J. R. G. 2007. Metering and dispensing of powder; the quest for new solid freeforming techniques. *Powder Technology,* 178**,** 56-72.

YONGJIN YI, D. H., AND ALLAN S. MYERSON 2005. Development of a Small-Scale Automated Solubility Measurement Apparatus. *Ind. Eng. Chem. Res.,* 44**,** 5427-5433.

ZHANG, Y., JIANG, Y., ZHANG, D., LI, K. & QIAN, Y. 2011. On-line concentration measurement for anti-solvent crystallization of β-artemether using UV–vis fiber spectroscopy. *Journal of Crystal Growth,* 314**,** 185-189.

ZIMMERMAN, J. H. K. 1952. The Experimental Determination of Solubilities. *Chemical Reviews,* 51**,** 25-65.